THE ASTROPHYSICAL JOURNAL SUPPLEMENT SERIES, 76:55–114, 1991 May

SINGLE AND BINARY STAR EVOLUTION[1]

ICKO IBEN, JR.[2]
University of Illinois and Pennsylvania State University
Received 1990 April 20; accepted 1990 August 22

CONTENTS

ABSTRACT

The theory of stellar evolution, when coupled with the observed properties of stars, has taught us much about stellar interiors and about the theory itself. This review presents first: (1) a general description of the observed global properties of single stars of low, intermediate, and high mass; a description of the theoretical evolution in the Hertzsprung-Russell diagram of such stars; and an assessment of what the amalgam has taught us about the interior and surface physics of real stars; and (2) a description of the observed properties of various types of evolved close binaries; a summary of the concepts which have been found useful in constructing scenarios for the transformation of primordial binaries into evolved systems; and a judgement about what the comparison between the observations and the results of a crude theory has taught us about the physics of mass transfer within interacting binary systems and about the manner and extent of mass and angular momentum loss from these systems.

The discussion then focuses on several specific topics: (1) the role of H^- opacity in determining red giant surface temperatures; (2) interior composition changes due to nucleosynthesis and mixing, followed by (the first) dredge-up and changes in surface composition; (3) stellar evolution in globular clusters—mass loss on the giant branch, the horizontal and suprahorizontal branches, the primordial helium abundance, and cluster ages; (4) RR Lyrae stars in globular clusters; (5) theoretical Cepheid period-luminosity relationships and distances to Galactic and extragalactic Cepheids; (6) solar neutrino pedagogy; (7) asymptotic giant branch (AGB) stars of intermediate mass—the second dredge-up, thermal pulses, and the activation of the ^{22}Ne neutron source, nucleosynthesis of s-process elements in the convective shell, and the third dredge-up, which brings freshly synthesized elements to the surface; (8) AGB stars of low mass, activation of the ^{13}C neutron source, the production of *s*-process elements in the solar system distribution, the third dredge-up and the formation of carbon stars (9) termination of the AGB phase and post–AGB evolution—planetary nebula nuclei, born-again AGB stars, and self-induced novae; (10) white dwarf evolution—diffusion, nuclear burning, composition, and the age of the Galactic disk; (11) response

[1] The 1989 Henry Norris Russell Lecture.
[2] Supported in part by the National Science Foundation Grant AST88-00773 and by endowment funds for the Eberly Family Chair in Astronomy and Astrophysics at the Pennsylvania State University.

of stars in binaries to rapid mass loss—the relationship between initial mass and the mass of the compact remnant; (12) response of white dwarfs in binary systems to mass accretion—classical and symbiotic novae, helium star cataclysmic variables; (13) scenarios for binary star evolution leading to close white dwarf pairs, some of which may merge to become subdwarf O and B stars, R CrB stars, or Type Ia supernovae; (14) star bursts, stellar mergers, and blue stragglers in clusters from the young disk to the halo.

This very personal account is not intended to be comprehensive. The major aim has been to provide perspectives on a number of topics in stellar astrophysics that have interested the author over the past quarter of a century.

Subject headings: clusters: globular — galaxies: distances — neutrinos — nucleosynthesis — stars: abundances — stars: binaries — stars: carbon — stars: Cepheids — stars: evolution — stars: horizontal-branch — stars: interiors — stars: novae — stars: pulsation — stars: RR Lyrae — stars: white dwarfs

I. NEARBY AND VISUALLY BRIGHT STARS IN THE HERTZSPRUNG-RUSSELL DIAGRAM

One of the major goals of the theory of stellar evolution has been to understand the positions of stars in the Hertzsprung-Russell diagram. The original Hertzsprung version, with absolute visual magnitude and color as coordinates, was published in 1911 (Rosenberg 1911; Hertzsprung 1911), and the original Russell version, with absolute visual magnitude and spectral type as coordinates, was published in 1914 (Russell 1914 *a, b*). Now, over three-quarters of a century later, we have a good notion as to how and why various regions of the diagram are populated.

A modern version of the Hertzsprung-Russell (H-R) diagram is shown in Figure 1, where coordinates are absolute luminosity and surface temperature. All but three of the nearby and/or bright stars placed in this diagram are taken from Allen's compilation (Allen 1961) and the selection criterion for the brightest stars is that their names were imprinted on the author's mind over 40 years ago while reading fairy tales, romantic novels, and nineteenth century English poetry. Two sequences defined by nearby stars are clearly distinguished in Figure 1: (1) a "main sequence" extending from Spica A down to L726−8 B and (2) a "white dwarf" sequence extending from Sirius B down to L870-2. The designation "main" derives from the high space density of member stars and the designation "dwarf" derives from the small size of the member stars. These two sequences have been recognized since the time of Hertzsprung and Russell, and we now know that main-sequence stars are supported against gravity by gas and radiation pressure and are burning hydrogen into helium at their centers, and hence may be called core hydrogen-burning stars, and that the white dwarfs are supported against gravity by the pressure of degenerate electrons and are shining primarily because of the loss of thermal energy by nondegenerate nuclei.

The brightest stars in Figure 1 above and to the right of the main sequence may be imagined to form two additional sequences: (3) a sequence which is nearly parallel to the main sequence and which extends from Rigel and Deneb down to Capella and Pollux and (4) a nearly constant-temperature sequence extending from Betelgeuse and Antares down to Mira and Aldebaran. By comparing with theoretical models, we know now that most of the stars in the third sequence are burning helium at their centers; this sequence may therefore be called the core helium-burning band, even though most of the light emitted by stars in the band comes from hydrogen burning in a shell. Members of the fourth branch are usually called red giants or red supergiants, an appellation that their colors and large size make obvious. The red giant branch actually extends all the way down to the main sequence, those near the main sequence being called subgiants, but only one representative (the cool component of RS CVn) is shown. The brightest red giants (supergiants) are burning hydrogen in a shell and most are also burning helium at the center. The lowest luminosity red giants (e.g., Pollux and Aldebaran) are burning hydrogen in a shell above a compact, hot core which is of a size comparable with that of the lowest-mass white dwarfs known. Red giants of intermediate luminosity, such as Mira, alternate in burning first hydrogen and then helium in a shell above a

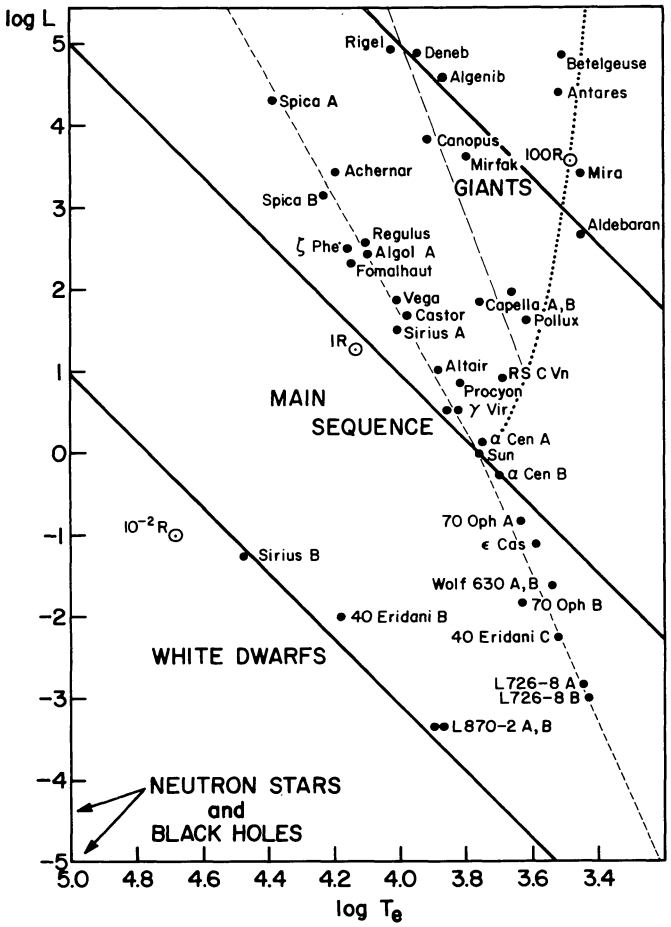

FIG. 1.—The locations of some nearby stars and of some bright stars in the Hertzsprung-Russell diagram. Coordinates are the logarithms (base 10) of luminosity L (in solar units) and of surface temperature T_e (degrees K). Three lines of constant radius are also shown. Data mostly from Allen's (1973) compilation.

white dwarf–like core composed of carbon and oxygen. These stars, called thermally pulsing AGB stars for reasons described in the next section, experience intermittent thermonuclear runaways and are responsible for producing most of the carbon and neutron-rich "*s*-process" isotopes in the universe.

The theory of single star evolution tells us that high-mass stars evolve from the main sequence to the core helium-burning band at a luminosity comparable with their main-sequence luminosity and then evolve into Type II supernovae. Stars of intermediate mass evolve to the giant branch, then to the core helium-burning band; after exhausting central helium, they evolve into intermediate-luminosity red giants (AGB stars), and finally, after the ejection of a nebular shell, they become white dwarfs. The existence of a nebular ejection phase has not yet been satisfactorily predicted from first principles, but its occurrence has been established by comparing theoretical models with the observed properties of stars in globular clusters in the Magellanic Clouds and by making use of the statistical properties of planetary nebulae. Low-mass stars evolve onto the low-luminosity portion of the giant branch where they possess an electron-degenerate core composed of helium. After igniting helium in a thermonuclear runaway, they descend to the core helium-burning band; subsequent evolution parallels that of intermediate-mass stars.

Neutron stars and black holes, not envisioned in the days of Hertzsprung and Russell, have enjoyed membership in the stellar club for over 20 years. They are detected either by their beamed radio and/or optical emission, as in the case of single neutron stars known as pulsars, by the emission of X-rays from the surface and from the base of a circumstellar disk, as in the case of accreting neutron stars and black holes, or by their large dynamical mass and lack of radiant emission, as in the case of several black hole candidates in binary systems. These objects, with radii 1000 times smaller than the radii of white dwarfs, lie beyond the bounds of the H-R diagram of Figure 1.

The sample of nearby stars shown in Figure 1 contains a high frequency of binary and tertiary systems. Examples are Spica A and B, L726−8 A and B, and Sirius A and B. It is from these and from many other multiple systems that we have derived reliable masses of stars other than the Sun. From binary systems widely enough separated that individual components may be expected to behave more or less as single stars, we have learned that there is a very tight correlation between mass and luminosity for main-sequence stars. For $-1 < \log L < 4$, $L \sim M^4$; for $-3 < \log L < -1$, $L \sim 0.355\, M^{2.2}$. Here, both mass M and luminosity L are in solar units. The mass-luminosity relationships derived from theoretical models agree quite well with the empirical relationships.

The distribution of "single" white dwarfs with respect to mass is based primarily upon observed positions in the H-R diagram and on a theoretical mass-radius relationship (Chandrasekhar 1931, 1939; Hamada and Salpeter 1962). This distribution is strongly peaked at $M \sim 0.55$–$0.6\ M_\odot$. The distribution extends downward to $M \sim 0.4\ M_\odot$ and falls off exponentially beyond $M \sim 0.6\ M_\odot$. Masses of the four white dwarfs shown in Figure 1 are dynamical ones obtained from the orbital characteristics of the binary systems of which they are components. Their masses span the observed mass range and agree, within the uncertainties, with the masses derived from the theoretical mass-radius relationship.

Sirius B, with $M \sim 1\ M_\odot$ is among the most massive white dwarfs known, being only $\sim 0.1\ M_\odot$ less massive than the theoretical upper limit for white dwarfs composed of carbon and oxygen. The theory suggests that its main-sequence progenitor was of mass of ~ 6–$8\ M_\odot$, the upper mass limit for the class of intermediate-mass stars, and that the separation of its progenitor from its $2\ M_\odot$ companion Sirius A was barely large enough to prevent mass transfer between the two components when the progenitor grew to red supergiant proportions. It is highly likely that, as the progenitor shed its hydrogen envelope to evolve into the central star of a planetary nebula, the two components moved several times further apart than when they were born.

The white dwarf 40 Eridani B, with $M \sim 0.43\ M_\odot$, is among the smallest-mass white dwarfs known. Its mass is less than the mass of the smallest-mass white dwarf ($\sim 0.5\ M_\odot$) which the theory of evolution and the observations suggest can be produced by a single star in a Hubble time. Fortunately, the nascent theory of close binary star evolution provides an explanation for the formation of such a light white dwarf via a scenario which involves two episodes of mass transfer between components of a low-mass binary. In this scenario, each component begins to lose mass to its companion shortly after it leaves the main sequence with an electron-degenerate helium core and continues to lose mass until most of its original hydrogen-rich envelope has been lost. The remnant then evolves into a white dwarf which was once the helium core of its progenitor. Following the second interaction, which entails the formation of a common envelope and orbital shrinkage, the two helium white-dwarf remnants are forced even closer together by the loss of angular momentum due to the emission of gravitational wave radiation. Eventually, the lighter white dwarf spills over onto the heavier one to form a single star which first ignites and burns helium as a hot subdwarf O or B star, and then evolves into a low-mass hybrid white dwarf (an object with a core composed of carbon and oxygen and an envelope of comparable mass composed of helium). The sum of the masses of the merging white dwarfs is expected to be in the range 0.3–0.6 $M_\odot$, and thus it is possible to achieve white dwarf masses smaller than the smallest mass which a single star can produce in a Hubble time.

The white dwarf pair L870−2 A and B (Saffer, Liebert, and Olszewski 1988) provides confirmation of several of the basic premises of the scenario just invoked to explain Eridani B and at the same time demonstrates the wide variety of evolutionary paths one may expect close binary stars to follow, consonant with the wide variety of initial conditions (individual masses and orbital separations) that nature provides. Both white dwarfs in L870−2 are of about the same mass, $M \sim 0.4$–$0.5\ M_\odot$ (Iben and Webbink 1988; Bergeron *et al.* 1989), and both are of about the same luminosity. In order to have developed electron-degenerate cores as large as this, the components of the main-sequence progenitors must have been separated from one another by a distance of the order of $400\ R_\odot$. Further, the masses of the main-sequence progenitors must have been at least as large as $1\ M_\odot$ and probably more like 3–$4\ M_\odot$. And yet, now, the remnant components are separated by only $\sim 6\ R_\odot$ and have a total mass of only $\sim 1\ M_\odot$. Thus, it is clear that orbital shrinkage occurs in the process of mass exchange, and it is likely that the mechanism which drives this shrinkage is related to mass and angular momentum loss from the system. A mechanism which involves a frictional interaction between

two stellar cores imbedded in a common envelope that is formed in the course of mass exchange is described in § III.

The next two sections of the paper describe in general terms the theory of evolution of single stars (§ II) and of close binary stars (§ III). The theory of binary star evolution relies heavily on quantitative properties of models of single stars, and so § III actually contains considerable further discussion about single stars. Sections IV–XIV describe several detailed results of theoretical modelling and make further comparisons with the observations that are touched upon only briefly, if at all, in §§ II and III.

No attempt has been made in this very personal account to provide a comprehensive and up-to-date discussion of all topics introduced or to provide a complete list of the most relevant references. It is hoped that the thoughts and perspectives offered will nevertheless be useful to the specialist as well as to the general reader. In more than one instance, inferences are drawn that are based on comparisons between theoretical models and interpretations of observational data which have since been substantially revised. The revisions have not been cataloged, but it is hoped that the proffered inferences are of a sufficiently general nature to have survived the inevitable changes in detail which occur as a subject matures.

II. SINGLE STAR EVOLUTION: THEORETICAL AND OBSERVATIONAL INSIGHTS

The track of a theoretical model star of intermediate mass (5 $M_\odot$) and of Population I composition is shown in Figure 2. The morphological characteristics of this track and the basic phenomena occurring in the stellar interior along each portion of the track (as given by the arrowed description along each portion) are generic to all intermediate-mass stars, if we define such stars to be those which do not develop an electron-degenerate helium core before igniting helium, but do develop an electron-degenerate core composed of carbon and oxygen after exhausting central helium. Approximately 80% of such a model's active nuclear-burning lifetime is spent on the main sequence converting hydrogen into helium in a convective core. After exhausting central hydrogen, it evolves rapidly to the giant branch, burning hydrogen in a thin shell above a rapidly contracting and heating core composed essentially of pure helium. As it approaches the giant branch, the base of a

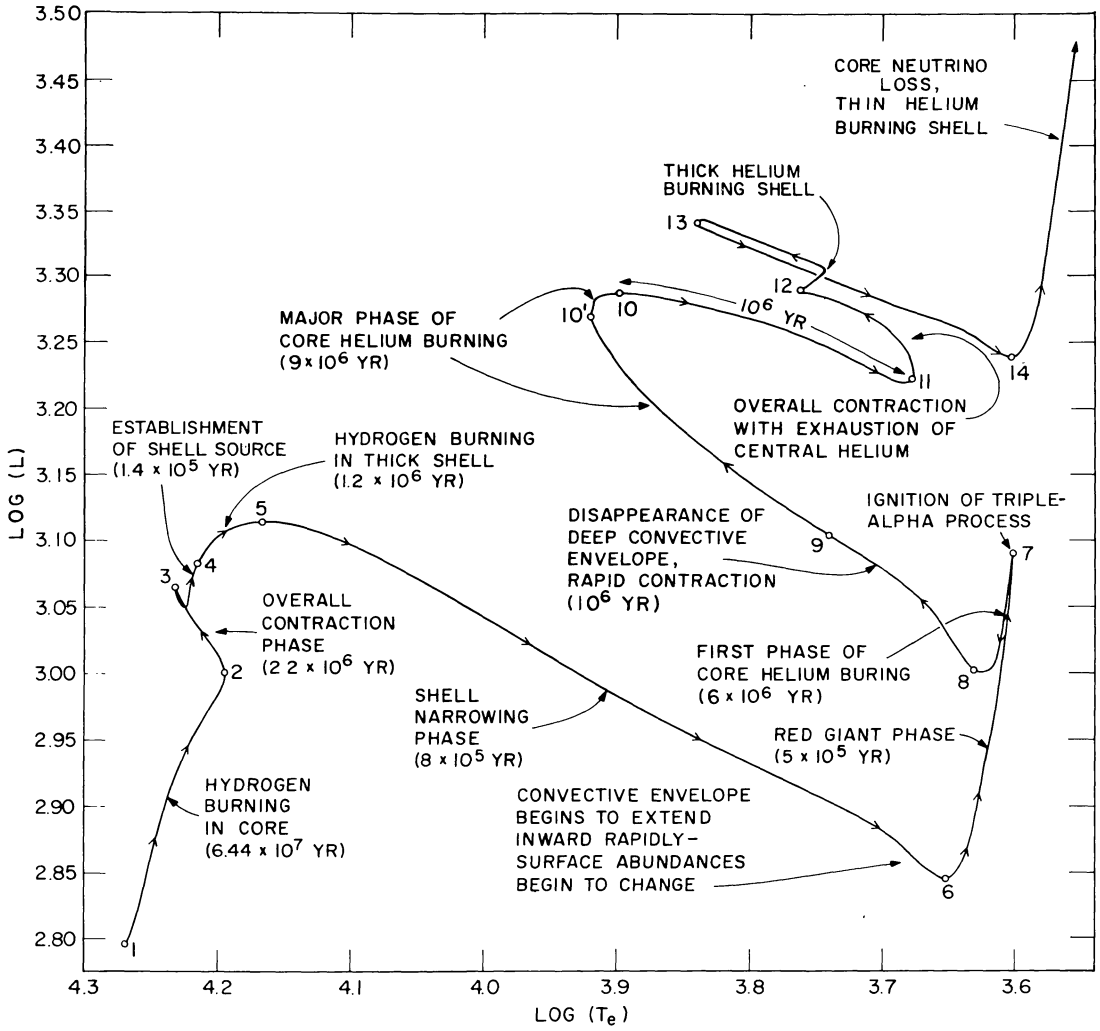

FIG. 2.—The track in the H-R diagram of a theoretical model star of mass 5 $M_\odot$ and of Population I composition. Text beside various portions of the track describe an important physical process occurring within the star at the indicated position. From Iben (1967*c*).

surface convective layer extends inward until it reaches layers in which carbon has been converted into nitrogen; the surface abundances of these two elements then begin to change in a potentially detectable way. The process of convectively mixing nuclearly processed layers into the convective envelope is called the "first dredge-up."

Once the central temperature reaches $\sim 10^8$ K and central density reaches $\sim 10^4$ g cm^{-3}, helium is ignited at the center, and this terminates and reverses the upward climb along the giant branch. The model star then embarks on an extended phase of burning helium in a steadily growing convective core. Hydrogen-burning in a thin shell continues to provide the bulk of the luminosity at the surface, and so the mass of the hydrogen-exhausted core continues to grow, even as the matter in the convective core within it is being converted into carbon and oxygen. In the H-R diagram, evolution on a nuclear-burning time scale takes place in two distinct regions: one on the giant branch and the other removed to the blue of the giant branch and at higher luminosity than on the giant branch. The times spent in the two regions are comparable and the total duration $\tau_{\rm He}$ of the core helium-burning phase is $\sim$25% of the duration $\tau_{\rm H}$ of the core hydrogen-burning phase.

The time development of global characteristics (luminosity L, surface temperature T_e, and radius R) as well as of several interior characteristics (central density ρ_c, central temperature T_c, and mass in the convective core M_{cc}) are shown in Figures 3*a* and 3*b*. During the core helium-burning phase, $\sim$80% of the energy escaping the star derives from hydrogen burning.

As the abundance of helium in central regions declines to nominal values, helium continues to burn in a shell that works its way outward in mass. The helium-exhausted core contracts and heats while the hydrogen-rich envelope expands and cools. In fact, much of the helium-rich matter between the location of the helium-burning shell and the hydrogen-helium interface participates in envelope expansion and cooling to the extent that hydrogen ceases to burn. In the H-R diagram, the model star evolves once again to the giant branch and, once again, the base of a growing convective envelope extends inward, this time eventually crossing the hydrogen-helium interface and entering into layers in which hydrogen has been completely converted into helium and most of the original carbon and oxygen has been converted into nitrogen. Fresh helium and nitrogen are brought to the surface in what is called the "second dredge-up" episode. As the base of the convective envelope moves inward in mass and the helium-burning shell moves outward in mass, as shown in Figure 4, it would seem that they must meet. Of course, they do not actually "meet." Instead, matter at the base of the convective envelope heats up and becomes more dense as it approaches the helium-burning shell, where $T_{\rm shell} \sim 2 \times 10^8$ and $\rho_{\rm shell} \sim 10^4$ g cm^{-3}; ultimately hydrogen is reignited, forcing the base of the convective envelope to retreat outward in mass ahead of the reestablished hydrogen-burning shell.

Early on in the second dredge-up phase, the matter in the helium-exhausted core becomes compacted to such an extent ($\rho_c \sim 10^6$ g cm^{-3}) that the electrons there have become degenerate; electron conduction thereafter helps maintain core material at temperatures within a factor of 2 of the mean core temperature ($T_{\rm mean} \sim 2 \times 10^8$ K). At the high densities and temperatures in the core, neutrino losses by the plasma and photoneutrino processes become important, and much of the gravitational potential energy liberated in consequence of the rearrangement of matter in the outer portions of the core as it grows in mass is lost in the form of neutrinos, helping to maintain the temperatures in the core close to the temperature in the helium-burning shell. The core of the model star now has the dimensions of a white dwarf and, in fact, it is a hot white dwarf.

The evolution of the model star following the reignition of hydrogen is rather complex and will be discussed in more de-

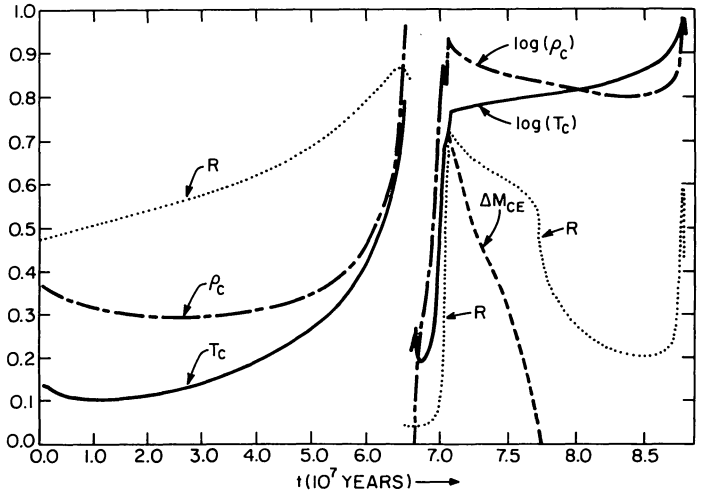

FIG. 3*a*

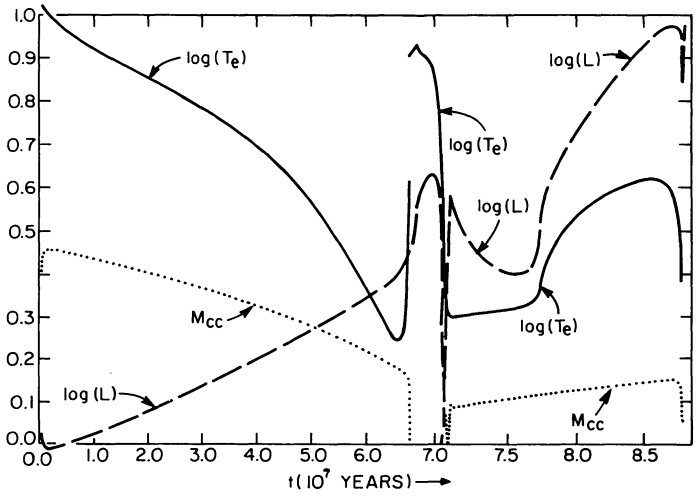

FIG. 3*b*

FIG. 3.—(*a*) Time dependence of global and interior characteristics of the model described in Fig. 2. Adapted from Iben (1965). Quantities and scale limits to the left of the break in t are radius R(0.0–5.0$R_\odot$), central density ρ_c (12–27 g cm^{-3}), and central temperature T_c(26–36 $\times$ 10^{6}K). To the right: R(0–100$R_\odot$), log ρ_c (1.8–4.3), log T_c(1.32–2.32), and mass in the convective envelope ΔM_{CE}(0–1$M_\odot$). (*b*) Time dependence of additional global and interior characteristics of the model described in Fig. 2. Adapted from Iben (1965). Quantities and scale limits to the left of the break in t are log T_e(4.17–4.27), log L(2.8–3.3), and mass in the convective core M_{cc}(0.0–0.5$M_\odot$). On the right: log T_e(3.3–4.3), log L(2.8–3.3), and M_{cc}(0.0–0.4$M_\odot$).

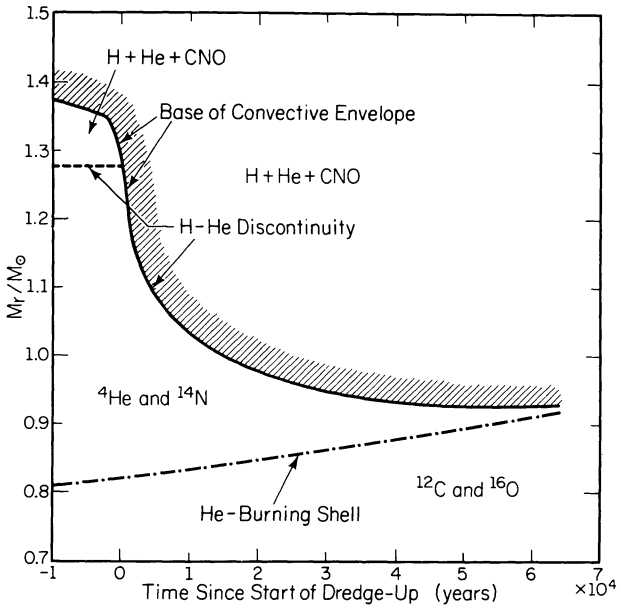

FIG. 4.—Interior composition, position of the helium-burning shell, and position of the base of the convective envelope during the second dredge-up episode in a model of mass 7 $M_\odot$. Adapted from Becker and Iben (1979).

tail in § VIII. Suffice it to say here that (1) hydrogen and helium burn alternately in shells, (2) the ignition of helium is mildly explosive, (3) extensive nucleosynthesis involving the capture of neutrons builds up hundreds of neutron-rich isotopes, and (4) these isotopes, along with carbon, the major product of incomplete helium burning, are brought to the surface in a series of "third dredge-up" episodes. This phase of evolution is sometimes called the thermally pulsing AGB phase.

In theoretical models of constant mass, this phase continues until the mass of the carbon-oxygen core reaches $\sim 1.4\,M_\odot$, the effective Chandrasekhar limit, at which point carbon is ignited in the core (Hoyle and Fowler 1966; Arnett 1969). After a brief episode during which neutrino losses by a generalized Urca process balance the energy generated by carbon burning (Paczyński 1972; Couch and Arnett 1975; Iben 1978*a*, *b*; 1982*a*; Barkat and Wheeler 1990), the rate of carbon burning increases exponentially, creating a burning front that works its way to the surface, converting matter into iron-peak elements and imparting greater than escape velocity to this matter. In short, the core is completely disrupted (Arnett 1969). The kinetic energy associated with the explosion is comparable with the kinetic energy of the matter ejected by a Type Ia supernova. However, the mass of the hydrogen-rich envelope of the model is large enough that the highly processed core material will be diluted with hydrogen to such an extent that hydrogen lines would prominently appear in the spectrum of a real counterpart. Since one of the major defining features of a Type Ia supernova is the absence of hydrogen lines, it is clear that Type Ia supernovae are not the consequence of the evolution of an intermediate-mass star of constant mass.

Could it be that, instead, such stars become Type II supernovae? If one supposes that the rate at which stars are born is given approximately by the Salpeter mass function (Salpeter 1955) normalized to give one new star per year in the Galaxy, then the number of low- and intermediate-mass stars formed with initial mass larger than 1.4 $M_\odot$ is over 20 times the total supernova rate estimated for our Galaxy. Thus, a very firm conclusion is that most real intermediate-mass stars do not evolve to the supernova stage. Their lives must somehow be terminated before the mass of the CO core reaches the explosive stage. Real stars are aware of an instability, not inherent in the simple theory used to construct quasi-static model stars, which causes them to eject their hydrogen-rich envelopes before their CO cores reach explosive conditions. Estimates of the rate at which planetary nebulae are formed in the Galaxy are not inconsistent with estimates of the rate of star formation, and it is tempting to believe that the immediate precursors of planetary nebulae are low- and intermediate-mass stars in the thermally pulsing stage. This topic will be pursued in § IX.

Following the enforced ejection of most of its overlying hydrogen-rich envelope, the remnant core of a model star of initial mass 5 $M_\odot$ evolves rapidly to the blue in the H-R diagram along an essentially horizontal track, as shown in Figure 5. The luminosity of the model is still due to hydrogen burning in a thin shell, but, by the time the surface temperature of the model has increased to $T_e \sim 10{,}000$ K, the total amount of

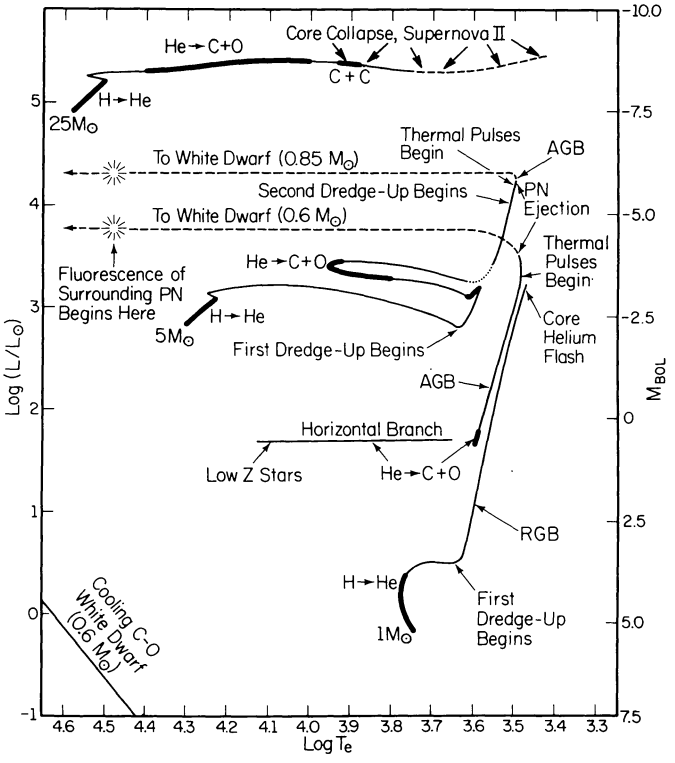

FIG. 5.—Tracks in the H-R diagram of theoretical model stars of low (1 $M_\odot$), intermediate (5 $M_\odot$), and high (25 $M_\odot$) mass. Nuclear burning on a long time scale occurs along the heavy portions of each track. The places where first and second dredge-up episodes occur are indicated, as are the places along the AGB where thermal pulses begin. The third dredge-up process occurs during the thermal pulse phase, and it is here where one may expect the formation of carbon stars and ZrO-rich stars. The luminosity where a given track turns off from the AGB is a conjecture based on comparison with the observations. From Iben (1985).

hydrogen remaining above the shell is such that active nuclear burning can continue for only another ~300 yr. Once T_e exceeds 30,000 K, the ejected material in a real analog can be photoionized by the radiation from the compact remnant, and the system will have taken on the characteristics of a planetary nebula with a hot central star.

The upper and lower mass limits of the category of intermediate-mass stars are uncertain, both limits depending on how far mixing between processed and unprocessed matter extends beyond the formal edge of the convective core during the main-sequence phase (Chiosi and Maeder 1986). Without overshoot beyond this edge, the lower limit for Population I stars is ~2.3 $M_\odot$. With overshoot, it could be as small as 1.5 $M_\odot$ and the comparison with the observation suggest that it may be between 1.6 $M_\odot$ (Eggen and Iben 1988) and 2.1 $M_\odot$ (Weidemann, Jordan, and Iben 1991).

Tracks of representatives of high-mass (25 $M_\odot$) and low-mass (1 $M_\odot$) model stars of Population I composition are also shown in Figure 5. Prior to the core helium-burning phase, the track of the 25 $M_\odot$ model (Lamb, Iben, and Howard 1977) is morphologically equivalent to tracks of intermediate-mass stars: the model evolves to the red and to higher luminosity as hydrogen burns in a shrinking convective core during the main-sequence phase, a characteristic hook to the blue follows the exhaustion of hydrogen at the center, and evolution to the red recommences as hydrogen burns in a shell and the hydrogen-exhausted core contracts and heats. In this instance, however, helium is ignited in central regions before the model reaches the red giant branch, and the model continues to evolve monotonically to the red while helium burns in a growing convective core; hydrogen burning in a shell continues to supply most of the model's luminosity.

Almost immediately following the exhaustion of helium at the center, the core of the model attains high enough temperatures and densities to ignite carbon while electrons are still nondegenerate. Ignition occurs before the model reaches the giant branch. This latter occurrence is, however, a very sensitive function of the detailed input physics chosen to construct the model, reminiscent of the situation with regard to where in the H-R diagram helium is ignited and burns in somewhat less massive stars. A 15.6 $M_\odot$ model star constructed by Hayashi and Cameron (1962) ignites helium as a red star and then returns to the blue, while a model of nearly the same mass (15 $M_\odot$) and composition constructed by Iben (1966*b*) ignites and continues to burn helium as a blue star. In both instances the major phase of core helium burning occurs when the model is a blue star. Similarly, the major portion of the core carbon-burning phase of a 25 $M_\odot$ model is spent far to the blue of the red giant branch, regardless of where in the H-R diagram the model is when carbon is first ignited.

During the carbon-burning phase of the 25 $M_\odot$ model, the helium-exhausted core is effectively isolated from the rest of the model. All of the nuclear energy generated in the core is radiated as neutrinos and antineutrinos, and the sole source of surface luminosity is hydrogen and helium burning in shells above the core. It has been demonstrated that the helium-exhausted core develops in its interior a Chandrasekhar-mass nugget within which all nuclear constituents are near the peak in the binding-energy versus nucleon-mass curve (iron peak nuclei) and that this nugget subsequently collapses to form a neutron star or black hole (Hoyle and Fowler 1960; Fowler and Hoyle 1964; Colgate and White 1966; Arnett 1969; Wilson 1983; Woosley and Weaver 1986) and ejects the mantle above the core by depositing neutrino energy in this mantle (Wilson 1980, 1983); the net result is presumably a Type II supernova explosion which produces an unbound extended remnant and a compact bound remnant (either a neutron star or black hole). It has been argued that, during and after the carbon-burning phase in massive stars, since the helium-exhausted core is effectively decoupled from the rest of the star and since the time scale for evolution following the carbon-burning phase is so short, the position of the precursor star in the H-R diagram at the moment of core collapse is identical with its position near the end of the core carbon-burning phase. If this is the case, then the 25 $M_\odot$ model, if evolved further, should explode as a Type II supernovae at a surface temperature of ~8000 K, far to the blue of the red giant branch.

The precursor of supernova 1987A in the Large Magellanic Cloud is known to have been a blue star ($T_e \sim$ 10,000 K) with a luminosity appropriate to that of a model star of mass ~20 $M_\odot$. At its brightest, it was much dimmer in absolute magnitude than the majority of previously identified Type II supernovae. After the fact, theoreticians were quick to demonstrate that the theory naturally predicts a monotonic relationship between the size of the precursor and the radiant energy emitted in the explosion (see, e.g., Arnett *et al.* 1989). The basic cause for the dependance of maximum optical brightness on precursor size is that (1) the maximum rate of energy emission from the supernova occurs at large radii and (2) more energy is used up in expanding a small star to an appropriately large radius than in expanding an already large star to this same radius. If this is true, then, since there are more stars in the 12–25 $M_\odot$ range than there are in the range greater than 25 $M_\odot$, the rate of formation of neutron stars may be much larger than an estimate of the rate of Type II supernova based on examples in which the radiant energy release is far larger than that of SN 1987A. On the other hand, the abundance of heavy elements in Magellanic Cloud stars is considerably less than in our Galactic disk; all other things being equal, models of lower metallicity are bluer and therefore smaller than models of higher metallicity in the same evolutionary stage (§ IV); hence, typical Type II supernovae in metal-rich aggregates will tend to be optically brighter than those in metal-poor aggregates.

An important consideration that differentiates quasistatic stellar models of constant mass from real massive stars is the fact that real massive stars are known to lose mass at a considerable rate during the main-sequence phase due to a radiatively driven wind (Morton 1967*a, b;* Conti 1978; Morton, Jenkins, and Brooks 1969; Cassinelli 1979; Abbot and Conti 1987). The mass loss rate is roughly correlated directly with luminosity and inversely with surface temperature, but there is considerable dispersion. For stars of sufficiently large initial mass ($M >$ 40–50 $M_\odot$), mass loss may proceed to such an extent that layers which have experienced hydrogen burning are exposed (Massevitch *et al.* 1979; Maeder 1982). It is in this way that N-type Wolf-Rayet stars are believed to be formed. Mass loss during the Wolf-Rayet phase is at an even higher rate than during the main-sequence phase (Barlow and Cohen 1977),

and it is believed that N-type Wolf-Rayet stars evolve into C-type Wolf-Rayet stars once all hydrogen-containing layers are stripped off, exposing regions which have experienced helium burning. Their high space density relative to the space density of main-sequence stars of similar luminosity implies that Wolf-Rayet stars must be evolving on a nuclear-burning time scale, probably burning helium in their cores (Chiosi and Maeder 1986).

Low-mass stars may be defined as stars which, shortly after leaving the main sequence, develop an electron-degenerate core composed of helium. The track in Figure 5 of a model of mass 1 $M_\odot$ and of Population I composition is representative of the class. From the observational point of view, the most striking characteristic of this track relative to the tracks of intermediate-mass stars is the tremendous extent of the red giant branch which it traverses prior to the onset of helium burning. The reason for the difference is simple: the hydrogen-exhausted cores of stars of intermediate mass continue to heat as they contract, and helium burning begins shortly after such stars reach the giant branch in the H-R diagram; the hydrogen-exhausted cores of low-mass stars temporarily cool down as electron degeneracy sets in and energy escapes the core efficiently by electron conduction, thus delaying the onset of helium burning which terminates ascent of the giant branch. As a low-mass model reaches the base of the giant branch, the mean temperature in its helium core reaches a minimum which is close to the temperature of the hydrogen-burning shell. Thereafter, as its mass increases due to the deposition of helium by the hydrogen-burning shell, the core shrinks spatially and temperatures in the hydrogen-burning shell (which is being drawn ever closer to the center) and in the core (in which electron conduction is becoming more efficient) increase. The luminosity increases due to the increase in shell temperatures, and the rate of heating in the core increases due to the increase in the rate of release of gravitational potential energy in the core (this rate is proportional to the rate at which mass is added to the core and, hence, is proportional also to the luminosity).

Ultimately, when the mass of the helium core reaches $\sim$0.45 $M_\odot$ (the precise value depends weakly on the composition, on the model mass, and on the input physics), a helium runaway is initiated in the core (Schwarzschild and Härm 1962), and this runaway continues until electron degeneracy is "lifted." Thanks to neutrino losses which induce a negative temperature gradient in central regions of the core, helium ignition actually occurs off center and the burning progresses inward in a series of "flashes" that take place at successively smaller distances from the center (Thomas 1967; Mengel and Sweigart 1981).

Eventually, the model settles down to experience a period of quiescent core helium burning analogous in every way to that experienced by intermediate-mass stars. The position in the H-R diagram during this phase depends on several factors, a major one being the metallicity and another being the extent of mass loss from the red giant precursor. This second factor cannot be determined from first principles, and one must rely on the observations to provide the necessary information, as discussed further in § V. For now, suffice it to say that, for metal-rich stars, the core helium-burning phase is confined to a very stubby region, or "clump" on the giant branch $\sim$3 mag below the red giant tip, whereas for metal-poor stars evolution covers a much broader range in surface temperature to the blue of the giant branch, leading to the designation "horizontal branch" for this phase of evolution.

The near constancy of luminosity during the core helium-burning phase is a consequence of the convergence of the cores of precursor red giant models of different total mass toward a common electron-degenerate helium core. Since the mass of the helium core at the onset of the quiescent core helium-burning phase is nearly the same for all models, the contribution to the luminosity by helium-burning reactions is also nearly the same for all models. This is true also for the contribution to the luminosity by hydrogen-burning reactions, but to a lesser extent; in models not too far from the giant branch, the hydrogen-burning shell contributes the bulk of the surface luminosity, as in intermediate-mass stars, but for models far to the blue of the giant branch (constructed by considerably reducing the mass of the hydrogen-rich envelope), the hydrogen-burning luminosity can be considerably less. Thus, the theoretical horizontal branch actually "droops" in going from red to blue. The duration of the core helium-burning phase is determined only by the rate of helium burning and is therefore nearly constant at $\tau_{\rm He} \sim 10^8$ yr. This is another contrast with intermediate-mass stars for which $\tau_{\rm He} \sim \tau_{\rm H}/4$, where $\tau_{\rm H}$ is the main-sequence lifetime. The mass in the hydrogen-exhausted core at the end of the horizontal-branch phase is typically $\sim$0.5 $M_\odot$, $\sim$0.05 $M_\odot$ larger than at the onset of the phase.

Following the exhaustion of central helium, a low-mass model adopts a structure similar to that achieved by intermediate-mass stars: an electron-degenerate CO core, a helium-burning shell, and a hydrogen-rich envelope in which hydrogen does not burn strongly, even at its base. As the CO core grows, the model evolves in the H-R diagram along a track which is very close to that followed by models possessing an electron-degenerate helium core and a hydrogen-burning shell. This similarity has led to the designation "asymptotic giant branch" or AGB, a term which is now applied to intermediate-mass stars with an electron-degenerate CO core, even though the term is not warranted by position in the H-R diagram. The AGB may be broken into two parts, the early-AGB or EAGB, which lasts until hydrogen is reignited for the first time, and the thermally pulsing AGB or TPAGB, which lasts until most of the hydrogen-rich envelope is lost via a normal giant wind (low-mass progenitors) or via a superwind (intermediate-mass progenitors).

For a low-mass model, the duration of the EAGB phase is of the order of 10^7 yr, versus $\sim 10^8$ yr for the duration of the first red giant branch phase of its precursor. How long the TPAGB phase lasts depends, at present, on information that can only be given by the observations. In Galactic globular clusters, where the most massive stars in the main-sequence phase are of mass $\sim$0.8 $M_\odot$, it appears that the AGB does not extend beyond the tip of the first red giant branch, showing that very low mass metal-poor stars may not even reach the TPAGB phase. Instead, they appear to lose (presumably by an ordinary stellar wind) all but a very low mass layer of hydrogen-rich material and become white dwarfs of mass essentially equal to the mass of the hydrogen-exhausted core of their horizontal-branch precursor, namely, $\sim$0.5 $M_\odot$. It is interesting to note

that this mass agrees with estimates of the masses of W Virginis stars that are obtained by making use of observed pulsational properties in conjunction with results of pulsation theory (Böhm-Vitense *et al.* 1974; see § VI). W Vir stars are very few in number (only ~15 in all 200 Galactic globular clusters) and must therefore be crossing the instability strip on a time scale of only a few times 10^4 yr. A more direct check on the terminal mass along the AGB in globular clusters would be to compare the properties of member white dwarfs in these clusters with theoretical white dwarf models. Such a check would become possible if the Hubble space telescope were to operate at full potential.

In somewhat younger disk aggregates such as the HR 1614 group (Eggen 1989), the luminosity of the brightest AGB stars is $\sim 10^4\ L_\odot$, which suggests that the mass of the CO core at the termination of the AGB is $\sim 0.65\ M_\odot$ (§§ III and VIII describe how this estimate can be made). Thus, Population I stars of initial mass $\sim 1.4\ M_\odot$ increase the mass of their CO cores by $\sim 0.15\ M_\odot$ while on the TPAGB and, in the course of giant branch and AGB evolution, return about half of their initial mass to the interstellar medium. The matter returned during the AGB phase is probably enriched in carbon and neutron-rich *s*-process elements (§ VIII).

Additional information comes from the number-mass distribution of nearby white dwarfs. Since the peak in this distribution is at a mass of ~0.55–0.6 $M_\odot$ (Koester, Schulz, and Weidemann 1979; Weidemann and Koester 1984; Weidemann 1990), typical low-mass stars in the solar vicinity reach the TPAGB and increase the mass of their CO cores by ~0.05–0.1 $M_\odot$ while in this phase. Further, since the dominant contributors to the observed white dwarf population in the solar vicinity are stars of $\sim 1\ M_\odot$ and slightly larger, we know that such stars also lose about half of their initial mass in the course of their nuclear-burning evolution.

The discussion thus far has highlighted motion in the H-R diagram, with the connection between location in the diagram and the internal constitution being made for the most part in a very qualitative fashion. To partially remedy this neglect of a beautiful part of the theory, the evolution of the thermodynamic state of matter at the centers of stellar models of various models is presented in Figure 6. The figure caption describes all features of this diagram which are not described in the text or in the figure itself.

In the H-R diagram of Figure 7, details of individual tracks are suppressed, and the hatched regions show schematically where members of a very large ensemble of stars of Population I composition and of all different masses would reside most of the time. The similarity with the distribution of stars in Figure 1 is striking. Within the instability strip in Figure 7 (§ VI), stars are unstable to periodic radial pulsation in the fundamental mode or in the first harmonic mode or both. Intersections between the instability strip and the shaded bands should correspond to locations of well-represented classes of variable stars. Indeed, at the intersection between the instability strip and the core helium-burning band defined by models of intermediate mass are the Cepheids; at the intersection between the instability strip and the core helium-burning band defined by low-mass models which have lost mass are the RR Lyrae variables; the intersection between the instability strip and the main sequence is where δ Scuti and Ap variables are found; and, finally, the intersection between the instability strip and the white dwarf cooling band is where the ZZ Ceti variables are found.

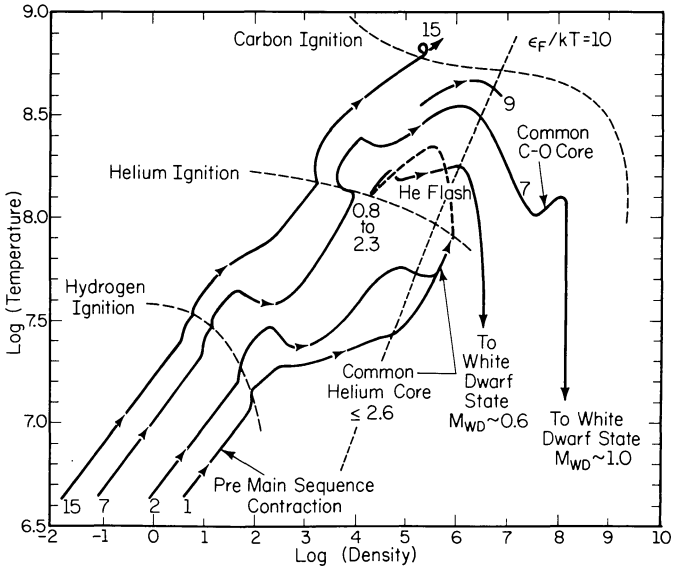

FIG. 6.—Evolutionary tracks of theoretical models in the density-temperature plane. Coordinates are the logarithms (base 10) of density ρ (g cm^{-3}) and of temperature $T(10^6\text{K})$ and each track describes the behavior of matter at the center of the relevant model of mass given in solar units at the low T, low ρ terminus of each track. Dashed lines with curvature indicate where fuels of three different types are ignited, and the relevant fuel is indicated at the leftmost end of each curve. Along the dashed straight line labeled $\epsilon_F/kT = 10$, the electron Fermi energy is 10 times kT, where k is Boltzmann's constant. Low-mass stars develop an electron-degenerate core composed of helium before igniting helium at their centers and, after experiencing a thermonuclear runaway, evolve to a lower central density near the helium ignition curve. Low- and intermediate-mass stars develop electron degenerate cores composed of carbon and oxygen and do not reach the carbon ignition curve before ejecting most of their hydrogen-rich envelopes. The places in the ρ-T diagram where this is indicated to occur are conjectures based on comparison with the observations. From Iben (1973 *a*; 1974).

III. BINARY STAR EVOLUTION: THEORETICAL CONCEPTS AND OBSERVATIONAL PARADIGMS

The theory of close binary star evolution has a much different character than does the theory of single star evolution. Interior models of single stars can in most instances realistically be assumed to be spherically symmetric. Further, quasi-static models suffice to describe evolution during most phases, with hydrodynamical situations appearing only as terminal one-dimensional implosions and explosions (as in supernova events) or as regular limit cycle oscillations (as in the case of classical radial pulsators). In the case of close binary stars, which may be defined as stars that interact by mass exchange at some point in their evolution, the situation is fully three-dimensional. Tidal interactions can cause significant distortions from spherical symmetry and can lead to rapid rotation for one or both components; the resultant meridional currents may not be regarded as mere perturbations as is the case for most single stars, and tidal heating may be very important. When

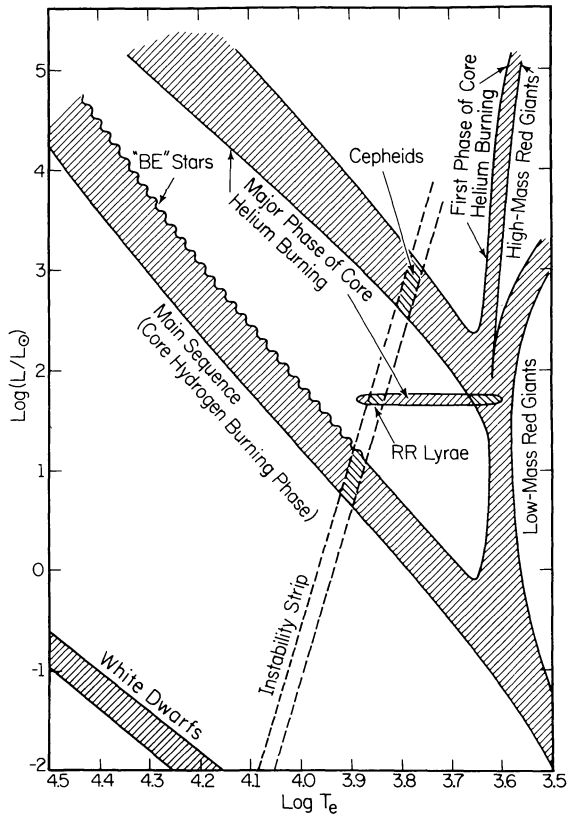

FIG. 7.—Distribution in the H-R diagram of a large ensemble of model stars. The shaded regions describe where in the H-R diagram model stars of Population I composition are to be found during the core hydrogen-burning and core helium-burning phases. The oval "horizontal" branch at $\log L \sim 1.7$ contains stars that are conjectured to have lost mass via a stellar wind during a prior sojourn on the giant branch. An instability strip, the blue edge of which is derived with the help of linear pulsation theory, marks where stars are expected to be unstable to pulsation in the fundamental and/or first harmonic radial modes. Adapted from Iben (1967*c*, *d*, 1985).

mass transfer occurs, physical processes such as turbulent viscosity and meteorological phenomena such as electrodynamical storms enter the picture in ways for which we have not developed even rudimentary quantitative descriptions.

Because of this, there are no beautiful sequences of mathematically impeccable binary star models to which one can point with pride and compare successfully with the observations. Instead, a body of broad concepts, precepts, and algorithms has emerged and has been used to construct qualitative scenarios to describe how close binary systems may evolve through various phases of interaction. Absolutely crucial in this development has been the existence of observational paradigms—highly evolved systems which quite clearly must have passed through a phase (or phases) of strong interaction in the past as well as systems which quite clearly must interact in the future. The paradigms may sometimes be ordered in ways which are consistent with the scenarios. Sometimes, in order to achieve consistency with the properties of the paradigms, adjustments must be made in the choice of the principles and algorithms which are invoked to construct the scenarios. And sometimes, of course, a combination of both exercises is necessary.

a) Roche Lobes

The first basic concept in the theory is that of Roche lobes. Assuming that each component of a binary is a point mass and moves in a circular orbit, one may write down the force on a test particle in a coordinate system rotating with the orbital frequency. The effective force on a particle *at rest* in the rotating coordinate system is a combination of the gravitational force exerted by the two binary components and the "centrifugal" force; this effective force is derivable from a potential. Among all possible surfaces of constant potential, there is one unique surface that consists of two separate parts, or lobes, each lobe completely enclosing one of the components (Roche 1849*a*, *b*, 1851, 1873; Kopal 1978). The two lobes touch at a single point along a line joining the centers of the binary components (see Fig. 8) and each lobe is called a Roche lobe.

The most relevant property of a Roche lobe is that a particle within it experiences a force in the direction of the enclosed component. Thus, if a real star were to slightly overfill its Roche lobe for one reason or another, at least some of the matter in the periphery of this star would begin to fall onto the other component. A basic assumption or principle of the theory is that *all* of the matter extending beyond the Roche-lobe filling star will eventually strike the companion (usually first striking an accretion disk and passing through this disk onto the companion).

Although Roche lobes are clearly not spherical, one may define a "Roche-lobe radius" R_L which is the radius of a sphere having the same volume as the lobe. This radius is related to the orbital separation and, for purposes of making simple comparisons with stellar model radii, the relationship (Iben and Tutukov 1984*a*)

$$R_{iL} \sim 0.52(M_i/M_{\rm tot})^{0.44}A \qquad (1)$$

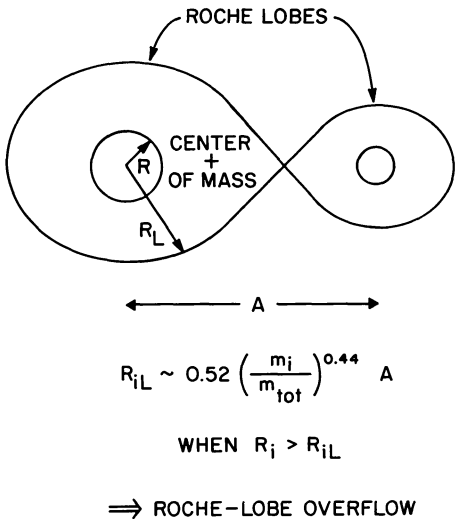

FIG. 8.—A schematic illustrating the Roche-lobe geometry. Shown is a cross section of the unique surface of constant potential which consists of two "lobes" which make contact at single point along the line joining the centers of the two binary components. Here, A is the separation between the centers of the two components, R is the radius of either component, and R_L is the radius of a sphere having the same volume as the Roche lobe about that component.

suffices. Here, R_{iL} is the Roche-lobe radius of the ith component, M_i is its mass, and M_{tot} is the sum of the masses of the components.

There are at least four ways of achieving Roche-lobe overflow. One is occasioned by the growth of either component due to evolutionary changes in its interior. Another is occasioned by orbital shrinkage due to the loss of orbital angular momentum via a magnetic stellar wind or via gravitational wave radiation, and a third is occasioned by swelling due to rejection of accreted matter or due to ignition of a nuclear fuel at the base of an accreted layer. A fourth way, which can occur in a dense cluster of stars, is due to a hardening collision between the binary and another star in the cluster.

b) Remnant Masses and Compositions

The outcome of a mass-transfer episode depends on the evolutionary status of both the donor and the potential accretor. The second major assumption or principle of close binary star theory, supported by numerical experiments in which mass is abstracted from evolved models, is that the remnant of a donor will have a composition and mass similar to that of the compact core of the donor when it first fills its Roche lobe. It is therefore important to be familiar with the relationship between the radius of a component (whose structure is assumed to be similar to that of a single star of the same mass and radius) and the mass and composition of the compact core. The radii of model single stars of Population I composition in various stages of evolution are shown as a function of model mass in Figure 9 (Iben and Tutukov 1985). The distinction between models of low and intermediate mass is made somewhat arbitrarily at 2.3 $M_\odot$. The positions of all borders at large radius are sensitive to the treatment of convection. The terminal radius of an AGB star relative to the border defining the onset of the TPAGB phase is particularly uncertain—the borders shown in Figure 9 are based on the assumption that the duration of the TPAGB phase is between $\sim 10^6$ yr (low-mass stars) and 10^5 yr (stars with CO core mass larger than $\sim 0.8\ M_\odot$).

The larger a star is during its main-sequence phase (the lower stippled region in Fig. 9), the more massive is the helium-rich core which it develops. On leaving the main sequence (the hatched region to the left in Fig. 9), a low-mass star develops a growing electron-degenerate helium core. The mass of this core is related to the model radius by (Iben & Tutukov 1984*a*, as normalized to the observations by Eggen and Iben 1990)

$$R \sim 10^{3.38} M_{\rm He}^4 . \qquad (2)$$

On leaving the main sequence (the clear region between the two stippled regions in Fig. 9), a model of intermediate mass possesses a non–electron-degenerate, but compact helium core; the mass of this core is related to the model mass approximately by (Iben and Tutukov 1985)

$$M_{\rm He} \sim 0.08\ M^{1.4} . \qquad (3)$$

Finally, once a model exhausts central helium and becomes a TPAGB star (clear region near the top of Fig. 9), the mass M_{CO} of its electron-degenerate carbon-oxygen core is related (during the quiescent hydrogen burning phase) to model luminosity approximately by (Uus 1970; Paczyński 1970)

$$L \sim 6 \times 10^4\ (M_{\rm CO} - 0.5) \qquad (4)$$

and model radius is related to core mass by (Iben 1984, as normalized to the observations by Eggen and Iben 1990)

$$R \sim 10^{3.14}\ (M_{\rm CO} - 0.5)^{0.68}\ (M/1.175)^{-0.315} , \qquad (5)$$

where $S = 0$ if stellar mass $M < 1.175$ and $S = 1$ if $M > 1.175$. In relationships (2)–(5), R, L, and M are in solar units.

Many numerical experiments have been performed to estimate the mass of the compact remnant which remains after a Roche-lobe filling event has been completed. The results depend somewhat on the assumptions made as to how rapidly mass loss occurs, as described in the next two subsections, but the dependence is not great and therefore expressions (1)–(5) lead to useful first approximations. Refinements require extensive computation (§ XI). The curve labeled close binaries in Figure 10 shows the results of experiments in which mass is abstracted at a rapid rate from intermediate-mass (2–10 $M_\odot$) model stars of Population I composition which possess deep convective envelopes and are about to ignite helium at their centers (Iben and Tutukov 1985). The net result is a white dwarf composed predominantly of carbon and oxygen. If the model possesses an electron-degenerate helium core when it first fills its Roche lobe, the end result of mass loss is a helium

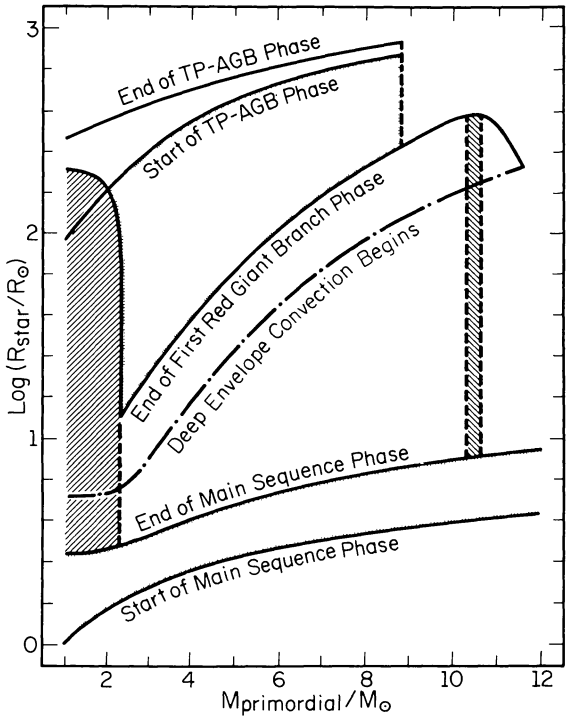

FIG. 9.—Radium vs. mass of models of single stars of Population I composition at various (labeled) stages in their evolution. For low-mass stars, the end of the first red giant branch phase occurs along the upper boundary of the hatched region at the left of the diagram. From Iben and Tutukov (1985).

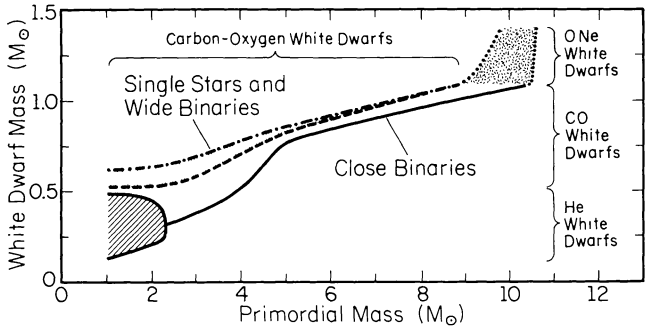

FIG. 10.—Mass and interior composition of a white dwarf remnant as a function of initial progenitor mass for single stars and binary star components after a case B mass Roche-lobe overflow event. A late case C Roche-lobe overflow event in an initially wide binary produces a remnant of mass similar to that of a single star.

white dwarf whose mass lies within the hatched region to the lower left of the figure. When model stars of initial mass in the 9–11 $M_\odot$ range experience mass loss just before helium is ignited, the net result is a white dwarf composed predominantly of oxygen and neon. The stippled region in the upper right portion of Figure 10 defines possible remnant masses.

In the notation introduced by the Kippenhahn group (Kippenhahn and Weigert 1967; Lauterborn 1970), mass-loss events in which a star fills its Roche lobe after having exhausted hydrogen at the center but before igniting helium are called "case B" events and the events which lead to the curve labeled close binaries in Figure 10 could be called late case B events. Shown also in Figure 10 are the estimated masses of remnants of single stars (*upper dash-dotted curve*) and the estimated masses of models which fill their Roche lobes after having developed an electron-degenerate CO core and lose mass in late case C events (*stippled region between dash-dotted and dashed curves*). The curve for single stars is based on the assumption that the TPAGB lifetime of a real star varies from $\sim 10^6$ yr at small core mass to $\sim 10^5$ yr when $M_{CO} > 0.80\ M_\odot$. Note that the range of white dwarf progenitor masses is larger for stars in close binaries than for single stars.

c) Mass Transfer Rates and the Mass-Conservative Assumption

Rough analytical and numerical estimates have been made of the rate at which a component will lose mass after it fills its Roche lobe for the first time; the estimated rate is a function of (1) the structure of the component at the moment of Roche-lobe filling, (2) the degree to which orbital angular momentum and system mass are assumed to be conserved during mass transfer, and (3) the supposed response of the companion to mass accretion. If the donor does not possess a deep convective envelope, and if it is assumed that both the orbital angular momentum and the total mass of the system remain constant, the mass donor initially loses mass at a rate given roughly by $dM/dt \sim -M/\tau_{th}$, where $\tau_{th} \sim GM^2/RL$ is defined as the thermal time scale of the donor, M is the initial mass of the donor, and R and L are its radius and luminosity, respectively (Paczyński 1971*b*). Mass loss at this rate continues at least until the initial mass ratio has been reversed; that is, until $M_1'/M_2' \sim M_2/M_1$, where M_2 and M_1 are the initial masses of the two components and M_2' and M_1' are the masses of the components at the end of the phase of rapid mass transfer. Mass loss proceeds at a high rate because, under the given assumptions of total orbital angular momentum and mass conservation, the Roche-lobe radius of the donor remains smaller than its value at the moment of initial Roche-lobe contact until this condition is met.

After mass reversal has been achieved, if the helium core of the donor was already electron-degenerate when Roche-lobe filling first occurred or if this core became electron-degenerate in consequence of mass loss, equality between Roche-lobe radius and stellar model radius can be maintained by a rate of mass loss which is much more modest than on the thermal time scale. The donor is now a low-mass subgiant, even though it may have initially been an intermediate-mass star, and the accretor has become a main-sequence star which can be brighter than its subgiant companion. The precursors of Algol binaries have followed some approximation to this evolutionary path, although some system mass and orbital angular momentum have undoubtedly been lost in real cases.

The current rate of mass transfer in Algol binaries is determined by a competition between (1) the rate at which the radius of the subgiant donor can increase in response to the increase in the mass of its helium-exhausted core and (2) the rate at which a magnetic stellar wind can abstract orbital angular momentum from the system (§ III*e*). Mass-transfer rates of the order of 10^{-9}–$10^{-7}\ M_\odot\ \mathrm{yr}^{-1}$ are estimated. If the mass-loss time scale is shorter than the main-sequence lifetime of the accretor and short compared with the time scale for the growth of the helium core of the subdwarf, the end result of the Algol phase of evolution will be a somewhat evolved main-sequence star and a helium white dwarf of mass not much larger than the mass of the helium core of the donor at the onset of the mass-transfer episode. In the typical Algol system, and indeed in the case of Algol itself, the mass of the helium core of the subgiant donor is of the order of $M_{He} \sim 0.2\ M_\odot$. The absence of Algol systems with M_{He} much larger than this is due to the fact that the mass-transfer rate does not abate when mass reversal occurs if the donor has developed a deep convective envelope before it fills its Roche lobe (§ III*d*).

If it is initially an intermediate-mass or a massive star and if it is already evolving toward the giant branch on a thermal time scale when it first fills its Roche lobe, the donor will continue to overfill its Roche lobe until the mass of its hydrogen-rich envelope decreases below a critical mass which is typically $\sim 0.01\ M_\odot$ or less. This is particularly true of model stars which have developed a deep convective envelope by the time they first fill their Roche lobes (late case B events). Once the mass of the hydrogen-rich envelope of the donor decreases below the critical value, the model contracts within its Roche lobe and evolves into a helium star—a compact object which is composed initially of nearly pure helium (capped by a thin, inactive hydrogen-rich envelope) and which is initially burning helium at the base of a convective core. The location of model helium stars in the H-R diagram is approximately midway between the main sequence and the region of white dwarfs; real analogs of such models are the subdwarf O and B stars. The mass of the helium star formed in this way is close to the mass of the compact core of the donor when it first fills its Roche

lobe, thus demonstrating the validity of the second basic tenet of the theory.

It is usually assumed that, in early case B events (those for which the donor does not have a deep convective envelope), when mass transfer proceeds on the thermal time scale of the donor or longer, the total mass of the binary system is conserved if the accretor is a main-sequence star of mass similar to that of the donor at the onset of mass transfer. This may be called the third major principle of the theory of close binary star evolution. The justification for assuming mass conservation is that, when components are of similar mass and similar size (which will be the case when the Roche-lobe filling component has not proceeded too far toward the giant branch), the thermal time scales of both components are also similar and so the secondary can adjust its structure in response to the addition of matter without expanding beyond its Roche lobe.

The extent to which orbital angular momentum is conserved is an important consideration which has as yet not been satisfactorily resolved. The assumption of exact conservation certainly presents a well-defined problem leading to relatively unique solutions and, therefore, many such solutions appear in the literature. The orbital separation at the end of the completely conservative mass-transfer episode is larger than at the beginning by an amount given by

$$A_f = A_0(M_1/M_{1R})^2[M_2/(M_{tot} - M_{1R})]^2 , \qquad (6)$$

where M_1 and M_2 are the initial masses of the components, M_{1R} is the mass of the remnant of the primary, $M_{tot} = M_1 + M_2$, and A_0 and A_f are the initial and final orbital separations, respectively. What this means is that the second star, which is now more massive than the primordial primary, must evolve to a larger radius before filling its Roche lobe than did the initial primary. The second star, of mass $M_2' = M_{tot} - M_{1R} > M_1$, will develop a more massive helium core before filling its Roche lobe than did the first, so that the second remnant to be formed will be more massive than the first.

d) Common Envelope Concept and Orbital Shrinkage

Models that evolve beyond the base of the giant branch possess deep convective envelopes (see Fig. 9). Such models expand in response to mass loss (see, e.g., expression [5]), provided the mass-loss rate is not too great. This behavior forces mass transfer in model systems to occur on a time scale intermediate between the thermal time scale and the dynamical time scale (Paczyński 1971*b*). For assumed mass-loss rates larger than a critical value, even a model with a deep convective envelope will shrink in response to mass loss (Iben and Tutukov 1985; Iben 1986). Thus, there is a self-regulating mechanism which prevents runaway mass transfer and in fact permits one to estimate an upper limit to the transfer rate expected in real systems and this is accomplished by adjusting the adopted mass-loss rate in such a way that model radius remains constant. For intermediate-mass models in late case B events, one finds $dM/dt \sim 10^{-4}$–$10^{-2} M_\odot$ yr^{-1}, corresponding to a mass-transfer time scale of the order of 100–10,000 yr.

A typical companion of a low- or intermediate-mass star which undergoes a case C or late case B mass-loss event will be a low-mass main-sequence star or a white dwarf. The time scale for mass transfer is much shorter than the thermal response time scale of a small main-sequence star, and is much, much shorter than the thermal response time scale of a typical white dwarf. This means that the matter which is transferred (initially through a disk) onto a low-mass main-sequence or white dwarf companion must form a hot layer which expands as its mass increases. In the case of a white dwarf companion, once the accreted layer becomes massive enough ($\sim 0.001\ M_\odot$ for a white dwarf of mass $\sim 0.6\ M_\odot$), hydrogen is ignited within the accreted layer (Nomoto, Nariai, and Sugimoto 1979) and the companion swells rapidly to achieve red giant proportions. In either case, the companion will quickly fill its Roche lobe, and the situation can no longer be described as one in which matter is being transferred from one star to the other.

The picture that has evolved to describe what may now occur is the fourth grand concept of the theory of binary star evolution: the formation of a common envelope (see Fig. 11). It is envisioned that, once both Roche lobes are filled, additional matter from the primary donor spills beyond both lobes into an expanding "common envelope" and that a frictional interaction between the matter in the common envelope and the imbedded stellar cores (the compact core of the primary donor and the white dwarf or main-sequence companion) provides energy which ultimately drives the matter in the common envelope from the system. These same frictional forces exert a torque on the imbedded stellar cores, forcing them to spiral toward each other. When most of the hydrogen-rich matter which was once in the envelope of the mass donor has entered the common envelope and escaped from the system, the compact remnant of the primary and its companion are in a more tightly bound orbit than before (Paczyński 1976; Meyer and Meyer-Hofmeister 1979).

Motivation for the invention and elaboration of this concept is the existence of observational paradigms which share the property that the current separation between components, one of which is typically a degenerate star (white dwarf or neutron star), is much smaller than the radius of a single star which could have been the immediate precursor of the degenerate star. The example chosen by Paczyński (1976) in his classic paper introducing the concept of a common envelope is V471

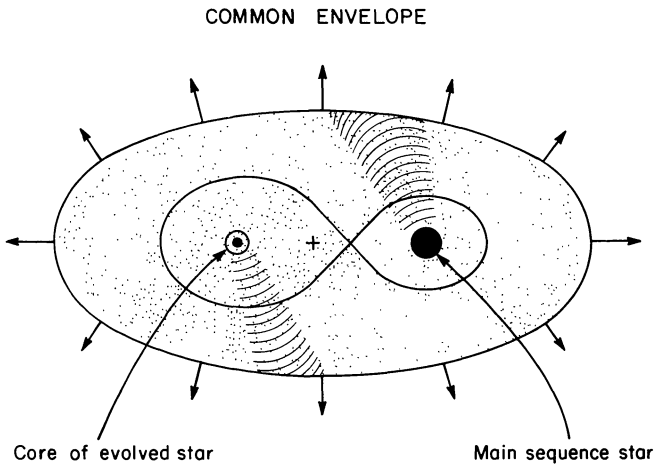

FIG. 11.—Schematic showing a conjectured common envelope event

Tau. One of the components of V471 Tau is a white dwarf, and the other is a red star near the main sequence, but perhaps ~0.6 mag. above the main sequence (Eggen and Iben 1988). The components are of comparable mass, ~0.7 $M_\odot$, and the separation between components is ~3 $R_\odot$, ~5 times the radius of the red star, which underfills its Roche lobe (of radius $R_L \sim 1\ R_\odot$) by a factor of ~2. In order to produce a white dwarf of mass ~0.7 $M_\odot$, a precursor must have a mass of the order of 3.5 $M_\odot$ (if it experiences a case C event) or 4.5 $M_\odot$ (if it experiences a case B event) and it must have acquired a radius larger than its terminal main-sequence radius of ~4 $R_\odot$ before filling its Roche lobe. Consequently, the progenitor system must have been characterized by an orbital separation at least as large as ~10 $R_\odot$. The fact that the red star is only of mass 0.7 $M_\odot$ even though the progenitor of its white dwarf companion must have had a mass near 4 $M_\odot$ means that most of the mass lost by the white dwarf precursor was also lost from the binary system, implying that the mass-loss event was of the case C or late case B variety. The inescapable conclusion is that the precursor of the white dwarf was a giant with a deep convective envelope and a radius in the range 30–400 $R_\odot$. This means that some agency caused the orbital separation to shrink by one to two orders of magnitude.

Consideration of the energetics of the common envelope scenario permits one to estimate the degree of orbital shrinkage one might expect as a function of binary parameters (Tutukov and Yungelson 1979). The quantity $E_{\rm expel} = GM_{\rm lost}\langle M_{\rm system}\rangle/A_0$ is a measure of the energy needed to expel common envelope material and the quantity $E_{\rm orbit} = GM_{1R}M_2/2A_f$ is a measure of the change in orbital binding energy (assuming that the initial orbital binding energy is small compared with the final orbital binding energy). In these expressions, $M_{\rm lost}$ is the mass from the system, $\langle M_{\rm system}\rangle$ is the time average of the mass remaining in the system during the common envelope phase, A_0 is the initial semimajor axis of the system, M_{1R} is the mass of the remnant of the primary, M_2 is the mass of the secondary, and A_f is the semimajor axis of the system following the common envelope event. If the initial mass M_1 of the primary is much larger than both M_2 and M_{1R}, $M_{\rm lost} = M_1 - M_{1R} \sim M_1$ and $\langle M_{\rm system}\rangle \sim (M_1 + M_{1R} + 2\times M_2)/2 \sim M_1/2$. Setting $E_{\rm expel} = \alpha\, E_{\rm orbit}$, it follows that

$$A_f \sim \alpha A_0 M_{1R} M_2 / M_1^2 . \qquad (7)$$

Here, α may be called a parameter of ignorance which may be taken to be ~1 in the absence of any further inquiry. Expression (7) may be used to learn more about observational paradigms. For example, setting $\alpha = 1$, $M_1 \sim 4\ M_\odot$, $M_{1R} \sim M_2 \sim 0.7\ M_\odot$, expression (7) yields $A_f \sim A_0/33$, suggesting that the progenitor of the white dwarf in V471 Tau filled its Roche lobe as an EAGB star with a radius of ~50 $R_\odot$.

One may also adopt the point of view that α is a parameter which can be estimated from properties of observational paradigms, thereby learning something about the physics of the common envelope event. Assuming that the radius of the progenitor of V471 Tau was between 30 $R_\odot$ and 400 $R_\odot$, as estimated from earlier considerations, one infers that $0.12 < \alpha < 1.65$. A value of $\alpha \ll 1$ means that much more orbital energy was expended in raising the kinetic energy of matter in the common envelope (in the form of heat or in the form of directed motion, or both) than in expelling this matter. The existence of planetary nebulae containing close binary stars (e.g., UU Sge in Abell 63 [Bond 1976] and MT Ser in Abel 41 [Grauer and Bond 1984]), demonstrates that the common envelope evolves into a planetary nebula when the compact remnant of the mass donor has contracted sufficiently for its surface temperature to exceed $T_e \sim 30{,}000$ K. The kinetic energy $E_{\rm kin}$ in the expanding nebula is related to the energy $E_{\rm expel}$ by $E_{\rm kin}/E_{\rm expel} \sim 10^{-3}\,(A_0/{\rm M}_1)(v/15\ {\rm km\ s^{-1}})^2$, where v is the expansion velocity of the nebula, and A_0 and M_1 are in solar units. Given that typical expansion velocities are of the order of 15 km s^{-1}, and $A_0/M_1 \sim 10$–100, it would appear that expansion kinetic energy is not an important energy sink. On the other hand, several two-dimensional simulations of a white dwarf spiraling inward through a red giant envelope have been conducted (Livio and Soker 1988; Taam and Bodenheimer 1989) and these suggest significant heat losses, leading to values of $\alpha \sim 0.3$–0.6. Clearly, both interpretations of the meaning of α are useful in learning about common-envelope evolution.

e) *Additional Modes of Orbital Angular Momentum Loss*

A fifth important precept of the theory of close binary star evolution is that orbital angular momentum can be abstracted from very close systems by mechanisms other than common envelope action and that such angular momentum loss can play a crucial role either by driving one component of the system closer to Roche-lobe contact or by maintaining this component in Roche-lobe contact after contact has first been achieved. Mechanisms that have been identified include (1) a magnetic stellar wind (MSW); (2) gravitational wave radiation (GWR); (3) tidal torques and tidal dissipation; and (4) three-body gravitational interactions.

The system V471 Tau is an example in what must be a continuum of possible outcomes of the common envelope evolution of an initial pair of main-sequence stars of disparate mass. Cataclysmic variables (CVs), which consist typically of a fairly massive white dwarf and a much less massive (almost or actually) Roche-lobe filling main-sequence star, are additional examples (Patterson 1984). One might guess that, all other things being equal, immediately following the common-envelope episode, the separation between components is monotonically related to the separation of the components prior to this episode. Thus, there may be some cases in which the main-sequence star overfills its Roche lobe and itself begins to contribute matter to the common envelope even before its companion has ceased to contribute; the likely outcome in such cases is that the main-sequence star dissolves into the envelope of what becomes a single red giant star (Webbink 1976). Such systems are evidently not precursors of CVs.

On the other hand, there must be many cases in which the main-sequence star does not fill its Roche lobe on emerging from the common envelope. Further, the probability that the main-sequence star precisely fills its Roche lobe immediately after the common envelope event must be very small. How, then, is contact achieved before the less evolved component exhausts central hydrogen and begins to expand? This conundrum is also raised during the CV phase of evolution. The fact that many CVs are identified after they have experienced a

nova outburst, coupled with the theoretical interpretation of nova oubursts as the consequence of the accumulation of a critical mass of hydrogen-rich material by a white dwarf (Gallagher and Starrfield 1978), makes it clear that the main-sequence component of a CV has transferred matter to the white dwarf component prior to the identifying outburst, and the statistics of CV and nova frequency show that a typical CV must undergo many outbursts in its lifetime. Yet, mass loss should force the main-sequence star to shrink and remain permanently detached from its Roche lobe. The inference is that there is some agency which abstracts angular momentum from the orbit in such a way as to maintain the shrinking component in contact with its Roche lobe for some period of time between outbursts.

It is reasonable to suppose that this same agency can also abstract orbital angular momentum from white dwarf, main-sequence star systems such as V471 Tau even when the main-sequence component is far from filling its Roche lobe. The key to the mechanism resides in several features which CVs and systems such as V471 Tau are thought to have in common in addition to having similar components: the main-sequence companion (1) has a surface temperature small enough to ensure that turbulent convective motions prevail over a substantial region inward from the photosphere, (2) exhibits a high degree of magnetic activity, and (3) is spinning about its own axis in synchronism with the orbital period. The first two features plus the property of spinning are shared with the Sun and with stars later than type F5 in young clusters such as the Hyades and Pleiades. The spin rate and the magnetic activity of late-type Pleiades stars (age $\sim 10^8$ yr), late-type Hyades stars (age $\sim 10^9$ yr) and the Sun (age = 4.6×10^9 yr) are correlated (Kraft 1967) and decline as roughly the inverse square root of the age (Skumanich 1972). The Sun is known to lose mass at a modest rate ($<10^{-14}\ M_\odot\ \mathrm{yr}^{-1}$, Hundhausen 1972) and an analysis of the coupling between the outward stream of ionized particles and the Sun's known dipolar field shows that the Sun is currently losing spin angular momentum on a 5×10^9 yr time scale (Weber and Davis 1967). Thus, the empirical data and the theory together demonstrate that stars of the type under discussion lose spin angular momentum via a "magnetic stellar wind" at a rate which is correlated with the spin rate.

The rapidly spinning, magnetically active main-sequence components in very close binaries must also be losing spin angular momentum via a MSW. However, the fact that in these very close systems the spin rate is very near the orbital rotation rate means that tidal torques continuously restore the angular momentum lost via the MSW. Since the ultimate source of the lost angular momentum is orbital angular momentum, the orbital separation must decrease (e.g., Verbunt and Zwaan 1981). The basic elements in the MSW–tidal torque (MSW for short) mechanism for angular momentum loss are shown schematically in the top panel of Figure 12.

The manner in which a system such as V471 Tau can evolve into a CV is now clear. Because of a MSW, the orbital separation of V471 Tau will decrease at a steadily accelerating rate (the spin rate of the main-sequence component increases with decreasing separation, causing an increase in the strength of the MSW) until the main-sequence component fills its Roche lobe and mass transfer begins. Once $\sim 10^{-5}\ M_\odot$ has been transferred, a nova explosion will occur, and, thereafter, the system will behave as a CV.

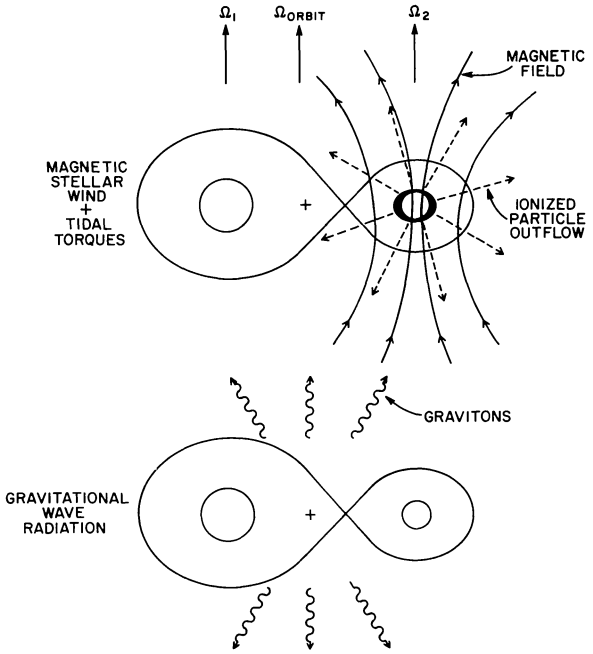

FIG. 12.—Schematic describing two modes of angular momentum loss: due to a magnetic stellar wind and tidal torques (MSW), and due to gravitational wave radiation (GWR).

A MSW is important in many other contexts. For example, an RS CVn star such as UX Ari (Huenemoerder, Buzasi, and Ramsey 1989), which consists of a main-sequence star and a more massive subgiant that is magnetically active and is a rapid rotator but does not fill its Roche lobe, would become an Algol in any case as the radius of the subgiant component grows in response to a growing electron-degenerate helium core; but it will evolve more quickly into the Algol configuration thanks to angular momentum loss due to a MSW. After the subgiant has filled its Roche lobe and the system has experienced the phase of rapid mass transfer which reverses the mass ratio, the subgiant will continue to fill its Roche lobe and transfer mass on a time scale intermediate between the time scale for angular momentum loss by a MSW and the time scale for the growth of the electron-degenerate helium core of the subgiant (Iben and Tutukov 1984c).

A MSW is also exceedingly important in the evolution of W UMa stars. These are low-mass systems in which the underlying components share a "common envelope" which is *not* being driven from the system and which is magnetically active and rotating with the period of the system. The mass ratio of the components is typically 2 to 1 or larger and can be as large as 9 to 1, as in the case of AW UMa in the HR1614 group. In this situation the MSW is emitted by the common envelope which is kept in corotation by actually being a part of the system. It has traditionally been assumed that the two components are basically main-sequence stars and that the fact that the less massive component is overluminous and overlarge for its mass is a consequence of energy transfer from the more massive component. However, attempts to understand in detail the characteristics of W UMa stars in terms of such models

have not been very successful (e.g., Lucy 1976; Lubow and Shu 1976; Flannery 1976; Robertson and Eggleton 1977, Vilhu and Rahunen 1979; Mochnacki 1981), and this may be due to (*a*) the neglect of the effect of a MSW in driving the underlying components together and (*b*) the assumption that the less massive component is not very evolved. Circumstantial evidence from old disk clusters, where both W UMa stars and blue stragglers are found side by side at comparable frequencies, indicates that W UMa stars are in the process of merging (Eggen and Iben 1989; Mateo *et al.* 1990) and this is hard to understand unless the less massive (mass-losing) component in W UMa stars is chemically somewhat evolved. It may be the case that the lighter star possesses a small hydrogen-exhausted core which is less massive than the Schönberg-Chandrasekhar (1942) limit for this component when it first filled its Roche lobe. Models of such a configuration have yet to be constructed. The connection between blue stragglers and W UMa stars is discussed further in § XIV.

Mechanism 2, the radiation of angular momentum by gravitational waves, is important in systems in which components are separated by less than ~ 1.5–$3\ R_\odot$. The radiation occurs because a binary has a time-dependent mass quadrupole moment and the time required for components to touch one another, if they were point masses in a circular orbit at an initial separation A, is (Landau and Lifschitz 1962)

$$\tau_{\rm GW}({\rm yr}) \sim 10^{8.176} A^4 / M_1 M_2 M_{\rm tot}\,. \qquad (8)$$

The most direct confirmation that GWR can bring about merger at a rate predicted by theory is the binary pulsar PS 1913+16 (Taylor and Weisberg 1982). Component masses and other orbital parameters for this system are known very accurately and the observed rate of period change agrees very precisely with the theory. The semimajor axis of PS 1913+16 is $\sim 2.8\ R_\odot$ and equation (8) suggests that a merger will occur in $\sim 2 \times 10^9$ yr. Actually, PS 1913+16 has a very eccentric orbit and the time scale to achieve a merger is less than this (formula [8] holds exactly only for $e = 0$).

Angular momentum loss by GWR plays a role in the evolution of several systems already discussed: short-period W UMa stars and short-period CVs. In the case of W UMa stars, the MSW is probably more important than GWR for all phases of evolution. In the case of CVs, the MSW dominates for periods longer than ~ 3 hr, and GWR dominates for periods less than ~ 2 hr. It is in systems consisting of *very* close binary white dwarfs with periods less than 10 hr, which are theoretically predicted but which have yet to be discovered, that the role of GWR is of overriding importance. Pairs of close white dwarfs must arise in systems in which the first episode of mass transfer leaves a white dwarf and a main-sequence star which is massive enough to evolve into a giant in less than a Hubble time and which is close enough to the white dwarf that it will fill its Roche lobe in the process of growing to giant dimensions. In such systems, the second mass-transfer episode is sure to lead to the formation of a common envelope accompanied by orbital shrinkage. A very clear demonstration that this is not simply speculation is the existence of the $1\overset{\rm d}{.}6$ white dwarf binary L870–2 discussed in § I. This particular binary will not be forced into a final phase of Roche-lobe contact by the emission of GWR until another $\sim 10^{11}$ yr has elapsed, but there must be other white dwarf pairs formed with much shorter periods. A system similar to L870–2 has been identified by Bragaglia *et al.* (1988) and more close candidate double degenerates are being identified (Bergeron, Greenstein, and Liebert 1990; Bergeron, Saffer, and Liebert 1990).

Estimates making use of the known distribution of main-sequence binaries with regard to masses and orbital separations (Kraicheva *et al.* 1978; Popova, Tutukov, and Yungelson 1982) and making use of algorithms similar to equation (7) suggest that the formation rate of white dwarf pairs at separations close enough for mergers to occur in less than a Hubble time should be of the order of 10% of the formation rate of all white dwarfs (Iben and Tutukov 1984*a*, 1985, 1986, 1987; Tutukov and Yungelson 1987*a*, *b*, 1988*a*, *b*; Tutukov and Fedorova 1989). Several attempts to find these predicted very short period binaries have given negative results [Robinson and Shafter 1987 ($P_{\rm orb} < 3$ hr), Foss, Wade, and Green 1991 ($P_{\rm orb} < 10$ hr)], but this can be explained as a consequence of the fact that, for very short periods, the high rate at which pairs are destroyed by GWR–induced mergers prevents the buildup of a large space density of pairs at short period (Iben and Tutukov 1991*a*; Iben 1990*a*). The evidence that mergers do occur is provided by the existence and properties of many sdO and sdB stars and of Type I supernovae vis-a-vis the properties of theoretical merger products (§ XIII).

Mechanisms 3 and 4 are expected to operate most effectively in dense stellar systems such as globular clusters and perhaps in galactic bulges where close encounters between initially unbound stars or encounters between bound systems and unbound interlopers may occur. The three processes involved—tidal capture, binary hardening, and exchange capture—are illustrated schematically in Figure 13. During a close encounter between two stars, large tides are raised on one or both

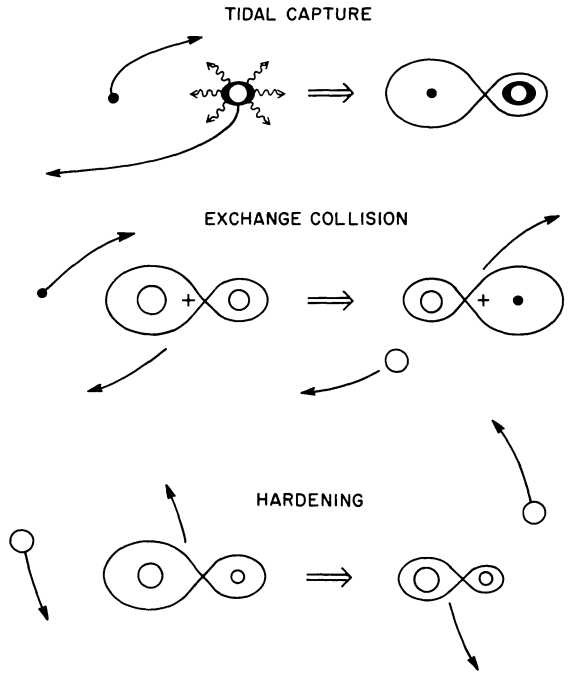

FIG. 13.—Schematic showing phenomena in dense stellar systems: tidal capture, exchange capture, and hardening collision.

stars, depending on the size of each star relative to the distance of closest approach, and some of the kinetic energy of relative motion is converted into the energy of fluid motions in the tidally distorted regions. This energy is ultimately radiated as light (mechanism 3). If the separation between components becomes small enough relative to the radial dimensions of one (or both) of the components, tides can become large enough that the gravitational potential energy exceeds twice the kinetic energy of relative motion and the interacting pair becomes gravitationally bound (Fabian, Pringle, and Rees 1975; Ray, Kembhavi, and Antia 1989). Thus, a neutron star passing close enough to a low-mass main-sequence star can raise sufficiently large tides in the main-sequence star that capture must follow.

Mechanism 4 operates when a preexisting binary experiences a close encounter with a single star. Such an encounter can lead to a "hardening" (or a "softening") of the binary (Hills 1975*a, b,* 1978; Heggie 1975) or it can lead to the replacement of one of the initial components by the interloper (Fullerton and Hills 1982; Hills 1975*a*). The frequency of hardening collisions is larger than the frequency of softening collisions for systems in which the orbital velocity exceeds the velocity dispersion in the cluster. Although the degree of hardening is usually quite modest (Hut and Paczyński 1984), the frequency of "catastrophic" collisions which actually lead to the initiation of mass transfer may be significant over the lifetime of a cluster (Krolik, Meiksin, and Joss 1984) and this may lead to a greater frequency of occurrence of merger products near the center of a cluster than in the peripheral regions of this cluster (Bailyn and Iben 1989).

Exchange collisions can occur if the mass of the interloper is larger than the mass of either component in the initial system, and it is the lighter component which is ejected. If there is a significant primordial population of tight binaries in globular clusters, this could be a way in which binaries containing a neutron star and a low-mass main-sequence star are formed (Hut and Verbunt 1983). As in the case of the post–common-envelope precursors of CVs, the main-sequence component in the immediate postcapture, postexchange, or posthardened system is unlikely in the general case to fill its Roche lobe. Thus, angular momentum loss by a MSW or GWR may be crucial to the formation of a low-mass X-ray binary (LMXB) in a Galactic globular cluster or in a galactic bulge.

f) *Scenario Building*

An important goal of the rudimentary theory of binary evolution is to devise scenarios which describe how a binary system of given primordial characteristics evolves into a more exotic system (containing at least one compact component) similar to systems with which we are familiar from the observations, and then evolves still further into a final configuration which can be two compact objects (whether gravitationally bound or free), a single compact object achieved by merger, or gas expelled at high velocity in a star-disrupting explosion which follows a merger. An attempt at illustrating the wide variety of possible scenarios is made in Figure 14 (adapted from Iben and Tutukov 1984*a*). Obviously, the full wealth of possibilities cannot be presented in such a small space, and realism with regard to scale is sacrificed in the interest of achieving conceptual clarity. Each subunit of the schema, usually consisting of a Roche-lobe outline and enclosed components, will be referred to as an element.

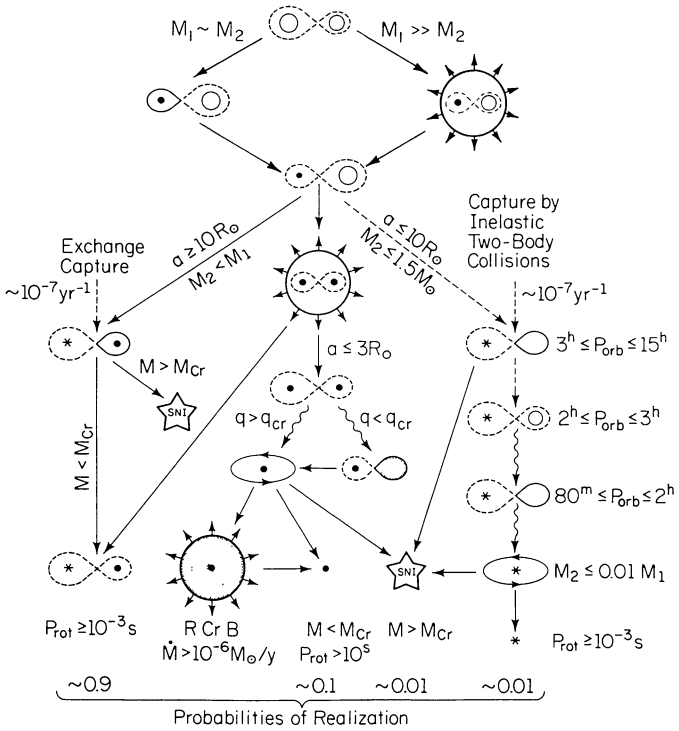

FIG. 14.—Scenarios for binary star evolution. Modified from Iben and Tutukov (1984*a*). Rings are unevolved stars; filled circles are electron-degenerate helium, carbon-oxygen, or oxygen-neon cores in giants; six-pointed stars are white dwarfs or neutron stars. Wavy lines mark transitions driven by the radiation of gravitational waves and counter-clockwise rotating ellipses are heavy disks. Open stars represent Type Ia supernova explosions. Roche lobes are shown by dashed loops (when not filled) or by solid loops (when filled). The probability of realization of different final products, assuming a total formation rate of close binaries as 1 yr^{-1}, is indicated at the very bottom of the figure.

The adventure begins with the element at the very top, which represents a pair of main-sequence stars which do not fill their Roche lobes (Fig. 14, *dashed lines*). The more massive star is within the left-hand lobe, and it is assumed to be of low or intermediate mass. If the two main-sequence stars are of comparable mass and are not too far apart, then, when the primary exhausts hydrogen over a large region about its center and grows to fill its Roche lobe, it transfers matter to its companion in a mass conserving but not necessarily angular-momentum conserving way. Evolution proceeds to the next element downward and to the left. The filled circle represents the helium core of the mass-losing component, and its Roche lobe is drawn as a solid line, indicating Roche-lobe filling. If the helium core is electron-degenerate and small, then the system becomes an Algol system and mass continues to be transferred at a slow rate until the mass left above the core decreases below a critical value; the system evolves into one consisting of a helium white dwarf and a low- or intermediate-mass main-sequence star (the second element from the top). If the helium core is not electron-degenerate (which will be the case more often than not if the initial primary is an intermediate-mass

star), mass transfer continues at a rapid rate until the donor shrinks within its Roche lobe to become a helium star, first converting helium into carbon and oxygen in its interior and then evolving into a CO white dwarf or a hybrid white dwarf (also the second central element from the top). If it is assumed that orbital angular momentum has been conserved during mass transfer, the orbital separation of the components will be much larger than in the primordial system.

In most instances, evolution in Figure 14 continues directly downward. If the orbital separation is less than $\sim 400\ R_\odot$, the second star will fill its Roche lobe before igniting helium; if larger, then it will not fill its Roche lobe before developing an electron-degenerate CO core. In either case, the stellar mass ratio is very large, and mass is transferred at a very rapid rate to a compact object which cannot absorb it; the transferred mass forms an expanding layer above the white dwarf, and ultimately the matter lost by the second star fills an expanding common envelope, as described by the third element from the top in the central column of Figure 14. The small filled circles in this element represent the white dwarf (*left*) and the helium core (or CO white dwarf core) of the second star (*right*). These compact objects form the "eggbeater" which is envisioned to drive off matter through the common envelope, whose outer edge is represented by the large circle capped by outwardly pointing arrows. In the next element downward, the second star has become (1) a helium white dwarf (if the helium core becomes electron-degenerate before it can ignite helium), (2) a helium star which evolves into a hybrid or a CO white dwarf, or (3) a CO white dwarf. Which of these possibilities is realized depends on the mass of the second star and on the size of its Roche lobe when it first fills this lobe. In most cases, thanks to the assumption of mass conservation during the first mass-transfer event, the second white dwarf to be formed is more massive than the first.

If the final pair of white dwarfs is too far apart ($>3\ R_\odot$ for massive white dwarfs and $>1.5\ R_\odot$ for light white dwarfs), then angular momentum loss by GWR occurs on a time scale longer than the Hubble time; the two white dwarfs simply cool down and disappear from view. Motion in Figure 14 is downward to the leftmost element at the bottom. This is the most frequently traveled path.

If the white dwarfs are formed in a tight enough orbit, GWR can force the lighter of the two into contact with its Roche lobe and mass transfer will begin at a rate determined by the ratio q of the lighter to the heavier dwarf. If the mass ratio is less than a critical value $q_{cr} \sim 0.6$, a stable mass- and angular momentum-conserving solution exists which allows the lighter white dwarf to remain within its Roche lobe as it loses mass. The semimajor axis and the period of the system continues to increase until eventually the lighter component can no longer be described as a white dwarf. The famous double star GP Com may be a system of this type (Nather, Robinson, and Stover 1981). The spectrum of this system shows no hydrogen lines and the ratio of nitrogen to carbon deduced from spectral lines is what would be expected if almost all of the carbon and oxygen in a solar system distribution of CNO elements had been converted into nitrogen, as occurs during complete hydrogen burning (Lambert and Slovak 1982).

If $q > q_{cr}$, mass transfer is unstable, and mass will flow to the heavier white dwarf at a rate greater than the Eddington accretion limit for this star (Webbink 1984). A common envelope forms (Iben 1988), but this is supplanted almost immediately by the transformation of almost all of the original matter of the light dwarf into a nearly spheroidal "thick disk" about the heavier white dwarf (Tutukov and Yungelson 1979). The element representing this situation consists of a filled circle (the heavier white dwarf) and a larger oval rotating in a counterclockwise fashion (the thick disk). Although the thick disk contains most of the angular momentum of the precursor white dwarf pair, it is of large radius primarily because of gas pressure (electrons are not degenerate) and radiation pressure support rather than because of centrifugal forces (Mochkovich and Livio 1989; Benz *et al.* 1990) and matter near the base of the disk can be hot enough to burn nuclear fuel (Nomoto, Nariai, and Sugimoto 1979; Benz *et al.* 1990; Iben 1990*a*).

What becomes of this configuration depends on the compositions and masses of the two precursor white dwarfs. If the two white dwarfs are composed of carbon and oxygen and if the sum of their masses is larger than the Chandrasekhar (1931, 1939) mass of $\sim 1.4\ M_\odot$, the final result may be a Type Ia supernova, but this is a long story with an as yet unknown outcome (§ XIII). If the sum of the CO white dwarf masses is less than the Chandrasekhar limit, then the net result is a single CO white dwarf or possibly a single ONe white dwarf (the single filled circle at the bottom center of Fig. 14). If the first white dwarf is made of helium and the second is made of carbon and oxygen (the second dwarf is heavier than the first because of the assumption of mass conservation in the first mass-transfer episode), then the merged product will take on the appearance of an R CrB star. Carbon burns at the base of the helium envelope above a growing CO electron-degenerate core, and mass is lost from the surface via a wind. The final result is a single CO white dwarf. If both white dwarfs are composed of helium, the merged product will evolve into a helium star, burning helium in its interior and adopting the characteristics of an sdO or sdB star; after exhaustion of much of its helium fuel it will evolve into a hybrid or CO white dwarf (Iben 1990*a*). In summary, many close main-sequence binaries of intermediate mass evolve ultimately into singly hybrid or CO white dwarfs, and some small fraction may evolve into ONe white dwarfs and Type Ia supernovae.

Return now to the first element at the top, and assume that the initial mass ratio is much larger than unity or that the orbital separation is so large that the primary does not fill its Roche lobe until after it has developed a deep convective envelope, or both. When the primary fills its Roche lobe, mass transfer will be unstable and a common envelope will be formed, as represented by the next element downward and to the right. The common envelope dissipates and the compact remnant of the primary evolves directly into a helium or CO white dwarf or evolves first into a helium star and then into a CO or hybrid white dwarf. The system is now represented by the second central element from the top. In this case, however, the orbital separation of the system is much smaller than the orbital separation of the initial system, in contrast with the case when the first mass transfer conserves mass and orbital angular momentum. Furthermore, the mass of the second star has not changed, remaining smaller than the mass of the primordial primary.

If the mass of this second star is less than $1\ M_\odot$, the system will remain rooted to the spot for over a Hubble time unless the separation between components is small enough to permit the

combined action of tidal forces and a MSW to force the relatively unevolved component into Roche-lobe contact. If the second star is massive enough and the system semimajor axis is large enough, this star will not fill its Roche before exhausting central hydrogen. In general, because of the orbital shrinkage occasioned by the prior common envelope experience, it will fill its Roche lobe before igniting helium. Because of the large disparity in thermal time scales between the second star and its white dwarf companion, the transfer of mass between the two stars will lead to the formation of a common envelope, and evolution in Figure 14 again proceeds directly downward to the third central element from the top. This time, however, the second white dwarf which eventuates is less massive than the first. Apart from this, progress downward through the central pyramid of elements, when relevant, is quite similar to that already described, and, in most instances, evolution proceeds directly to the leftmost element at the bottom of the figure.

Another less frequently traveled but observationally very important channel is the one which opens up when the second star can support a MSW and the orbital separation is small enough that tidal torques keep this component spinning at close to the orbital frequency. In this case, loss of orbital angular momentum will cause the second star to fill its Roche lobe while it still retains hydrogen at its center. If the mass of the less evolved component is less than ~ 0.8 times the mass of the white dwarf, the system will evolve along the set of CV configurations shown at the right of Figure 14. Evolution along the CV configurations can also be initiated by the tidal capture of a single low-mass main-sequence star by a single white dwarf. If the main-sequence star is heavier than the white dwarf, another common envelope is formed as hydrogen is ignited at the base of a layer of matter newly acquired by the white dwarf. As the mass of the donor is whittled down to be 20% or so smaller than the mass of the white dwarf, the common envelope phase ends and the system evolves downward along the CV sequence.

Along the CV sequence, the white dwarf accretor is on the left and the low-mass donor is on the right. The six-pointed star representing the white dwarf is meant to indicate that accretion and nova-like activity is taking place. It has been suggested that, if the white dwarf is initially massive enough, and if the mass-transfer rate is high enough, the white dwarf might grow in mass despite the loss of matter during the hydrogen-burning runaways that are intermittently initiated and, on achieving the Chandrasekhar mass, might explode as supernovae (Iben 1982*b;* Starrfield, Sparks, and Truran 1985). This may conceivably occur, but certainly not with a frequency close to the rate at which supernovae occur in the Galaxy (Iben and Tutukov 1984*a, c*). Furthermore, the expanding shell of the exploding star would ablate from and sweep up enough hydrogen from the companion that the explosion would not be mistaken for a Type Ia supernova.

In the normal situation, the white dwarf remains at about the same mass as the donor continues to lose mass and decrease in radius. Angular momentum loss due to the combined action of a MSW and tidal torques maintains the donor in Roche-lobe contact as the orbital separation and the period steadily decrease. It is known that there is a paucity of CVs with periods in the 2–3 hr range, and this is usually attributed to a cessation of the MSW due possibly to a change in the magnetic field configuration which occurs when the mass of the main-sequence star decreases to $\sim 0.3\ M_\odot$ and this star becomes convective throughout its interior (Rappaport, Verbunt, and Joss 1983). It is argued that, during the preceding mass-transfer stage, the donor is not completely in thermal balance and remains larger than a main-sequence star of the same mass; once the MSW ceases, for whatever reason, mass-transfer ceases and the erstwhile donor shrinks to be of normal size for its mass. Another possibility is that it is tidal heating that is primarily responsible for the inflation of the donor and that the rate of such heating is strongly reduced when the donor becomes completely convective. In either case, orbital shrinkage due to GWR will, typically in $\sim 2 \times 10^8$ yr, force the low-mass star to again fill its Roche lobe and thereafter GWR will drive mass transfer. The progression to shorter periods is reversed when matter in the interior of the donor becomes electron degenerate and donor radius increases with decreasing mass (Paczyński 1983). Ultimately the donor becomes planetary-like and is captured by the white dwarf.

The accretor could also be a neutron star (in a globular cluster or in a galactic bulge) which has acquired a low-mass companion either by tidal capture or by an exchange collision. In this case, the six-pointed star within the left-hand Roche lobe indicates that the system emits X-rays as accreted matter strikes the surface of the neutron star and the series of elements depicts the evolution of low-mass X-ray binaries (LMXBs). Since the gravitational binding energy of a gram of matter at the surface of a neutron star is 10 times larger than the nuclear fuel in a gram of accreted matter, exactly the inverse of the situation in CVs, thermonuclear runaways in LMXBs are completely contained, with the average amount of radiant energy emitted in consequence of thermonuclear flashes being 10 times smaller than the amount of energy emitted in consequence of the conversion of gravitational potential energy first into heat and then into X-rays. Since neutron stars in LMXBs grow in mass, and since there is an upper limit on the mass which a neutron star can have, there is a possibility that some small fraction of LMXBs may evolve into black holes. Further, it takes only $\sim 0.1\ M_\odot$ of matter accreted with Keplerian velocities to spin a neutron star up to near breakup velocities, so there is the additional possibility that some neutron stars accreting from a low-mass companion evolve into millisecond pulsars (Smarr and Blandford 1976). The large numbers of millisecond pulsars that are currently being discovered in Galactic globular clusters (Backer and Kulkarni 1990), when compared with the numbers of LMXBs in these same clusters, suggest to Grindlay and Bailyn (1988) that LMXBs are not the precursors of the millisecond pulsars, but this inference has been challenged by Verbunt, Lewin, and van Paradijs (1989). In any case, it is not inconceivable that somewhat longer-period precursor systems in which the mass-transfer rate is large enough to hide X-ray emission are the predominant precursors; they are not seen both because of their short lifetime and because of their masking of high-energy radiation.

An attractive precursor system is one in which the mass donor is a subgiant or giant with an electron-degenerate helium core which is more massive than chosen by Webbink, Rappaport, and Savonije (1983) to explain bulge LMXBs with luminosities near the Eddington limit. The time scale for mass transfer due to GWR alone depends inversely on the 5.6th power of the core mass, being of the order of 10^8 yr when core

mass $M_{He} \sim 0.2\ M_\odot$. Systems with large helium core masses will not be seen as LMXBs because of the rapid time scale for mass transfer, and the systems with very low mass helium cores will not be detected as LMXBs because of the low rate of X-ray emission. Thus, one anticipates that bright LMXBs in globular clusters may be formed at only a small fraction of the rate at which all mass-transferring systems of neutron star plus subgiant and giant are formed.

The final evolutionary channel depicted on the far left in Figure 14 can be reached in a dense stellar system by means of an exchange capture whereby one of the components in a low-mass main-sequence binary is replaced by a more massive white dwarf (or neutron star). Much more frequently, it is reached by a binary system in which the primary evolves into a massive white dwarf and the secondary, of mass less than 0.6–0.8 times the mass of the white dwarf, fills its Roche lobe after having developed an electron-degenerate helium or CO core. This channel has been occasionally cited in attempts to understand the formation of Type Ia supernovae in terms of the accretion of hydrogen-rich matter onto a white dwarf companion (Whelan and Iben 1973; Iben and Tutukov 1984*a*; Kato, Hachisu, and Saio 1989). Given the imposed demands on the mass of the first white dwarf and on the mass of its main-sequence companion, it is evident that a precursor system, if a binary, must develop a common envelope during the first mass-transfer episode, and that orbital shrinkage must be relatively modest if the orbital separation is to remain large enough to prevent the secondary from filling its Roche lobe before it has developed an electron-degenerate helium or CO core. A small donor-accretor mass ratio insures that, in the absence of a thermonuclear runaway in accreted matter, all of the matter lost by the donor will remain on the accretor. There is a narrow window of accretion rates (Fujimoto 1982; Iben 1982*b*) which will allow the accretor to burn hydrogen in steady state without expanding to fill its Roche lobe, and if a transfer rate can be maintained within this window, the mass of the white dwarf might reach the Chandrasekhar limit, resulting in a supernova explosion. The estimated frequency for this to occur is much smaller than the observed Type Ia supernova rate (Iben and Tutukov 1984*a*; Kato and Hachisu 1989) and, in any case, the presence of large amounts of hydrogen in the system makes this scenario somewhat unattractive as an origin of Type Ia supernovae.

A variant of this scenario, involving the transfer of hydrogen-rich matter from a giant to a massive white dwarf at a rate within the permanent accretion window, supposes that the donor is an AGB star which does not fill its Roche lobe, but which emits a wind from which its white dwarf companion may accrete at a rate within the window (Iben and Tutukov 1984*a*). Since, the AGB star does not fill its Roche lobe, there is no restriction on its mass.

In any event, systems involving stable mass transfer onto a white dwarf from a subgiant, a red giant, or an AGB star will occur and the final fate of most such systems will be a pair of noninteracting white dwarfs as depicted in the bottom element on the left in Figure 14.

In most instances, mass transfer will lead either to (*a*) nova outbursts and a loss from the system of a large part of the mass accreted by the white dwarf prior to outburst or (*b*) to a swelling of the accreted layer (in response to nuclear burning at its base) to such an extent that a common envelope is formed and all of the matter from the subgiant or AGB component is lost from the system. Evolution in Figure 14 proceeds once again to the leftmost element at the bottom of the figure.

The sketch that has been given here is exceedingly rough, and there are manifold refinements which one could explore in an attempt to understand the wealth of potentially realizable evolved binary systems (Massevitch and Tutukov 1988; Lipunov and Postnov 1988; Tutukov and Yungelson 1990). By including interacting binary systems which have made their mark in observational astronomy, the H-R diagram is enlarged significantly beyond the traditional confines defined by single stars in nuclear-burning phases. This is illustrated in Figure 15 (Iben and Tutukov 1984*a*). In this figure, the traditional region is an inverted triangle bordered roughly by a line of constant radius ($\sim R_\odot$) and a nearly vertical giant branch extending to a radius of the order of 1000 $R_\odot$. The tracks of single stars are indicated by solid lines and the tracks of mass-losing stars in close binary systems are indicated by dashed lines. The location of components (subgiants, low-mass main-sequence stars, or AGB stars) which are transferring mass to a companion, which may be a main-sequence star (Algols), a white dwarf (CVs, LMXBs), or either a main-sequence star or a white dwarf (symbiotics), are indicated by thin five-pointed stars. The paths of cooling degenerate remnants of various types follow along lines of constant radius far to the left of the region defined by single nuclear-burning models. Each thick five-pointed star along the white dwarf cooling curves gives the luminosity of the accretion disk about a white dwarf which is accreting at the indicated rate. An eight-pointed star along the neutron star cooling curve gives the luminosity of the accretion disk about a neutron star which is accreting at the indicated rate.

This concludes the general discussion of single and binary star evolution. What follows is a series of commentaries on a number of special topics that the author has found particularly interesting.

IV. POPULATION I MODELS AND THE OBSERVATIONS

a) *Contraction onto the Main Sequence and the* H^- *Ion*

The evolutionary tracks in Figure 16 are those of 1 $M_\odot$ model stars of Population I composition which initially (at the highest luminosity and lowest surface temperature) are homogeneous in composition, are supported against gravity by gas pressure, and are not burning nuclear fuel (Iben 1965*a*). The models, which describe how stars evolve from the T Tauri phase onto the main sequence, differ only in the choice of the abundance of heavy elements of low ionization potential (<7.5 eV); in the model which produces the dashed track, the abundance of such elements is 10 times smaller than in the model which produces the solid track. In the catalog of input physics which enters into the model calculations, the only item influenced by this difference is the contribution of the H^- ion (Wildt 1939, 1940; Chandrasekhar 1958) to the opacity. This contribution is directly proportional to the abundance of elements of low ionization potential.

The portions of the tracks at the lowest (essentially constant) surface temperatures are almost exact inverses of the

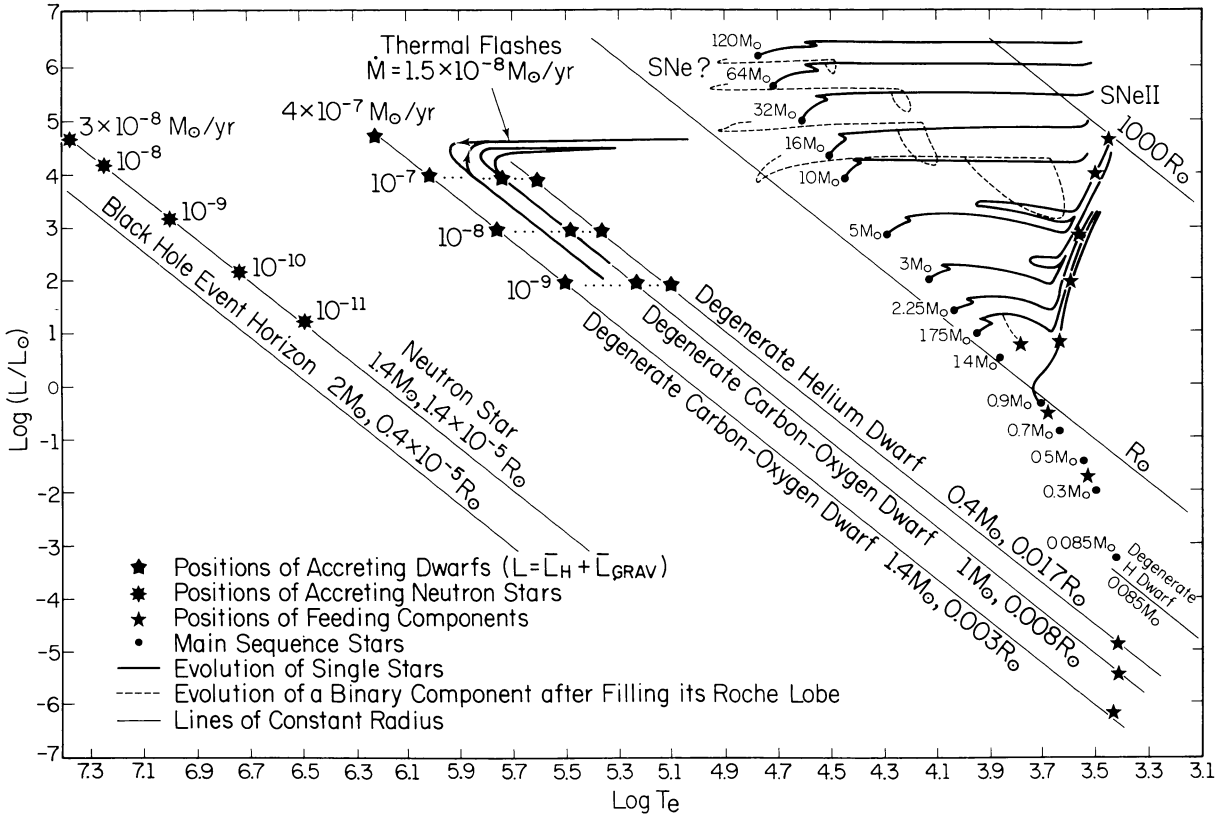

FIG. 15.—Populating the extended H-R diagram with interacting binaries. From Iben and Tutukov (1984*a*)

tracks followed by model stars of the same mass and input physics that have exhausted central hydrogen and are climbing the giant branch with an electron-degenerate helium core. What the two sets of models have in common is a very deep convective envelope and a surface photospheric region in which absorption by the H^- ion is the dominant source of opacity. In contrast with the opacity in the interior, an H^--dominated opacity decreases with decreasing temperature, and the dependence on temperature is very steep. The dependence on density is linear.

Along the nearly vertical portions of the tracks, the model stars are completely convective except for the very outer, photospheric layers. Motion is downward along the tracks because the only source of energy escaping the models is the release of gravitational potential energy, and this requires a decrease with time in model radius. A decrease in radius means that the model moves downward and/or to the left in the H-R diagram. A decrease in radius also means an increase in densities and/or an increase in temperatures everywhere within the model and therefore an increase in photospheric opacities. An increase in photospheric opacities means a decrease in demand for a high-energy flux from the interior, and this is why model luminosities drop as radii decrease. The model calculations show that the high-temperature dependence of the H^- opacity source acts as a thermostat to maintain the surface temperature at a nearly constant value and that the major burden of responding to contraction falls upon the luminosity.

When models reach the lowest-luminosity portions of the tracks, the opacity in central regions has become small enough that radiative diffusion has taken over from convection as the primary means of transporting energy outward. Model surface characteristics remain near the trough in the H-R diagram as the dominant star-wide mode of energy transport switches from convective flow to radiative diffusion, and the model is transformed from an index 1.5 polytrope to an index 3 polytrope. Thereafter, the model follows Eddington's (e.g., 1926) prescription:

$$L \propto \mu^4 M^3/\kappa\,, \tag{9}$$

where μ is the mean molecular weight, M is the stellar mass, and κ is an average interior opacity (which decreases with increasing temperature).

Eventually, central temperatures become large enough that hydrogen is ignited. The energy liberated by nuclear fusion is converted into heat, and the overpressure thereby created slows down and reverses contraction in an ever-widening region about the center. The decrease in the rate of release of gravitational potential energy is responsible for the drop in luminosity as the models settle onto the main sequence where the dominant source of surface luminosity becomes the release of nuclear energy.

The line in the H-R diagram to the blue of which lie contracting models of specified initial composition has been named after Hayashi, in recognition of his perception that red giants of large luminosity must have deep convective envelopes (Hayashi 1961), whatever the state of their deep interiors. In fact, the recognition that, if they are to mimic lumi-

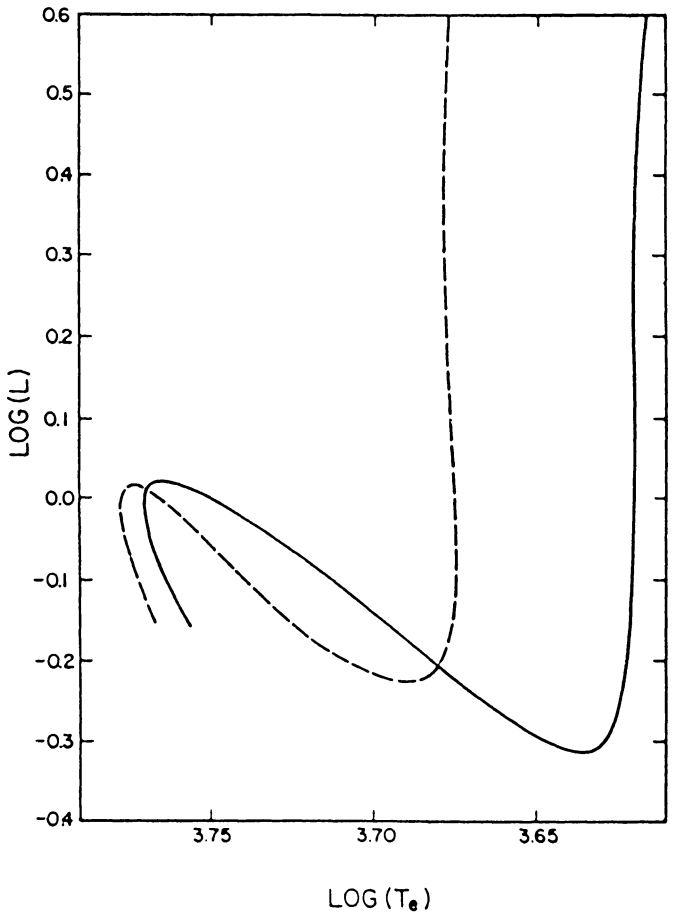

FIG. 16.—Evolutionary tracks of solar-mass models of Population I composition which are contracting onto the main sequence from an initial configuration which is completely convective in the interior (Iben 1965*a*). The total abundance of elements of low-ionization potential which contribute electrons for the formation of the H^- ion, which is the dominant source of opacity in photospheric layers, is smaller by a factor of 10 in the model following the dashed track than in the model following the solid track.

nous red giants in globular clusters (see the next section), low-mass stars must develop deep convective envelopes after leaving the main sequence was recognized earlier by Hoyle and Schwarzschild (1955*a*, *b*). Hoyle and Schwarzschild argued further that it was the use of boundary conditions more sophisticated than the conditions that $T = 0$, $\rho = 0$ at the surface that was responsible for the abrupt upturn from the subgiant branch to the giant branch. Comparison between the two tracks in Figure 16 shows, however, that the physics of a hydrogen-rich atmosphere at low temperature (leading to the formation of the H^- atom and the attendant dominant contribution of this atom to the opacity) plays an important role in defining the precise location of the minimum surface temperature in the H-R diagram beyond which a model may not stray. A nice discussion of much of the physics of the contracting phase and of the considerations which influence where on the theoretical quasi-static model tracks real stars take up residence is given by Stahler (1988).

b) Evolution Off the Main Sequence and Old Disk Clusters

Evolutionary tracks for low-mass models of Population I composition which are burning hydrogen are shown in Figure 17 (Iben 1967*a*). Times to evolve between labeled points along each track are given in Table 1. Several features of these tracks are useful in comparing with loci defined by stars in old Galactic disk clusters. Note that, because the solar-mass model does not develop a convective core, its track does not exhibit a sharp, short-lived hook to the blue after the exhaustion of hydrogen at the center. However, tracks for the more massive model stars do exhibit this hook and the time spent burning hydrogen in a thick shell $\tau_{\rm shell}$ (points 4–7 in Fig. 17) relative to the time spent burning hydrogen in a convective core $\tau_{\rm core}$ (points 1–3) is approximately $\tau_{\rm shell}/\tau_{\rm core} \sim (2/3)(M_\odot/M)^{2.5}$. The ratio of lifetimes decreases with increasing mass because the mass fraction of the convective core increases with increas-

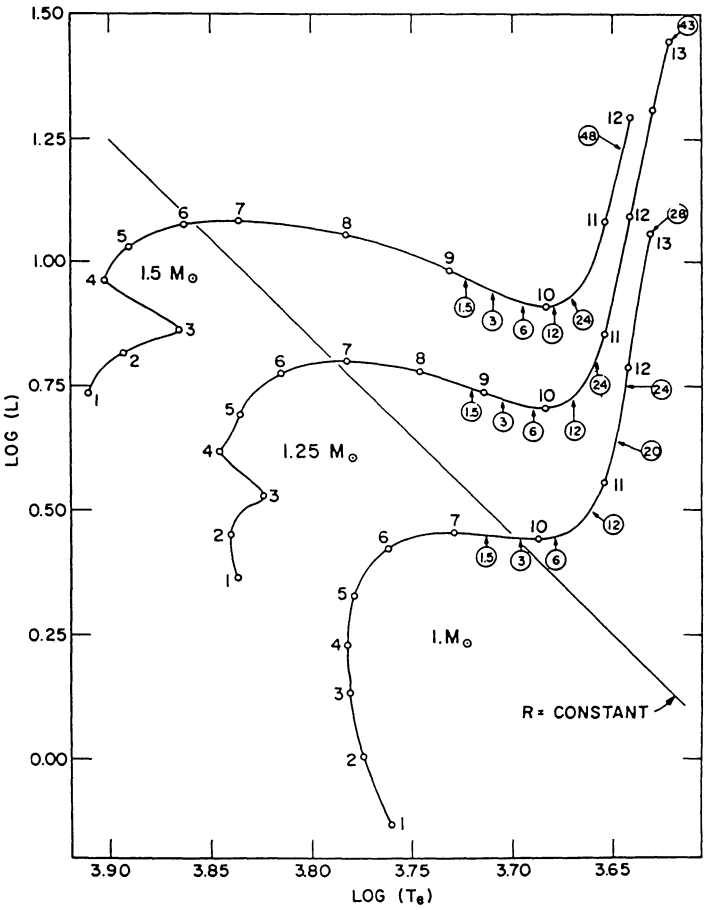

FIG. 17.—Evolutionary tracks of low-mass models of Population I composition during the main-sequence and early shell hydrogen-burning phases (Iben 1967*a*). models along the lowest surface temperature portions of the tracks possess electron-degenerate helium cores and deep convective envelopes. The circled numbers along the tracks at low T_e give the factor by which the surface lithium abundance has been depleted, assuming that no mass is lost during the main-sequence phase and that no forms of mixing other than convective mixing have taken place. Ages of models at other enumerated points are given in Table 1.

TABLE 1

EVOLUTIONARY LIFETIMES[a] OF MODELS IN FIGURE 17

Points	1.0 $M_\odot$	1.25 $M_\odot$	1.5 $M_\odot$
1–2	3.77/9	1.39/9	1.01/9
2–3	2.89/9	1.41/9	5.43/8
3–4	1.46/9	1.82/8	8.10/7
4–5	1.03/9	5.38/8	1.74/8
5–6	7.02/8	3.69/8	1.41/8
6–7	2.92/8	1.38/8	3.44/7
7–10	1.57/8	1.46/8	1.05/8
10–12	3.98/8	2.45/8	1.57/8

[a] In years.

ing model mass and the model can remain within the main-sequence burning hydrogen in a thick shell only as long as the mass of the hydrogen-exhausted core remains smaller than the Schönberg-Chandrasekhar (1942) limit of ~10% of the mass of the model.

The time spent in the overall contraction phase (points 3–4) for the 1.25 $M_\odot$ and 1.50 $M_\odot$ models is only ~5% of the core hydrogen-burning lifetime (points 1–3) and ~20% of the lifetime of the thick shell burning phase (points 4–7). Hence, for clusters in which stars near turnoff are massive enough to have developed a convective core of moderate mass, stars in the thick shell burning phase will be distinctly separated in the H-R diagram from stars in the core burning phase by a region containing relatively few stars. A classical example of a cluster which exhibits this property is M67, as shown in Figure 18. The points are from an early study by Johnson and Sandage (1955) and the solid curves have been inserted as a guide to offset the fact that the observed sample obviously contains some stars which are not cluster members.

Another feature of the model tracks in Figure 17 which is also reflected in the cluster locus of M67 is that the slope of the track between the point of maximum luminosity near the main sequence (point 7) and the point of minimum luminosity at the base of the giant branch (point 10) is steeper for models which have a convective core during the first portion of their main-sequence phase. The locus defined by stars in the very old disk cluster NGC 188 does not exhibit a gap near the main sequence and the portion of the locus leading from above the main-sequence turnoff to the subgiant branch is quite flat. Both characteristics identify the most massive stars in NGC 188 to be less massive than those in M67. Further, since the luminosity at the base of the giant branch is a well-defined function of stellar mass, one may easily estimate the relative masses of turnoff-point stars in the two clusters and therefore also relative ages. If, further, the lower main-sequence portions of the two cluster loci are normalized to fit the model zero age main-sequence, one may estimate absolute cluster ages. In this way one finds $\tau_{\rm NGC\ 188} \sim 2 \times \tau_{\rm M67} \sim 11 \times 10^9$ yr (Iben 1967*a*), and these estimates are not too different from the much more carefully obtained estimates of VandenBerg (1985).

c) Internal Composition Changes and the First Dredge-up

An additional phenomenon described in Figure 17 is the change in surface composition brought about by convective mixing. During the main-sequence phase of the models, lithium is destroyed over most of the interior (at temperatures larger than $\sim 2.5 \times 10^6$ K), leaving only a thin layer containing unburned lithium near the surface. As the models reach the giant branch, the base of the convective envelope extends inward in mass, spreading the remaining lithium over a larger and larger mass. The surface abundance of lithium must necessarily drop, and the circled numbers beside the tracks in Figure 17 show the factor whereby the initial abundance is depleted in the models. Since the mass of the layer in which lithium remains before dilution is ~1%–2% of the mass of the model, the dilution factors show that the convective envelope grows to contain over half of the mass of the star early on in its upward ascent of the giant branch.

The observations of the lithium abundance in real low-mass giants show that the process just described is certainly operating, but that there are a number of other physical processes (such as diffusion, meridional or turbulent mixing, and surface mass loss) which operate in real low-mass stars but which have not been taken into account in the models. For example, the predictions of the simple models appear to hold approximately for G and K giants of mass greater than ~1.3 $M_\odot$ (Lambert, Dominy, and Sivertsen 1980; Pilachowski 1986) but overestimate the abundances of Li for low-mass G and K giants and of M giants (Luck and Lambert 1982) by as much as two orders of magnitude. This means that, in real low-mass main-sequence stars, mixing processes which carry Li inward to high enough temperatures that it may be destroyed (Charbonneau and Michaud 1990) are operating, or that mass loss depletes the store of lithium near the surface and at the same time dilutes the surface abundance of lithium during the main-sequence phase (Hobbs, Iben, and Pilachowski 1989), or both. The importance of lithium as a tracer of epidermal physical

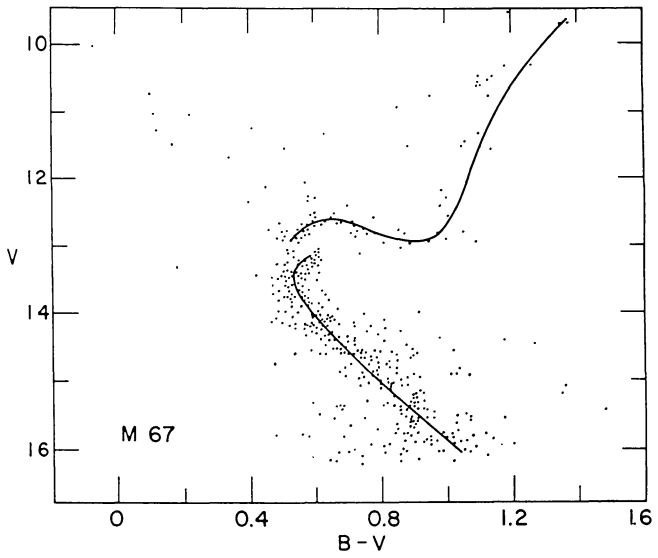

FIG. 18.—Positions of stars seen in projection near the center of the old disk cluster M67 (Johnson and Sandage 1955). The radial-velocity test for cluster membership has not been applied. The solid curve has been introduced as a guide to the eye.

processes is reviewed by Boesgaard (1988), Hobbs and Pilachowski (1988), and Wallerstein (1988).

The abundances of elements other than Li are affected by the deepening of the convective envelope along the giant branch. Figure 19 gives the distribution of several isotopes in a model star of mass 5 $M_\odot$ as it is crossing the Hertzsprung gap to become a red giant (Iben 1966*a*). Note that hydrogen has been exhausted over approximately the inner 10% of the mass of the star, ^{12}C has been converted into ^{14}N over the inner 50%, and ^{16}O has been converted into ^{14}N over the inner 20%. Both ^3He and ^{13}C have been created in middle regions of the model (the initial model does not contain these elements). Lithium (not shown) has been destroyed over the inner 99% of the model. As the model reaches the giant branch, first the lithium abundance decreases, then fresh ^3He appears at the surface, followed by fresh ^{13}C. Then the surface abundance of ^{14}N increases at the expense of ^{12}C (Iben 1964). The base of the convective envelope extends at its deepest down to a mass fraction of ~20%, so a change in the surface abundance of ^{16}O is not expected. The quantitative predictions of CNO abundance ratios from models of different masses are in reasonable agreement with the observations of giants (Lambert and Ries 1981), and predictions of the $^{12}C/^{13}C$ ratio agree with observed ratios for some 70% of these same giants, but 30% show ratios which are substantially smaller than the predicted ones, once again suggesting some form of "extra mixing" during the main-sequence phase (see the discussions in Iben and Renzini 1983, 1984).

V. GLOBULAR CLUSTER STAR EVOLUTION

Figure 20 (Iben 1971*b*) presents a summary of the type of theoretical information which is relevant to understanding the evolutionary state of most of the stars in Galactic globular clusters and is useful for estimating the ages of these clusters.

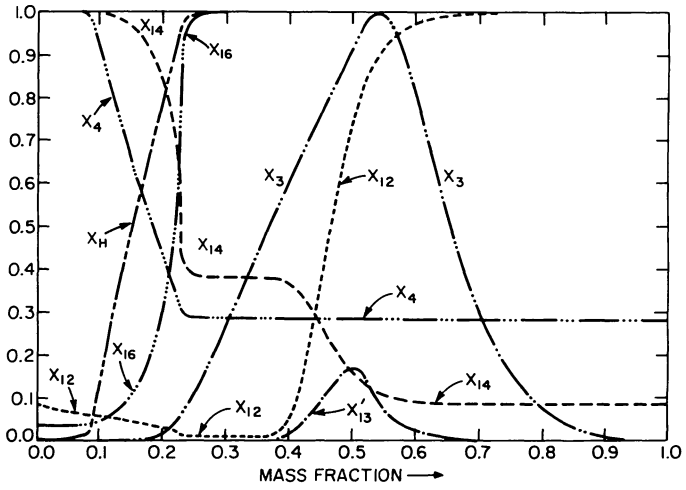

FIG. 19.—The variation with mass fraction of composition variables in a model star of mass 5$M_\odot$ and Population I composition at the end of the main-sequence phase (Iben 1966*a*). The X_i's are abundances by mass of $^1H(X_H)$, $^3He(X_3)$, $^4He(X_4)$, $^{12}C(X_{12})$, $^{13}He(X_{13})$, $^{14}C(X_{14})$, and $^{16}O(X_{16})$. Scale limits correspond to $0.0 < X_H < 0.7080$, $0.0 < X_3 < 1.296 \times 10^{-4}$, $0.0 < X_4 < 0.9762$, $0.0 < X_{12}, X_{13} < 3.610 \times 10^{-3}$, $0.0 < X_{14} < 1.445 \times 10^{-2}$, and $0.0 < X_{16} < 1.080 \times 10^{-2}$.

The models on which the summary is based are from Iben and Rood (1970*a*, *b*). Model masses have been chosen so as to populate the H-R diagram in a way which gives approximate quantitative agreement with the locus defined by real stars in a typical globular cluster. Note that the model tracks which lead from the termination of the main sequence to the giant branch actually have positive slopes, and this in itself indicates that globular cluster stars are older than the stars in NGC 188, one of the oldest disk clusters known.

Next note that, in order to match the spread in surface temperatures along an observed horizontal branch, it is necessary to suppose that there is a spread in mass among the model stars on this branch and that the mean model mass is significantly smaller than the initial masses of models that exhaust central hydrogen when they are near the location of the cluster turnoff point, this latter fact being first recognized, without comment, by Hayashi, Hoshi, and Sugimoto (1962). It follows that real globular cluster stars lose mass somewhere between the main sequence and the tip of the giant branch and that there is a "hidden" parameter (probably rotation rate) which forces the degree of mass loss to vary from star to star. This theme is developed by Rood (1973) and Renzini (1977).

The third fact to notice is that the luminosity of a horizontal-branch model is less sensitive to model mass than is the luminosity of a core hydrogen-burning model at the moment when hydrogen vanishes at the center. The luminosity of a horizontal-branch model is sensitive primarily to the composition of its main-sequence progenitor. If there were a way of estimating this composition directly from the observations, one could then theoretically estimate the luminosity of the horizontal branch at the position directly above the cluster main-sequence turnoff point. The observed depression of the cluster turnoff point below the horizontal branch would set the absolute luminosity of the turnoff point and comparison with theoretical time-constant loci would then provide an estimate of the mass of a star near the turnoff point and an estimate of cluster age. The problem with this algorithm is that, although the abundance by mass of elements heavier than helium is known with some precision (typically $Z \sim 10^{-4} - 10^{-3}$), globular cluster stars are in general too cool to allow a meaningful spectroscopic estimate of Y, the abundance by mass of helium at the surface. Less direct methods of estimating Y must be employed.

The exercise is illustrated in Figure 21 (Iben 1971*b*), where it has been assumed that $Z \sim 10^{-3}$ and $Y \sim 0.29$. Evolutionary tracks for models which are burning only hydrogen have been replaced by an approximation to an isochrone (which connects points of equal age along tracks of different initial mass) of age 12.5×10^9 yr. Along the straight line passing through the turnoff point along this isochrone, circles mark the location of the turnoff point for isochrones of different ages. The observations provide an estimate of the difference between the luminosity of the turnoff point and the luminosity of horizontal branch stars directly above turnoff. This difference is approximately a factor of 25, independent of Z (Sandage 1982), so one may guess the age of a typical globular cluster to be of the order of 12.5 billion years *if* $Y \sim 0.29$.

The rub, of course, is that we do not know Y directly from the observations of globular cluster stars. On the other hand, we do know something about hydrogen/helium ratios in hot

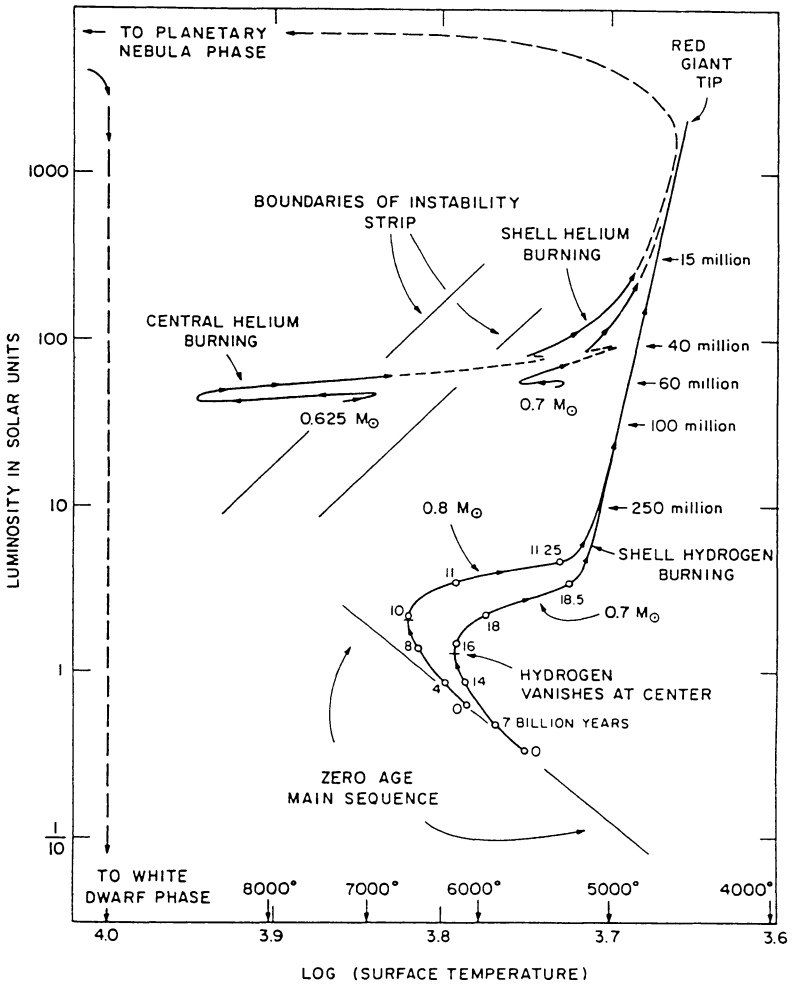

FIG. 20.—Tracks of mild Population II model stars during hydrogen and helium burning (Iben 1971*b*). Composition parameters are $Y = 0.3$ and $Z = 10^{-3}$. A number beside a circle gives the time in billions of years for a model to reach the circle from the zero-age main sequence. Times to reach the red-giant tip from points lower down on the giant branch are given in millions of years. The tracks are simplifications from the results of Iben and Rood (1970*a*, *b*).

Population I stars and in H II regions and the inferred values of Y are typically of the order of 0.26, and these should be larger than the values of Y for globular cluster stars. Further, big bang estimates of helium production suggest values of $Y \sim 0.23$ for the earliest generation of stars. A rough approximation to the relationship between cluster age t, Y, Z, and the brightness difference $\delta = \log L_{hb} - \log L_{tp}$ (where subscripts hb and tp denote horizontal branch and turnoff point, respectively) derived from data by Sweigart and Gross (1976, 1978), Rood (1972), Iben and Rood (1970*a*), and Simoda and Iben (1970) is

$$\log t_9 \sim 1.146 + 1.12\,\delta - 1.98\,\Delta Y - 0.084\,\Delta \log Z, \quad (10)$$

where t_9 is the age in units of 10^9 yr, $\Delta Y = Y - 0.23$, and $\Delta \log Z = \log Z + 3$. For $\delta \sim 1.36$, this expression gives the estimated ages in Table 2. Adopting $Y = 0.23$, it follows that the mean age of globular clusters is $\sim 15.5 \times 10^9$ yr. The uncertainty in this estimate is of the order of $\pm 3 \times 10^9$ yr.

The situation is far more complex than has been indicated here and there are many different points of view expressed in the literature (see discussions in Iben and Renzini 1984 and Renzini and Fusi-Pecci 1988). One view is that all of the globular clusters must be of essentially the same age (Sandage 1981, 1982; VandenBerg 1983). Expression (10) in conjunction with the observed near constancy of δ then requires that clusters with smaller Z also have a larger value of Y, a correlation that flies in the face of the most elementary theories of Galactic nucleosynthesis, and one might be inclined to distrust the theoretical models, especially the horizontal branch models, that have led to this result. Another view (Demarque 1980; see also Rood 1990) is that there is actually a spread in globular cluster ages, and the same near constancy of δ then implies (see Table 2) a variation in cluster ages from $\sim 12 \times 10^9$ yr to 17×10^9 yr. The ratio of oxygen (an important opacity source) to iron (the traditional element for defining Z) appears to be an order of magnitude larger in extreme Population II stars than in mild Population II stars (Sneden, Truran, and Wheeler 1989), and this works in the direction of reducing the spread in ages (VandenBerg, Bolte, and Stetson 1990).

In closing this section, the reader is warned that the horizontal branch models used in the discussion do not include con-

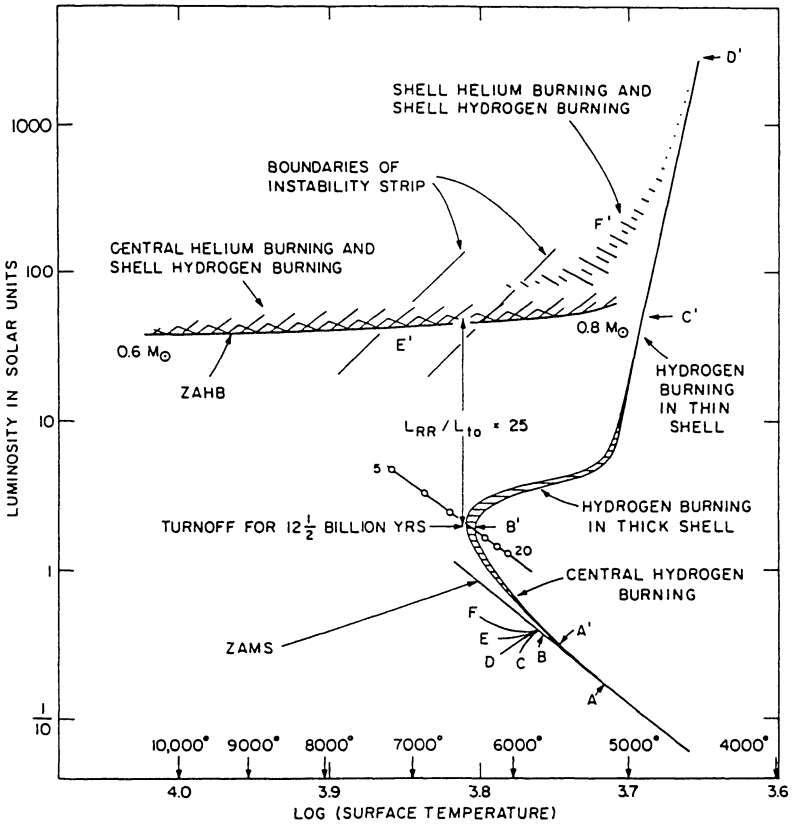

FIG. 21—A schematic showing an approximation to a theoretical isochrone of age 12.5×10^9 yr for models of initial composition $Y = 0.29$, $Z = 10^{-3}$ (Iben 1971*b*). On this isochrone, a model star at a position labeled with a primed alphabetic character originated at a position on the zero-age main sequence labeled with the corresponding unprimed alphabetic character. The age of the isochrone (12.5×10^9 yr) has been chosen in such a way as to give a luminosity difference between the turnoff point along the isochrone and the location of the horizontal branch directly above the turnoff to coincide with the observational luminosity difference of a factor of ~25.

vective overshoot or semiconvection, processes which have a sound physical basis and which have the effect of increasing the horizontal extent of tracks in the H-R diagram and the horizontal branch lifetime, both by a factor of ~2 over those presented here (Castellani, Giannone, and Renzini 1971*a, b;* Sweigart and Demarque 1972; Lee, Demarque, and Zinn 1990; Sweigart 1990).

VI. RADIAL PULSATIONS AND CLASSICAL VARIABLES

a) RR Lyrae Stars in Globular Clusters

Figure 22 describes the physical conditions in the envelope of a model horizontal branch star (Iben 1971*b*) which lies within the observed RR Lyrae strip sketched in Figures 20 and 21. The conditions in the minute helium and hydrogen ionization zones near the surface (the total mass above the base of the helium ionization zone is only $\sim 10^{-7}\, M_\odot$) are responsible for driving pulsations during which the star's luminosity can vary by a factor of 2 and radius can vary by 50%.

TABLE 2

GLOBULAR CLUSTER AGES VERSUS INITIAL COMPOSITION

Value of Y	$Z = 10^{-3}$	$Z = 10^{-4}$
0.20	$t_9 = 16.1$	$t_9 = 19.5$
0.23	$t_9 = 14.0$	$t_9 = 17.0$
0.26	$t_9 = 12.2$	$t_9 = 14.8$

In his pioneering efforts to understand the cause of Cepheid pulsations, Eddington thought that the major driving force is in some way connected with the interior energy source (Eddington 1926) and that the hydrogen ionization zone acts only to decrease dissipation in the envelope (Eddington 1941, 1942). Zhevakin (1953, 1954*a*, *b*) and Cox and Whitney (1958) were the first to suggest that the helium ionization zone could be responsible for driving, and Baker and Kippenhahn (1962) and Cox (1963) demonstrated with linear nonadiabatic calculations that this zone was a major source of driving. Christy (1962) and Baker and Kippenhahn (1965) then showed that the hydrogen ionization zone also contributes to driving. Figure 23 describes the driving (positive contribution to $\int PdV$ over a pulsation cycle) and damping (negative contribution to $\int PdV$ over a pulsation cycle) regions in a horizontal branch model as given by a linear nonadiabatic calculation (Iben 1971*a*). In this particular case, which is for the first harmonic radial mode, driving outweighs damping and, in a nonlinear calculation, the model would develop oscillations which increase in amplitude until a limit cycle where driving and damping exactly balance each other is reached (Christy 1962).

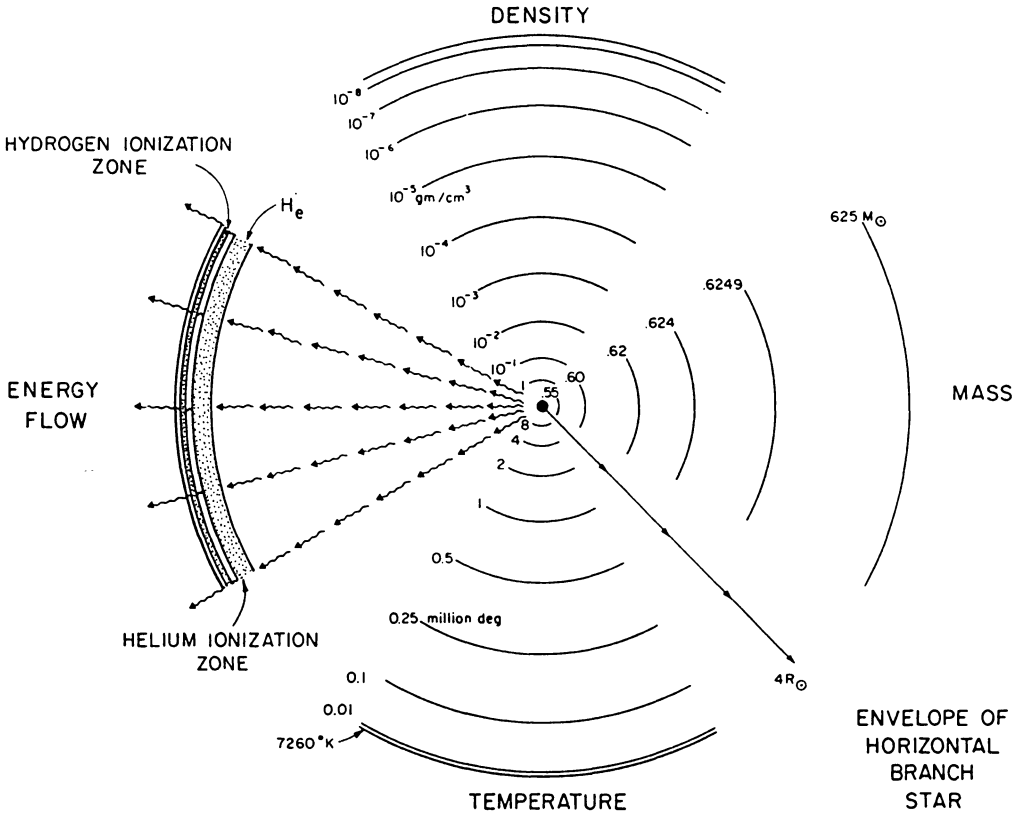

FIG. 22—Structure variables in the envelope of a model horizontal branch star which is unstable to pulsation in the first harmonic radial mode (Iben 1971*b*).

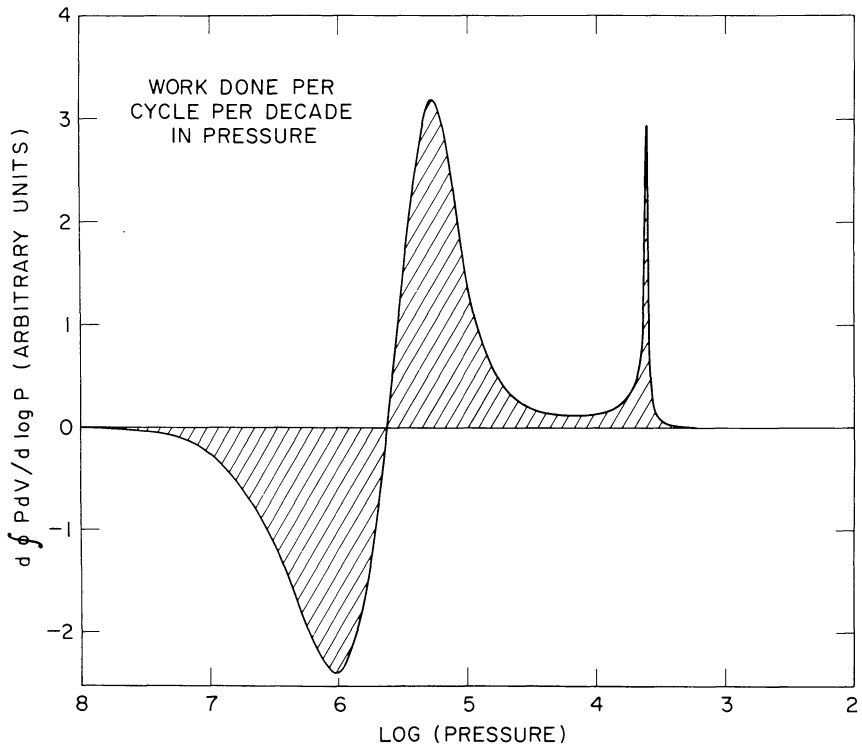

FIG. 23.—Damping (negative $\int PdV$) and driving (positive $\int PdV$) in the envelope of a model horizontal branch star with characteristics close to those described in Fig. 22. Pulsation is assumed to be in the first harmonic radial mode and the net contribution to $\int PdV$ is positive, indicating that the model is unstable to pulsation in this mode. From Iben (1971*a*).

Since all major contributions to damping and driving are confined to the envelope of a horizontal branch model, it is possible to determine the pulsational stability characteristics of such a model without reference to the properties of the interior at temperatures above, say, 10^6 K. In fact, the pulsational stability characteristics for models over a much larger portion of the H-R diagram can be explored in this way. The "blue edges" for pulsation in the fundamental and first harmonic radial modes shown in Figure 24 (Iben 1971*b*) have been constructed on the basis of a linear nonadiabatic pulsation analysis of 0.6 $M_\odot$ envelope models. All models to the left of a given blue edge are stable against pulsation in the stated pulsation mode. The reason for the existence of the blue edges has to do with the fact that, for a given model mass and luminosity, as surface temperature is increased, there is progressively less mass above the ionization zones, and the contribution of these zones becomes less and less effective.

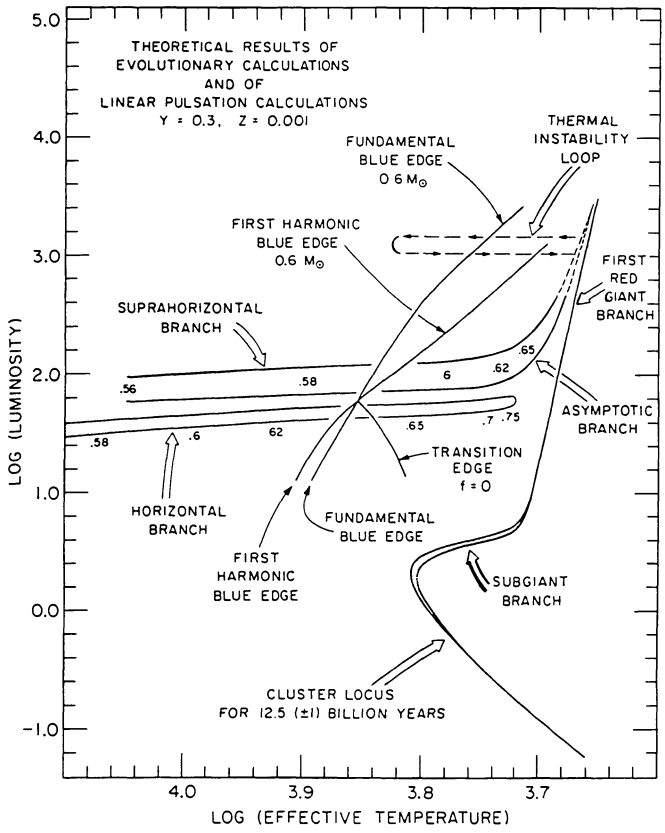

FIG. 24.—A variant of Fig. 21 with the additions of (1) blue edges for pulsation in the fundamental and first harmonic radial modes for models of mass 0.6 $M_\odot$, (2) the approximate location of thick shell helium-burning models (the suprahorizontal branch introduced by Strom *et al.* 1970), and (3) an early indication that thermal pulses could experience excursions forth from and back to the asymptotic giant branch (Iben 1971*b*). Intersections between the instability strip (to the red of the blue edges and to the blue of an unspecified red edge) and the horizontal branch, the suprahorizontal branch, and the postulated excursions from the AGB may be identified as the locations of RR Lyr stars, BL Her stars, and W Vir stars. The excursion from the AGB is now thought to be a one-time-only affair, and this accounts for the extreme rarity of W Vir stars in globular clusters. The transition is motivated by the observations which demonstrate that pulsation in the first harmonic mode is favored in a large region to the red of the fundamental blue edge where linear analysis shows models to be unstable in both the fundamental and first harmonic modes. From Iben (1971*b*).

Note that, at the luminosity level of the horizontal branch, there is a small region within which only the first harmonic mode is unstable. To the red of this region, both the fundamental and first harmonic modes are unstable. The observations quite clearly demonstrate that the first harmonic mode wins out over a substantial region to the red of the fundamental blue edge. The hypothetical curve labeled "transition edge" in Figure 24 is postulated to have the property that, for models between it and the first harmonic blue edge, full amplitude pulsation will be in the first harmonic mode and, for models to the red of this curve, full amplitude pulsation will be in the fundamental mode. The region of interest for making a comparison with real RR Lyrae stars is shown in Figure 25 (Iben and Huchra 1971), where also a red edge has been introduced. The position of the red edge is based on observation; to date, there has been no convincing theoretical calculation to define this edge. The best that theory has been able to accomplish is to note the fact that envelope convection begins to become important in the neighborhood of the observed red edge.

The horizontal branch is divided into three parallel segments, and it is assumed that each segment is populated uniformly by stars, but at a density which decreases with luminosity, as indicated. Stellar masses are taken from the results of evolution theory and the relationship between the period P and the model parameters M, L, and T_e is taken from the results of the linear pulsation theory. The net result is the theoretical number-period distribution shown in the top panel of Figure 26. Note that the four edges of this distribution coincide with the edges defined by the RR Lyrae stars in M3 (Hogg 1955), and this completes the demonstration that real stars are aware of a transition line which does not coincide with the theoretical fundamental blue edge. The fact that the relative numbers of stars in the two peaks of the observed distribution differ by a factor of ~2.5 from the relative numbers in the theoretical distribution says simply that, in the real situation, the stellar density increases with decreasing surface temperature and this is presumably a consequence of the physics of mass loss and rotation during the preceding giant branch phase.

Although nonlinear calculations suggest that the first harmonic mode wins out for a short distance to the blue of the fundamental blue edge (Christy 1966; Stellingwerf 1975; Cox 1980*b*) and thereafter the fundamental mode wins, a systematic study has yet to be performed. The simple comparison with the observations just given shows that the region over which the first harmonic wins out is somewhat larger than indicated by extant theoretical results.

b) Cepheid Distances and Number-Period Distributions

Theoretical blue edges can also be constructed in the luminosity-period plane. Examples for models of mass covering the range expected for Cepheids are shown in Figure 27 (Iben and Tuggle 1975). These edges have been constructed on the assumption that the mass of an average Cepheid is related to its luminosity according to the mass-luminosity relationship given by evolutionary models of Population I composition in the core helium-burning phase. The circles are defined by Ce-

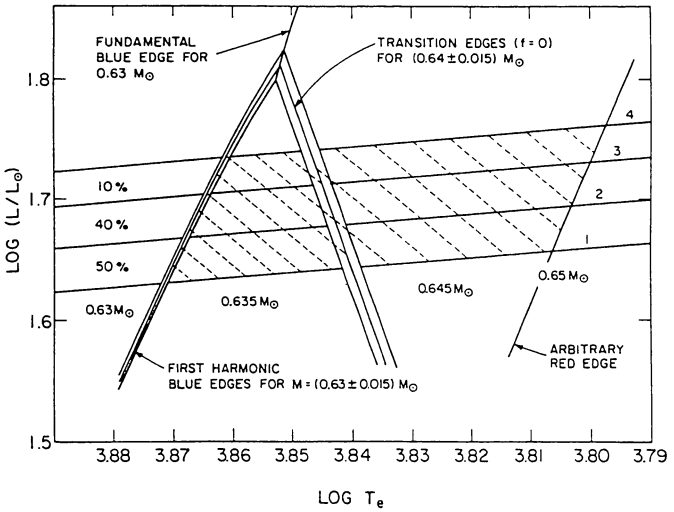

FIG. 25.—A simplified theoretical horizontal branch with blue edges, an arbitrary red edge, and conjectured transition edges for model masses of relevance (Iben and Huchra 1971).

pheids in Andromeda. Their positions in the left-hand panel have been derived by transforming from the photographic observations of Baade and Swope (1963) and by adopting a distance modulus of 24.12 mag (Sandage and Tammann 1971). The positions in the right-hand panel have been obtained by adjusting the distance modulus until the upper envelope of the observed distribution (excluding stars 11 and 27) is nearly touching the theoretical fundamental blue edge. This gives a distance modulus of 24.40 mag. Stars 11 and 27 are probably first overtone pulsators, and their positions with respect to the theoretical blue edges are not favored by either choice of modulus.

Using a PLT_eM relationship obtained from linear pulsation calculations one can also obtain a relationship between the mass and luminosity of individual Cepheids and the result for the 17 Andromeda Cepheids when a distance modulus of 24.4 mag is chosen is shown in Figure 28 (Iben and Tuggle 1975). The straight line,which satisfies the equation

$$\log M = 0.71 + 0.25\,(\log L - 3.25)\,, \qquad (11)$$

is a tolerable fit to the observed points, particularly when variables 11 and 27 are assumed to be pulsating in the first harmonic mode.

The same exercises can be carried out with Cepheids in the Magellanic clouds and in our Galaxy. For the LMC and the SMC one obtains distance moduli of 18.75 mag and 19.25 mag, respectively (Iben and Tuggle 1975). There are 12 Cepheids in Galactic clusters and one in front of a reflection nebula that Sandage and Tammann (1969, 1971) have used to define an observational period-luminosity relationship. Distances to these Cepheids were assigned by the main-sequence fitting technique normalized to the best estimate of the distance to the Hyades available at the time. If the distance moduli estimated in this way are increased by 0.25 mag and the theoretical PLT_eM relationship is then used to estimate masses of the 13 Cepheids, the results shown in Figure 29 (Iben and Tuggle 1975) are obtained. Note that the resultant mean mass-luminosity relationship obtained in this way is identical with the mass-luminosity relationship defined by Andromeda Cepheids at a distance modulus of 24.4 mag and this agreement has been achieved by increasing the distance moduli of both the Hyades and Andromeda by essentially the same amount.

Had no adjustment been made in assumed moduli, the derived mass-luminosity relationships for both Andromeda Cepheids and Galactic Cepheids would have the same slope, but the derived mass of each Cepheid would be some 40% smaller than given by evolutionary models (Cogan 1970; Iben and Tuggle 1972). It is not clear that this particular mass discrepancy has permanently disappeared (see Cox 1980*a*, *b* for an affirmative point of view) and there are other apparent discrepancies between theory and observation which definitely still remain (Cox 1980*a*, *b*; Simon 1982). Recently Feast and Walker (1987) have suggested that theoretical period-luminosity relationships overestimate the brightness of Cepheids in the Magellanic clouds by ~0.5 mag. They estimate distance moduli of 18.47 and 18.78 mag for the LMC and SMC, respectively, and present

$$\langle M_v \rangle = -1.35 - 2.78 \log P$$

as a summary of the observations in the visual. On the other hand, theoretical estimates which fold together the results of evolutionary theory and the results of pulsation theory in the linear approximation give (Becker, Iben, and Tuggle 1977)

$$M_{\rm bol} \sim -1.51 - 3.13 \log P\,, \qquad (12)$$

independent of metallicity, and (even on taking bolometric corrections into account) it would appear that a major part of the quoted 0.5 mag discrepancy comes from a difference in the

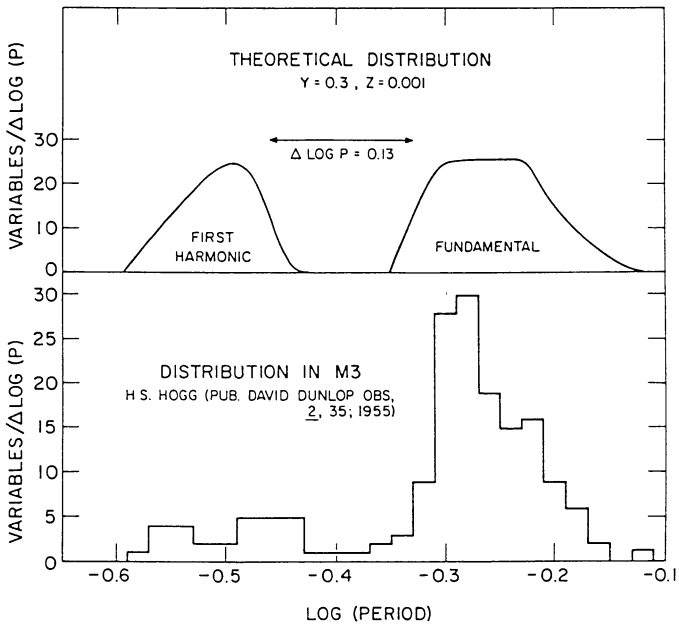

FIG. 26.—A theoretical number-period distribution (Iben and Huchra 1971) compared with the distribution for M3 (Hogg 1955).

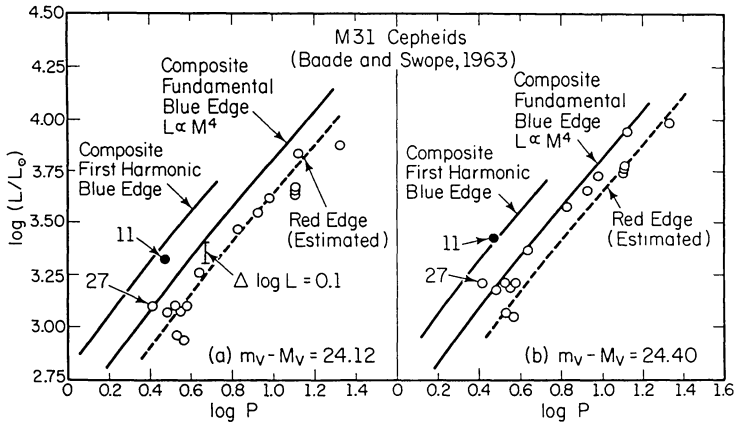

FIG. 27.—Andromeda Cepheids (Baade and Swope 1963) in the period-luminosity plane when the distance modulus is chosen as 24.12 mag (*left-hand panel*) or as 24.4 mag (*right-hand panel*). Along the composite blue edges, $\log M = 0.73 + 0.25 (\log L - 3.25)$. From Iben and Tuggle (1975).

slopes of the adopted period-luminosity relationships. It is interesting that the theoretical relationship fits the Andromeda data quite well (compare with the circles in the right-hand panel of Fig. 27), and it also fits the SMC and LMC data quite well (see Figs. 4 and 8 in Iben and Tuggle 1975). In summary, the theories of stellar pulsation and evolution provide a period-luminosity relationship that is, in the view of this reviewer, consistent with the observations, but this view is not shared by all.

Another combination of the results of pulsation calculations and of evolution calculations that can be used to interpret observational results is illustrated in Figures 30 and 31 (Becker, Iben, and Tuggle 1977). The theoretical tracks in Figure 30 are for models of the same initial helium abundance $Y = 0.3$, but the metallicity parameter Z is 10 times smaller for the tracks on the left than it is for tracks on the right. Note that the core helium-burning band, which is formed by joining together segments along which tick marks occur at the highest density, crosses the instability strip at a lower luminosity and for smaller masses for the models of lower metallicity. The period of a Cepheid at the intersection point is shorter for the metal-poor case than for the metal-rich case and, because the stellar mass is less, the lifetime in the instability strip is longer in the metal-poor case.

Interpolating within the tracks for any given composition, one can construct a plot which relates lifetime in the Cepheid strip to model mass and, using the theoretical PLT_eM relationship, one can determine the period as a function of position along the instability strip. Then, assuming that the Cepheid birthrate depends on mass in the same way as the Salpeter (1955) mass function, one can construct a theoretical plot of Cepheid number versus period, with results shown in Figure 31 (Becker, Iben, and Tuggle 1977). As expected, the smaller

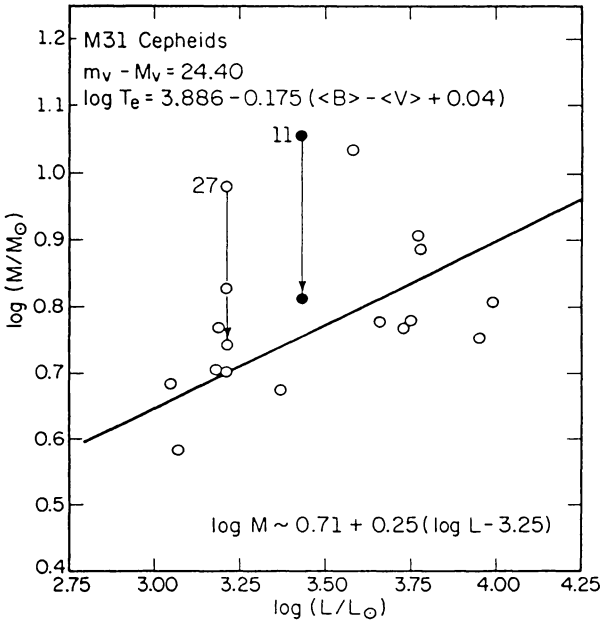

FIG. 28.—Andromeda Cepheids in the mass-luminosity plane when the distance modulus is chosen as 24.4 mag (Iben and Tuggle 1975). The higher masses for stars 11 and 27 obtain if pulsation in the fundamental mode is assumed; the lower masses are appropriate if these stars are pulsating in the first harmonic mode.

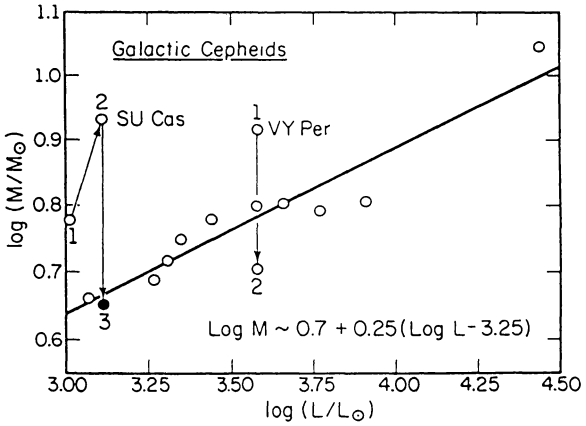

FIG. 29.—Cepheids in Galactic clusters in the mass-luminosity plane when the distance modulus to individual Cepheids is chosen to be 0.25 mag larger than in Sandage and Tammann (1969). The third mass estimate for SU Cas and the second for VY Per are to be preferred. From Iben and Tuggle (1975).

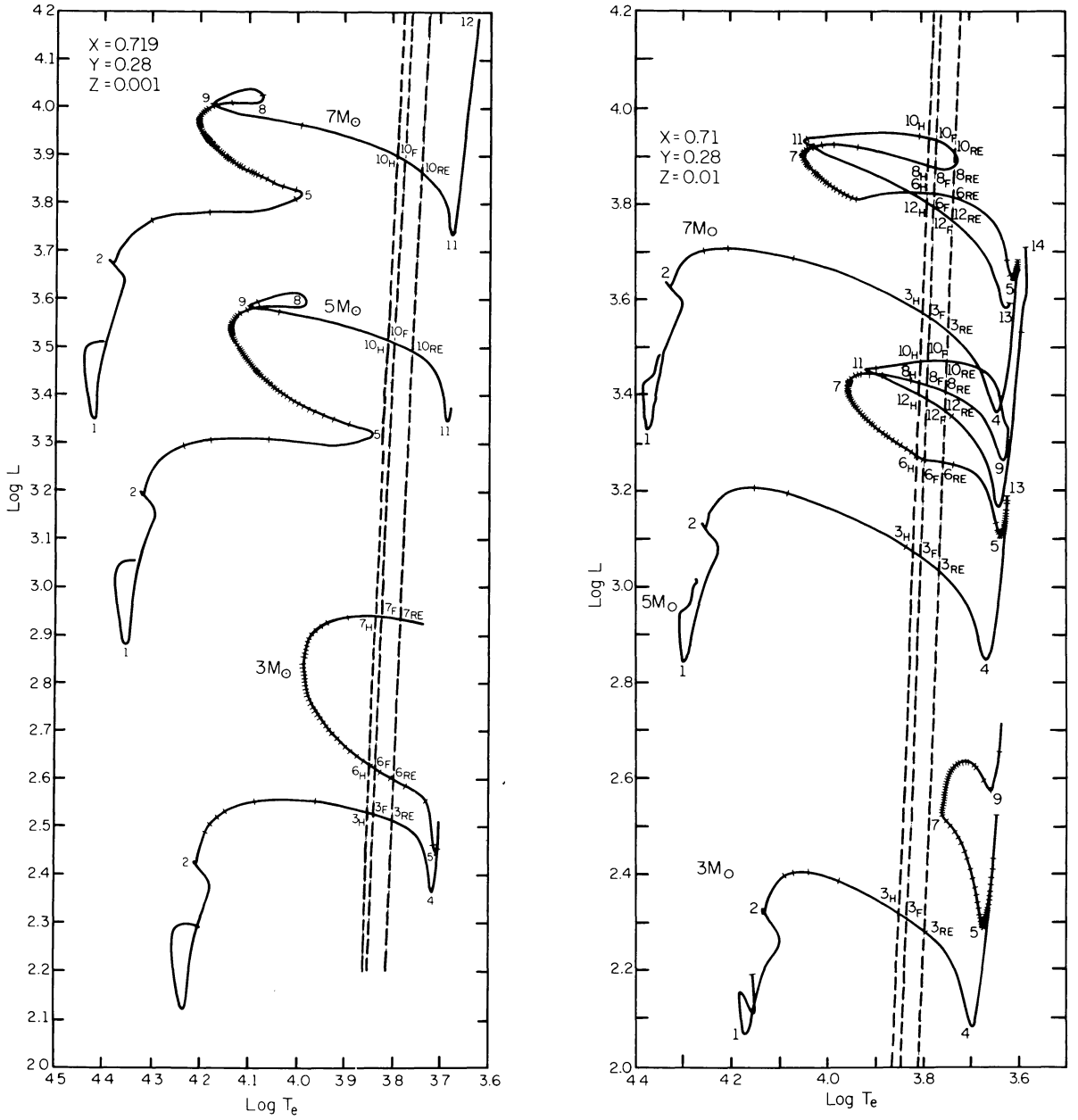

FIG. 30.—Evolutionary tracks of 3, 5, and 7 $M_\odot$ model stars in the H-R diagram for $Y = 0.28$ and $Z = 0.001$ (*left-hand panel*) and Z = 0.01 (*right-hand panel*). The dashed lines in order from left to right are the first harmonic blue edge, the fundamental blue edge, and an arbitrarily chosen red edge. After the main sequence, tick marks are placed at time intervals of 10^6 yr for the 3 $M_\odot$ model, 2×10^5 yr for the 5 $M_\odot$ model, and 10^5 yr for the 7 $M_\odot$ model. From Becker, Iben, and Tuggle (1977).

the metallicity, the shorter the mean period of the distribution. Most surprising, however, is the extremely strong dependence on metallicity of expected total numbers of Cepheids.

The qualitative and rough quantitative accord between the theory and observation is illustrated in Figure 32 where number-period distributions for Cepheids in the Magellanic Clouds are shown (Payne-Gaposchkin 1971*a*, *b*). A typical star in the SMC is known to be more metal poor than the typical star in the LMC by a factor of perhaps 2–4, and it is gratifying to see that the mean period of the number-period distribution for the SMC is smaller than that for the LMC, consistent with theoretical expectations. The fact that the widths of the observed number-period distributions are approximately twice as large as the theoretical distribution for an ensemble of homogeneous composition could be taken as an indication that there is a considerable spread in composition among stars in each Cloud (by factors of 3–10). The fact that there are as many Cepheids in the SMC as there are in the LMC, even though the total mass of the SMC is perhaps 10 times smaller than the mass of the LMC, is also in qualitative accord with the theory. For example, if $Z = 0.01$ is appropriate for the LMC, then the fact that there are 10 times as many Cepheids per total stellar mass in

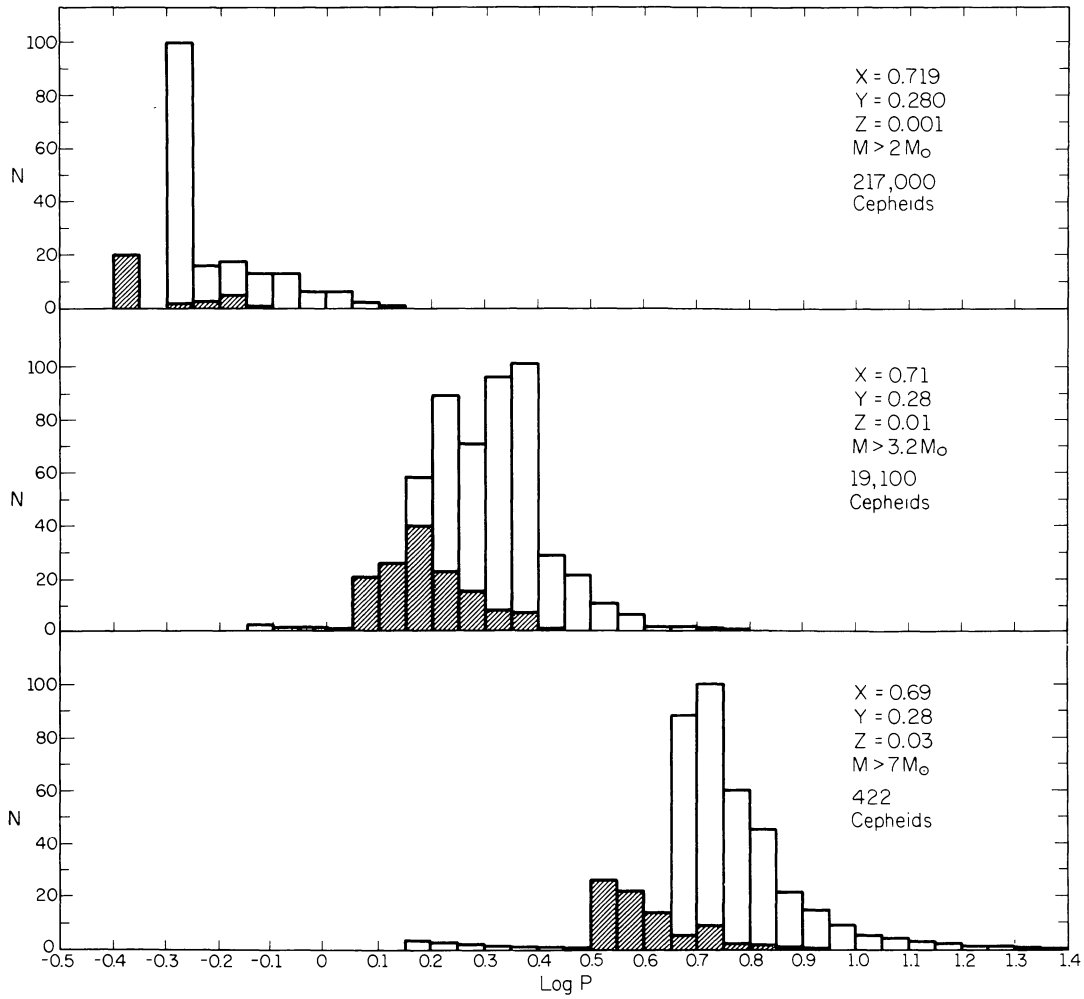

FIG. 31.—Theoretical number-period distributions for Cepheid variables as a function of the metallicity parameter Z when $Y = 0.28$ (Becker, Iben, and Tuggle 1977). All distributions are normalized so that the maximum number density N is 100 and it has been assumed that birthrate is proportional to $M^{-2.35}$.

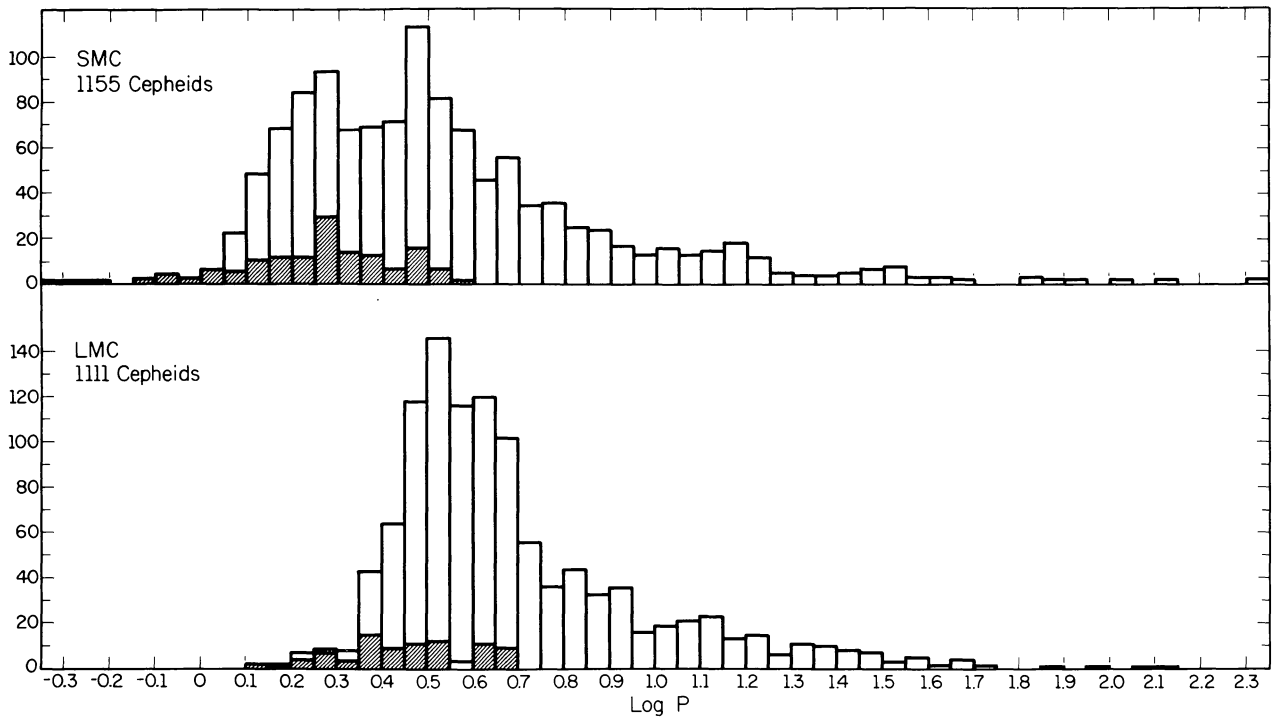

FIG. 32.—Number-period relationships defined by Cepheids (derived from data by Payne-Gaposchkin 1971*a*, *b*). From Becker, Iben, and Tuggle (1977).

the SMC as in the LMC could be used to estimate $Z = 0.001$ for the SMC (compare the upper two panels in Fig. 31). However, this would be placing far too much confidence in the ability of the models to mimic real stars, particularly with regard to surface temperature at a given stage of evolution. This latter characteristic is extremely sensitive to the treatment of convection and to the envelope opacity, and no model result should be taken at face value. A graphic demonstration is the fact that, although a correspondence between theoretical and observed Cepheid numbers can in this particular example be achieved by supposing that $Z_{SMC} \sim 0.1 \times Z_{LMC}$, the resultant theoretical difference in mean period far exceeds the observed difference. Furthermore, spectroscopic determinations of metallicities totally rule out such a large difference in Z.

VII. SOLAR MODELS AND SOLAR NEUTRINOS

The search for solar neutrinos became the "solar neutrino problem" with the publication by Davis, Harmer, and Hoffman (1968) of an experimental upper limit of 3 SNU (1 SNU = 10^{-36} neutrino captures per second per ^{37}Cl atom). The nature of the discrepancy is illustrated in Figure 33 (Iben 1968, 1969), where a predicted neutrino flux (in units of 3 SNU) is given as a function of the initial helium abundance Y. The major contributors to the predicted neutrino counting rate are neutrinos emitted in the reactions $^8\mathrm{B}(i^+\nu)^8\mathrm{Be}^*$ and $^7\mathrm{Be}(e^-, \nu)^7\mathrm{Li}$. Shown also are model central temperature and density. The metallicity or (more accurately) the opacity parameter Z is correlated with Y in a manner which equation (9) makes transparent.

The opacity used in the models on which Figure 33 is based is a fit to the opacity tables of Keller and Meyerott (1955), which do not include bound-bound transitions, and the nuclear cross section factors employed have long since been superceded (see also below). However, the basic lesson of Figure 33 is still true today: consistency with the experimental upper limit cannot be achieved except by choosing a value of Y which is (1) quite small compared with values of $Y > 0.25$ that are estimated by an analysis of lines in the spectra of hot Population I stars and H II regions and (2) is small compared with the value of $Y \sim 0.23$ produced by standard big bang models. It is reasonable to suppose that Y for the Sun is similar to that in other Population I stars and in the interstellar medium, especially since most other elements in stars (where measureable) are approximately in the solar-system distribution, and one must conclude that the real discrepancy represented in Figure 33 is at least a factor of 5. The same lesson is told by models constructed by using opacity tables of Cox and Stewart (1970), which do include bound-bound transitions, and nuclear reaction cross section factors that are quite similar to those in current favor (Abraham and Iben 1971).

Nuclear cross sections of relevance in solar models are in general an extrapolation from measurements at energies much higher than those of relevance in the models; an estimate of the cross section for the basic $p(p, e^+\nu)d$ reaction is, of course, obtained only by doing a theoretical calculation. Given these facts, it is appropriate to explore the sensitivity of predicted model neutrino fluxes to the nuclear cross sections. This sensitivity is illustrated in Figure 34 (Iben 1968, 1969), where variations in particular center of mass cross section factors, S_{ij}, are given in terms of the factors S_{ij}^0 used in constructing Figure 33. A rough analytical approximation to the detailed model results is (Iben 1977*b*)

$$F_\nu \sim 0.91 \text{ SNU } y^{2.65} S_{34} S_{33}^{-0.5} S_{11}^{-1.46} \times (1 + 8.1 y^{3.97} S_{17} S_{e7}^{-1} S_{11}^{-1.95}), \quad (13)$$

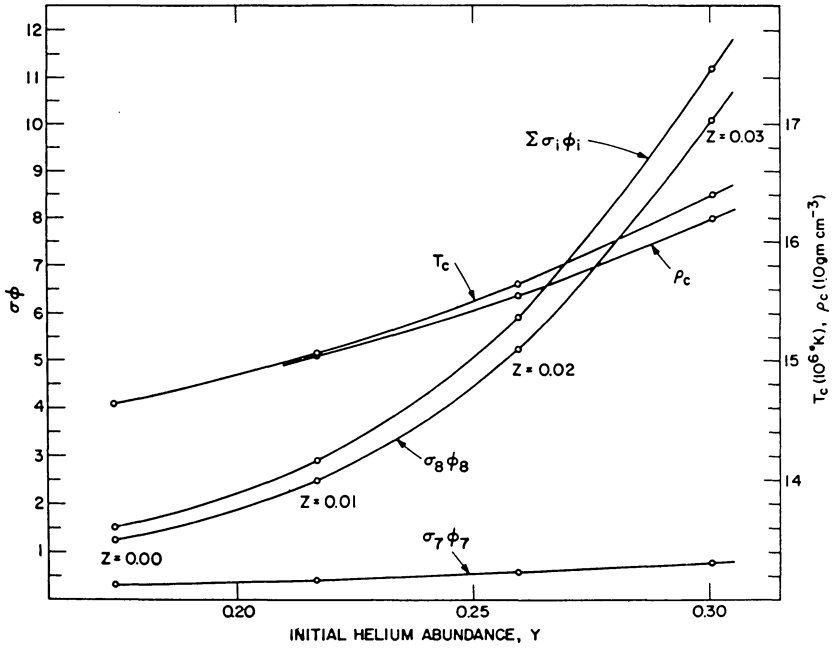

FIG. 33.—The relationship between the initial helium abundance Y (and the metallicity or opacity parameter Z) and the total neutrino counting rate ($\Sigma\sigma_i\phi_i$), the contribution of ^{7}Be neutrinos ($\sigma_7\phi_7$), the contribution of ^{8}B neutrinos ($\sigma_8\phi_8$), the solar central temperature (T_c), and the solar central density (ρ_c). All $\sigma_i\phi_i$ are given in units of 3 SNU, the original Davis, Harmer, and Hoffman (1968) upper limit. From Iben (1968, 1969).

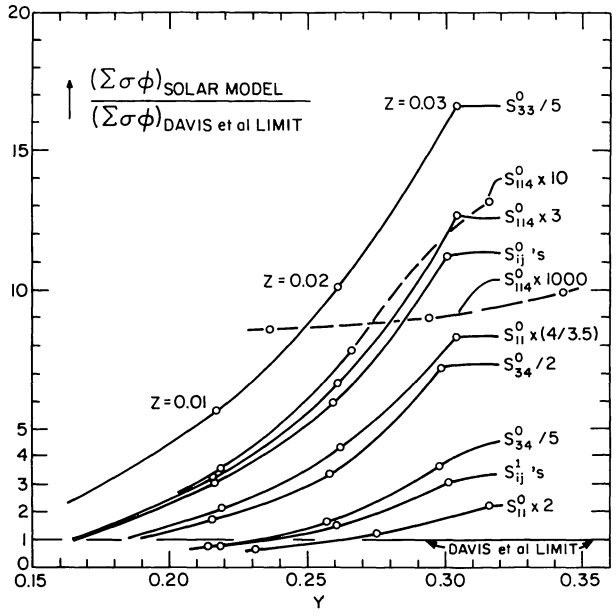

FIG. 34.—The dependence of neutrino counting rate on Y, Z, and center of mass cross section factors S_{ij} relative to a canonical set S^0_{ij}. From Iben (1969).

where $y = Y/0.25$ and the S_{ij}'s are measured relative to a choice of cross sections thought optimal at the time.

Over a period of two decades, the Davis experiment has yielded an average counting rate of 2 SNU, with variations of the order of ±2 SNU (Davis *et al.* 1990). The first results of the Kamiokande experiment (Hirata *et al.* 1989) are consistent with the concurrent results of the Davis experiment and, if one interprets fluctuations in the experimental counting rate as purely statistical, perhaps the most promising suggestion for removing the discrepancy is the so-called MSW (Mikheyev, Smirnoff, and Wolfenstein) effect which supposes that at least one flavor of neutrino has a very small mass, that the mass eigenstate neutrino is a mixture of flavors, and that, because the effective mass of the electron neutrino is a function of the electron density, the particular flavor which dominates in each mass eigenstate varies as the neutrino passes outward through the Sun (Mikheyev and Smirnoff 1986; Wolfenstein 1978; Bethe 1986; Rosen and Gelb 1986).

However, the variations in the counting rate may be anti-correlated with sunspot number (Davis 1990), implying that the neutrino may possess a magnetic moment (in contradiction with some theoretical considerations). In any case, the study of solar neutrinos may be telling more about the physics of neutrinos than about the solar interior. An excellent account of the current situation is given by Wolfenstein and Beier (1989). Several other schemes for understanding the solar neutrino problem are discussed by Taylor (1989).

VIII. ASYMPTOTIC GIANT BRANCH STARS: THERMAL PULSES, NUCELOSYNTHESIS, AND THE THIRD DREDGE-UP

Thermal pulses were first discovered in AGB models of low-mass Population II stars by Schwarzschild and Härm (1965) and in AGB models of intermediate-mass Population I stars by Weigert (1966). The understanding that these models are analogs of real stars, some of which become carbon stars and some of which exhibit evidence for extensive interior production of neutron-rich isotopes known as *s*-process isotopes, has been achieved rather slowly over a period of several decades. That red giants in some stage of evolution produce *s*-process isotopes has been known since Merrill (1952) discovered in several red giants the element technicium, the longest lived isotope of which has a half life of only $\sim 10^5$ yr. However, there was not general awareness that the Tc-exhibiting red giants or the red giant carbon stars are, in general, more luminous than red giants which possess an electron-degenerate helium core. It was not until the theoretical discovery of thermal pulses that it was realized that the red giants exhibiting lines of molecules containing Tc are in fact AGB stars, and it was not until surveys of carbon stars in the Magellanic clouds were conducted (Blanco, McCarthy, and Blanco 1980) that it became clear that carbon stars are AGB stars of low luminosity and that AGB stars of large luminosity do not become carbon stars.

The search for an understanding of the site of the production of *s*-process isotopes was initiated by the classic study of Burbidge *et al.* (1957), which introduced the concept of distinguishing between (1) situations in which the time scale for neutron capture by β-unstable nuclei is in general larger (slow [*s*-capture]) than the time scale for their β decay and (2) situations in which the time scale for neutron capture is smaller (more rapid [*r*-capture]) than the time scale for β decay, except when the neutron number is near the magic values of 50, 82, and 126. Cameron identified the endothermic reactions $^{13}C(\alpha, n)^{16}O$ (Cameron 1955) and $^{22}Ne(\alpha, n)^{25}Mg$ (Cameron 1960) as promising channels for producing neutrons. The studies of Clayton *et al.* (1961) and of Seeger *et al.* (1965) demonstrated that an exponential distribution of exposures is necessary to produce a solar-system distribution of *s*-process isotopes, and Ulrich (1973) demonstrated that such a distribution follows naturally in thermally pulsing AGB stars in consequence of the overlap of successive helium-burning convective shells. However, the manner in which neutrons become available for neutron-capture nucleosynthesis and the manner in which freshly synthesized elements make their way to the surface have been hotly contested topics for over two decades, and a final, definitive story has yet to be constructed.

a) AGB Stars of Large CO *Core Mass*

The structure of a Population I model star of mass 7 $M_\odot$ as it is beginning the thermally pulsing stage is shown in Figure 35 (Iben 1973*a*). Note that the size of the helium-exhausted CO core (*lower panel;* radius $R \sim 0.011\ R_\odot$) bears the same relationship to the size of the envelope (*upper panel*) as the size of the proton in a hydrogen atom bears to the size of the electron cloud about it (this is a convenient mnemonic which has primarily aesthetic significance). Note, further, that the temperature of the core is constant to within a factor of ~2; electron conduction is responsible for this near constancy. Because of neutrino losses, the temperature in central regions is less than in the middle of the core. The small bump in the temperature profile just beyond the outer edge of the CO core is due to the release of nuclear energy by the triple-alpha reaction as a thermal pulse gets underway.

In Figure 36 is shown the variation with time of several global and structural characteristics of the 7 $M_\odot$ model during

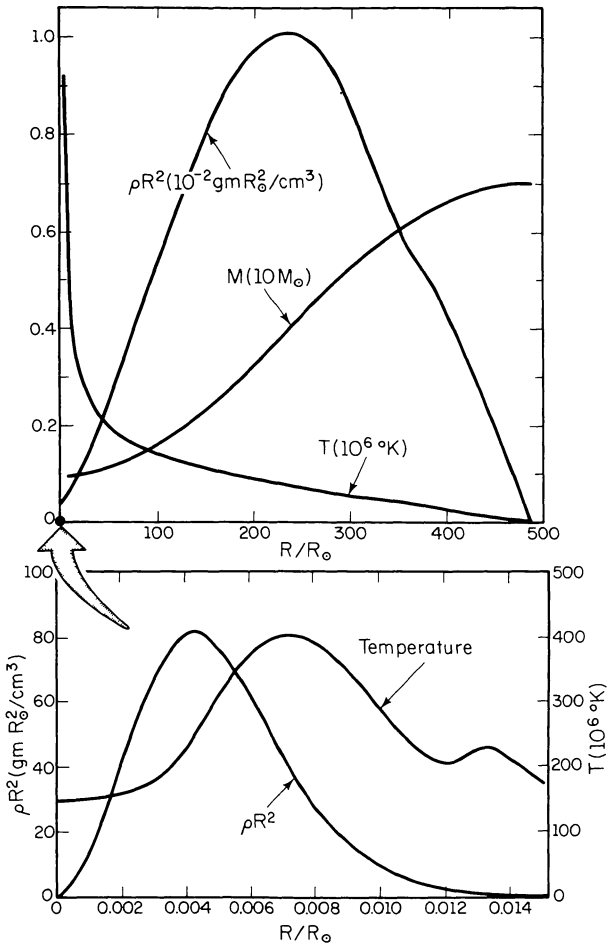

FIG. 35.—Structure of an AGB model of mass 7 $M_\odot$. The upper panel gives the temperature [$T(R)$], mass [$M(R)$], and dM/dR (ρR^2) as a function of radius R in the envelope of the model. The lower panel gives temperature and dM/dR within the hydrogen-exhausted core of the model.

and between two early (the seventh and eighth) thermal pulses (Iben 1975). Of particular interest is the fact that, following each thermonuclear flash, the base of the convective envelope (at mass point M_{CE}) reaches down past the XY discontinuity (the mass point M_{XY} below which there is no hydrogen), approaching the position below which a substantial amount of helium has been converted into carbon in a convective shell during the preceding flash (the outer edge of this carbon-rich region is labeled "carbon discontinuity"). Note that, with each successive pulse, the base of the envelope comes closer to the carbon discontinuity and, as shown in Figure 37 (Iben 1976), it actually soon extends into the carbon-rich region. This result was corroborated by Sugimoto and Nomoto (1975), by Fugimoto, Nomoto, and Sugimoto (1976), and by many authors since. In Figure 37, carbon-abundance profiles (*solid curves to the left*), the location of the convective helium-burning shell (*cross-hatched regions*), the location of the inner edge of the convective envelope (*single hatched regions*), and the position of the XY discontinuity are shown as a function of time; time increases upward.

As the base of the convective envelope extends into the carbon-rich region, fresh carbon and other products of helium-burning nucleosynthesis are mixed throughout the convective envelope and appear at the surface. This process is called the "third dredge-up." It is to be emphasized that the term "dredge-up" is a proper description only in the mass coordinate system. In the spatial coordinate system, matter in the carbon-rich region and above is actually moving outward, so in this coordinate system, carbon is being "thrown up" rather than being dredged up.

As is evident from the amount of fresh carbon dredged into the envelope after each helium shell flash, the illustrative model will develop a surface abundance of carbon in excess of the surface abundance of oxygen (and hence become a carbon star) by the time the mass of its CO core has increased by only $\sim 0.05\ M_\odot$, unless temperatures near the base of the convective envelope are high enough during the interpulse phase for carbon to be effectively converted into nitrogen by hydrogen-burning reactions. Unfortunately, whether or not carbon burns into nitrogen in a model depends on the choice of a parameter (the ratio of mixing length to scale height) in the standard treatment of convection. Furthermore, there are indications both from the observations (the existence of planetary nebulae) and from theory (Wood 1974, 1979; Tuchmann, Sack, and Barkat 1978, 1979) that dynamical instabilities may terminate the existence of an AGB star before it becomes a carbon star even if it otherwise has the potential for becoming a carbon star.

It is at this juncture that results of studies of carbon stars and of other AGB stars in the Magellanic Clouds and in our Galaxy may be invoked to clarify issues that cannot be answered unambiguously solely from theoretical calculations. Richer, Olander, and Westerlund (1979) have found that no more than about a half-dozen carbon stars in the Magellanic Clouds are of magnitude brighter than roughly −6 mag. A grism survey of the bar west field in the LMC (Blanco, McCarthy, and Blanco 1980) shows that the carbon star number-magnitude distribution is a bell-shaped curve extending from roughly −4 mag to roughly −6 mag. Studies of globular clusters in the Clouds (Frogel, Mould, and Blanco 1990) show that only clusters of intermediate age (10^8 yr < age < 10^9 yr) contain carbon stars and that these carbon stars are almost always among the brightest AGB stars in the clusters. This positioning of carbon stars among other AGB stars is in qualitative accord with the theoretical expectation that there is a minimum core mass below which dredge-up does not occur and that, for more massive stars, many pulses may be necessary for carbon star characteristics to be achieved.

The cluster studies demonstrate further that (1) the younger the cluster, the brighter the brightest AGB stars and (2) *no AGB stars* in clusters, whether carbon stars or not, are brighter than about −6 mag. From point 1 one may argue general qualitative agreement with the theory which predicts larger CO core masses and hence larger luminosities (see eq. [4]) for more massive progenitors. From point 2 and equation (4) it follows that envelope ejection must terminate the life of a real AGB star once its core mass exceeds $\sim 0.85\ M_\odot$, whether this occurs immediately upon reaching the TPAGB or whether it occurs during evolution along the TPAGB.

That real stars of fairly large initial mass become TPAGB stars with core masses larger than 0.85 $M_\odot$ and do not eject their hydrogen-rich envelopes immediately upon becoming

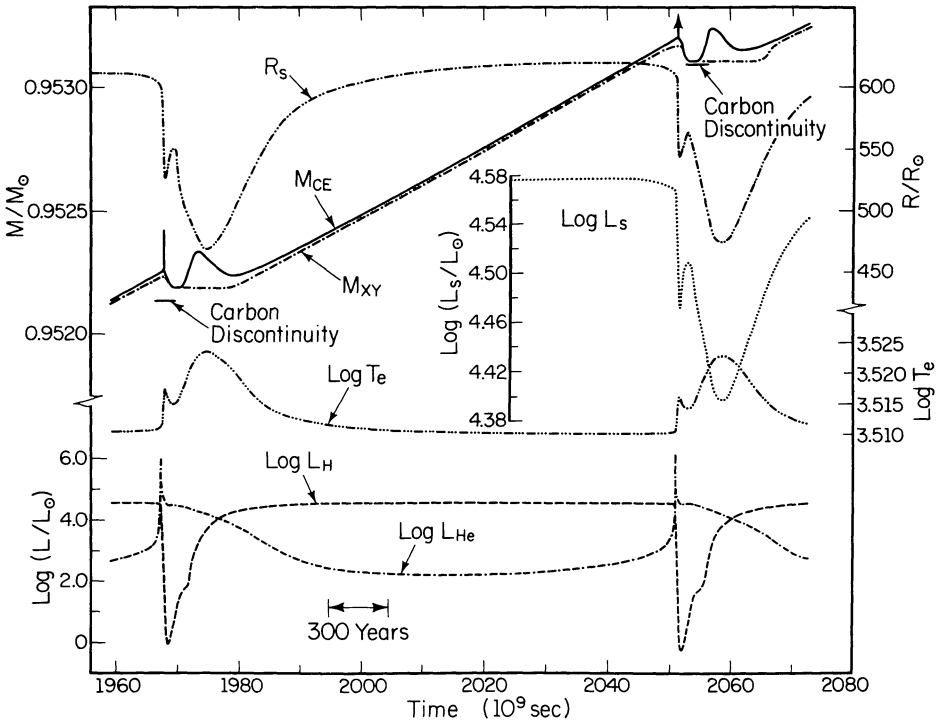

FIG. 36.—Variation with time of several global and interior characteristics of 7 $M_\odot$ AGB model of Population I composition during a period encompassing the seventh and eighth thermal pulses. Shown are surface radius (R_s), mass at the base of the convective envelope (M_{CE}), mass at the location of the hydrogen-helium "discontinuity" (M_{XY}), surface luminosity (L_s), surface temperature (T_e), hydrogen-burning luminosity (L_H), and helium-burning luminosity (L_{He}). From Iben (1975).

TPAGB stars has been demonstrated by Wood, Bessell, and Fox (1983) who divide the long period variables (LPVs) in the Clouds into two groups: those with normal strengths of ZrO bands and those with enhanced strengths. They identify members of the first group, which are scattered randomly through the luminosity-period diagram, as ordinary supergiants which do not experience AGB evolution and show that members of the second group fall within a band in the luminosity-period diagram extending up to and beyond luminosities given by TPAGB models of CO core mass $M_{CO} = 1.1\ M_\odot$. The members of the first group are in general more luminous than those in the second group, consistent with their being too massive to become AGB stars. Wood, Bessell, and Fox suggest that the ZrO enhanced LPVs are indeed TPAGB stars of core mass larger than the magic 0.85 $M_\odot$ and that the enhanced ZrO is a consequence of the formation of Zr in the convective helium-burning shell during a shell flash and of dredge-up of this fresh Zr following the flash.

The number of LPVs in the Clouds is an order of magnitude smaller than the number of Cepheids. Cepheids have masses which identify them as progenitors of AGB stars of large initial core mass. Since the lifetime of a typical Cepheid is $\sim 10^6$ yr (Becker, Iben, and Tuggle 1977), this means that the lifetime of a typical LPV is less than $\sim 10^5$ yr. In this short a time, the mean interpulse brightness can increase by no more than ~ 0.1 mag, the mass of the CO core can increase by only a few times 0.01 $M_\odot$, and the amount of fresh carbon that can be dredged up cannot convert the star into a carbon star, even if the carbon could resist conversion into nitrogen by hydrogen burning. The theoretical models of Tuchman, Sack, and Barkat (1978, 1979) predict that, once a critical luminosity is exceeded, an AGB star will eject its hydrogen-rich envelope in only 10^3 yr (which is less than the time between thermal pulses for a model of core mass $M_{CO} = 0.95\ M_\odot$). The difficulty comes in determining what this critical luminosity is as a function of core mass, of stellar mass, and of composition. The observations indicate that the critical mass is not exceeded until after the star has reached the thermally pulsing stage and experienced a sufficient number of pulses to produce overabundances of Zr at the surface. Therefore the critical mass must increase with increasing core mass, and the time scale for building up to a hydrodynamical instability is long compared with the interpulse lifetime.

The ZrO-rich LPV band extends to $M_{bol} \sim -7.3$, the theoretical upper limit for an AGB star with a CO core mass of 1.4 $M_\odot$. However, the maximum initial mass of an electron-degenerate CO core is $\sim 1.1\ M_\odot$, and we have inferred that a luminous AGB star can only live long enough to increase its core mass by a few times 0.01 $M_\odot$. A straightforward interpretation of the facts is that the degenerate cores of the most luminous LPVs are actually composed predominantly of oxygen and neon (ONe cores) and that the progenitors of these stars have initial masses in the 8–12 $M_\odot$ range (Nomoto 1984, 1987). If its mass reaches $\sim 1.37\ M_\odot$, an ONe core collapses in consequence of electron captures on the trace isotope ^{24}Mg and on the abundant isotope ^{20}Ne (Miyaji *et al.* 1980; Sugimoto and Nomoto 1975); the end result is a "silent supernova" which leaves a remnant neutron star (Nomoto 1984, 1987).

Complementary information about the abbreviated lifetime

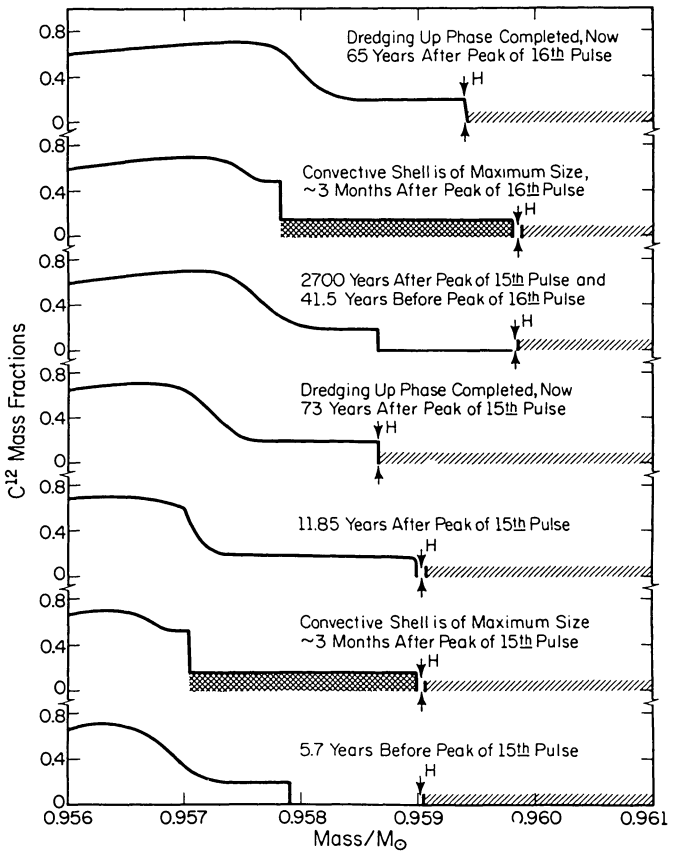

FIG. 37.—Carbon profiles and location of convective regions during two successive helium-shell flashes and dredge-up episodes in the AGB 7 $M_\odot$ model. Time increases upward. From Iben (1976).

of AGB stars comes from comparisons between the masses of the brightest white dwarfs in Galactic open clusters and the masses of stars near cluster turnoff (Weidemann and Koester 1983; Reimers and Koester 1982; Weidemann 1987, 1990). The amount by which the mass of the progenitor of the brightest white dwarf exceeds the masses of stars near turnoff can be estimated, and one can establish an empirical relationship between the mass of a white dwarf and the mass of its progenitor. As an example, Reimers and Koester (1982) estimate the mass of the progenitor of a $\sim 0.9\ M_\odot$ white dwarf in the cluster NGC 2516 to be $\sim 5\ M_\odot$, compared with a mass of $\sim 6\ M_\odot$ estimated by considerations involving the lifetimes of Magellanic cloud AGB stars (see Fig. 10).

A very recent discovery by Blöcher and Schönberner (1990) may substantially modify those arguments given in this section that assume the existence of a well-defined relationship between the luminosity of an AGB star of intermediate mass during the quiescent hydrogen-burning phase and the mass of its CO core. They find that, for a choice of mixing length over scale height large enough that a substantial fraction of the hydrogen-burning luminosity is formed in the convective envelope, the mean luminosity of the TPAGB models increases steadily with each pulse, becoming considerably larger than the Eddington luminosity of a star of mass equal to the mass of the CO core (the luminosity given by equation (4) is less than this luminosity). It is the absence of a finite radiative region between the hydrogen-burning shell and the base of the convective envelope that permits this to occur, and the phenomenon has apparently escaped detection because of the large number of pulses required to demonstrate it. If the model mass is held fixed, the mean luminosity could, in principle, continue to increase until it reached the Eddington limit appropriate to the total mass of the star. However, in a real star, the growth in luminosity and radius might be expected to give rise to an exceedingly high mass-loss rate. As the mass of the envelope decreases, the base of the convective envelope moves outward in mass and the temperature at the base decreases until, eventually, it becomes too low to support hydrogen burning. As more and more of the hydrogen-burning luminosity comes from the growing radiative zone below the base of the convective envelope, this luminosity must again shrink below the Eddington luminosity appropriate to the mass of the core. In the process, however, the star may have lost most of its envelope mass and may have done so on a very short time scale. This, then, may be the mechanism which leads to the OH/IR phenomenon, the long conjectured "superwind" that terminates the AGB phase for intermediate-mass AGB stars.

b) AGB Stars of Small CO *Core Mass*

The light curve for a low-mass TPAGB model of mass $M = 0.6\ M_\odot$ and of mild Population II composition is shown in Figure 38 (Iben 1982*c*). The progenitor of this model is assumed to have had a main-sequence mass larger than $\sim 0.8\ M_\odot$ and to have arrived on the horizontal branch with a mass $\sim 0.6\ M_\odot$. The mass of the CO core at the onset of thermal pulses is $\sim 0.5\ M_\odot$, and thermal pulses continue to occur until the mass of the CO core grows to $\sim 0.599\ M_\odot$, at which point the model leaves the region of red giants to become a compact object resembling the central star of a planetary nebula. A more realistic calculation would begin with a larger initial mass, a larger horizontal branch mass, and mass would be abstracted during the AGB phase in such a way that the total model mass decreases to $0.6\ M_\odot$ just as the core mass reaches a mass $M_{\rm CO} \sim 0.599\ M_\odot$ (Schönberner 1979). From the many calculations in the literature, one finds that the time between thermal pulses varies inversely with about the tenth power of the mass of the CO core. That is,

$$\tau_{\rm interpulse} \sim 2 \times 10^5\ {\rm yr}\ (0.6\ M_\odot/M_{\rm CO})^{10}\ . \qquad (14)$$

This relationship is valid only after a dozen or so pulses have transpired, as is evident from the fact that interpulse period first increases and then decreases as evolution proceeds in a model of given mass (see Fig. 38). The large variations in luminosity that occur in connection with thermal pulses may, on occasion, be used to estimate the CO core masses of real AGB stars (Wood and Zarro 1981).

In none of the TPAGB models of low mass constructed prior to 1983 does the base of the convective envelope reach the carbon-rich region formed during the peak of a preceding helium shell flash. A decade ago, Sackman (1980) pointed out that during the expansion phase that continues after convection in a shell subsides, matter at the edge of the carbon-rich region cools down to temperatures such that the contribution to opacity by absorption on carbon atoms can become significant. Iben and Renzini (1982*a*, *b*) then showed that this contribution (which previously had not been included in low-tem-

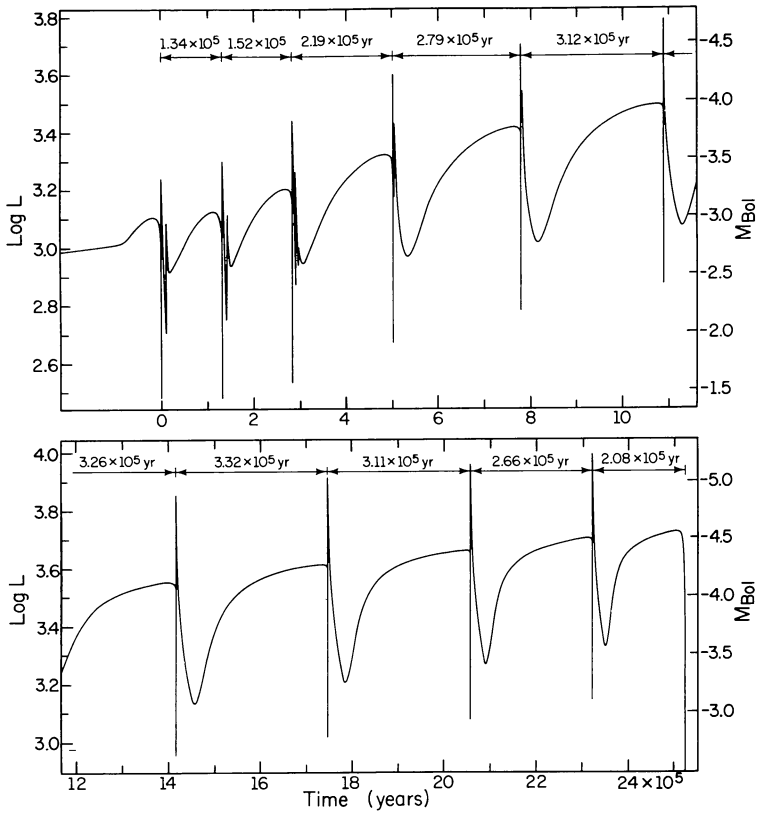

FIG. 38.—Light curve of an 0.6 $M_\odot$ AGB model of mild Population II composition. The mass of the CO core increases from 0.5 $M_\odot$ to 0.59 $M_\odot$ during 10 thermal pulses. Helium burns quiescently in a shell during the gradual luminosity decline between pulses and hydrogen burns quiescently during the subsequent gradual increase in luminosity. From Iben (1982).

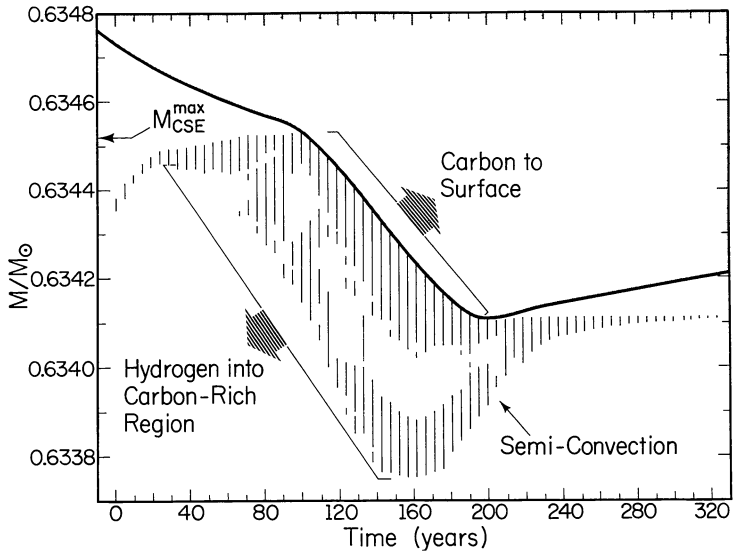

FIG. 39.—Mixing near the base of the convective envelope in an AGB model of mass 0.7 $M_\odot$ and of mild Population II composition when the contribution of carbon to opacity is properly taken into account. In the stippled region above the base of the convective envelope matter is mixed by turbulent convection. The temperatures in the region shown are near 10^6 K and, in matter below the base of the convective envelope, carbon atoms with one K-shell electron provide the major contribution to the opacity which is nearly linearly proportional to the carbon abundance. This property leads to a mixing of carbon outward (and hydrogen inward) in such a way that the radiative and adiabatic gradients nearly equal one another, and this is the characteristic of a classical semiconvective zone. In the computation, formal convective zones shift back and forth as mixing progresses in the semiconvective region. From Iben and Renzini (1982*b*).

perature opacity prescriptions used in model construction) assisted in the dredge-up process and, more important, led to the development of a semiconvective region which forced a trace of hydrogen to be mixed inward into regions of high carbon and helium content, as shown in Figure 39 (Iben and Renzini 1982*b*).

Primarily responsible for the dredging up of carbon into the convective envelope in the Iben-Renzini work is the use of an algorithm which forcibly mixes matter into mass zones (below the formal base of the convective envelope) which are initially stable against convection according to the Schwarzschild (1906) criterion but become unstable after mixing; this process is continued until a mass zone is encountered in which, even after mixing, the Schwarzschild criterion indicates stability against convection. It has since been corroborated that some form of "extra mixing" such as given by this crude "convective overshoot" algorithm is necessary to achieve dredge-up. Hollowell (1988; see Hollowell and Iben 1988, 1989) has devised a random walk treatment of convective mixing which leads to a more realistic convective overshooting and dredge-up and Boothroyd and Sackman (1988*a, b*) achieve dredge-up by use of a very large ratio of mixing length to pressure scale height.

The existence and properties of carbon stars demonstrate that dredge-up occurs in real low-luminosity AGB stars. The fact that the oldest clusters in the Magellanic clouds do not contain carbon stars demonstrates that the CO core mass of an AGB star must exceed some critical minimum value before dredge-up can occur, and this gives some confidence in the models which also suggest that, even with "extra mixing," dredge-up does not occur until core mass reaches a value of the order of 0.6 $M_\odot$ (e.g., Iben 1983; Hollowell and Iben 1988, 1989; Lattanzio 1986, 1987, 1988; Boothroyd and Sackmann 1988*a, b*).

According to equation (4), the luminosity during the quiescent hydrogen-burning phase of an AGB model of core mass $\sim$0.6 $M_\odot$ is $\sim$6000 $L_\odot$, corresponding to $M_{\rm bol} \sim -4.7$ mag. Yet, the distribution of field carbon stars in the LMC extends down to $M_{\rm bol} \sim -4$ mag, and this would appear to reveal a serious discrepancy with the models (Iben 1981) if it were not for the fact that equation (4) is actually a good approximation only toward the very end of the interpulse phase of a low-mass AGB star (see Fig. 39). That is, as a low core mass model emerges from the turmoil of a helium shell flash and embarks on a phase of quiescent helium burning, its luminosity declines gradually until it reaches a minimum which is approximately a magnitude dimmer than just prior to the flash; as helium burning goes out and hydrogen burning recommences, recovery to the prepulse luminosity is even more gradual. Thus, although its luminosity prior to a pulse must reach a value near 6000 $L_\odot$ if it is to become a carbon star, after it has become a carbon star its luminosity will remain for a substantial period of time from 1.5 to 2.5 times smaller than its prepulse luminosity. This explains why there is some overlap in luminosity between carbon stars and M stars along the AGB branch in those Magellanic cloud clusters of intermediate age which contain a substantial population of carbon stars (Frogel, Mould, and Blanco 1990).

c) s-Process Nucleosynthesis

The general character of the nucleosynthesis which occurs in the convective shell that is engendered by the high fluxes generated during a helium-burning thermonuclear runaway is shown schematically in Figures 40 and 41. Figure 40 emphasizes that there are two prime neutron sources which may be activated in the convective shell; the ^{22}Ne source is thought to be dominant in stars with large core masses, and the ^{13}C source is thought to be dominant in stars with small core masses. Figure 41 shows schematically the types of nuclear reactions and the mixing episodes which occur during different phases in a complete thermal-pulse cycle.

At the peak of a helium shell flash, the temperature at the base of the convective shell reaches $\sim 300 \times 10^6$ K in AGB models of small CO core mass and reaches even higher values in AGB models of large core mass. In all cases, high temperatures are maintained for a sufficiently long time that ^{14}N, into which the ^{12}C and ^{16}O initially present in the model have been converted during prior hydrogen-burning processing, is converted completely into ^{22}Ne.

Whether or not substantial amounts of ^{22}Ne can capture α particles with the release of neutrons depends on the poorly known cross section for this process, as well as on the duration of the highest-temperature phase of the thermal pulse. If the cross section recommended by Fowler, Caughlan, and Zimmerman (1975) is chosen, copious numbers of neutrons are produced in AGB models with core masses in excess of $\sim$0.95 $M_\odot$ (Iben 1975*a*, 1976, 1977*a*); in models with core masses in the range 0.6–0.7 $M_\odot$, only $\sim$1% of the ^{22}Ne is converted into ^{25}Mg and neutrons (Becker 1981; Iben 1982*b*). The experiments of Wolke *et al.* (1989) suggest that the cross section adopted in these studies could be orders of magnitude too large. If this is true, then the ^{22}Ne source of neutrons is simply not active in AGB stars. However, the demonstration by Wood, Bessell, and Fox (1983) of overabundances of the *s*-process element Zr in massive AGB stars and the demonstration by Gallino *et al.* (1988, see also Gallino 1989 and

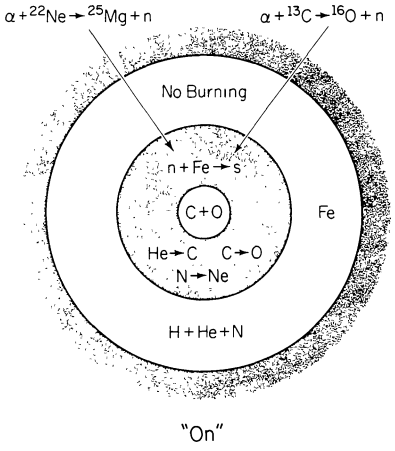

FIG. 40.—Nuclear reactions in the "nuclearactive" region of an AGB stellar model during the phase of shell convection forced by the helium-burning thermonuclear runaway. During this phase, the carbon abundance in the shell increases to $\sim$20% by mass, the oxygen abundance increases by $\sim$1% and nitrogen is converted into neon by the reactions ^{14}N(α, γ)^{18}F(β^+, ν)^{18}O(α, γ)^{22}Ne. Neutrons are released in consequence of the ^{22}Ne(α, n)^{25}Mg reaction in AGB models of large CO core mass and in consequence of the ^{13}C(α, n)^{16}O reaction in AGB models of small core mass. Neutron capture on the seed nucleus ^{56}Fe and its progeny form neutron-rich isotopes at abundances that approximate the classical *s*-process distribution, except at delicate branch points.

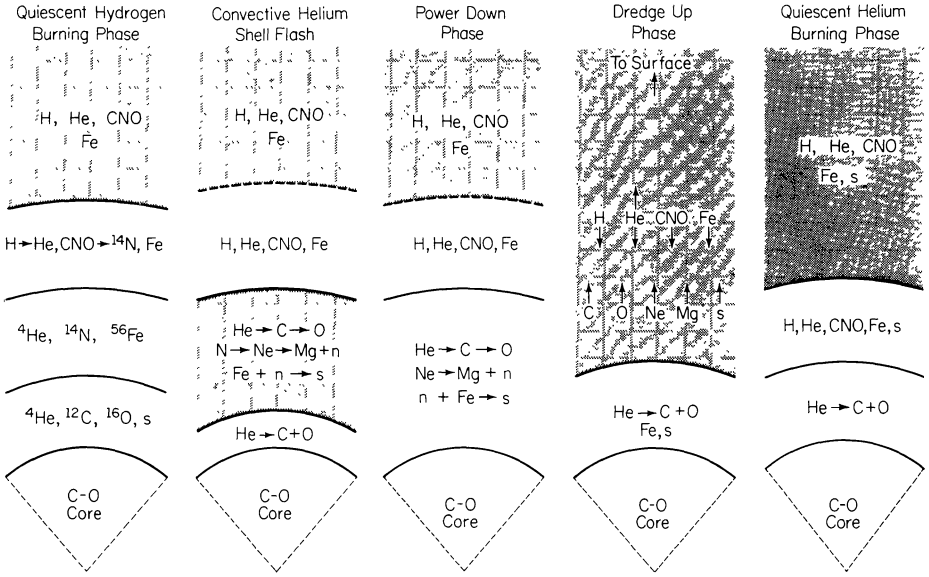

FIG. 41.—A schematic representation of the convective zones and the modes of nucleosynthesis in the nuclearactive region of an AGB model of large core mass. From Iben (1985).

Käppeler *et al.* 1990) that, in AGB models of small core mass, a ^{22}Ne source operating at the 1% level (see below) is capable of producing in the solar-system distribution several *s*-process isotopes near very temperature-sensitive branch points, suggests that the Wolke *et al.* estimates of the ^{22}Ne neutron-capture cross section may be overly conservative.

Using the cross section for the ^{22}Ne(α, n)^{25}Mg reaction given by Fowler, Caughlan, and Zimmerman (1975), it is found that, in models of CO core mass 0.96, 1.16, and 1.36 $M_\odot$, the ratio of neutrons released to the initial abundance of ^{22}Ne is 0.18, 0.96, and 0.98, respectively (Iben 1977). The short lifetimes of luminous AGB stars in the Magellanic clouds, coupled with the fact that the maximum initial CO core mass of a TPAGB star is 1.1 $M_\odot$, might suggest that results for the two larger core masses are of only academic interest. On the other hand, helium shell flashes occur also above the ONe electron-degenerate cores formed by model stars in the 8–10 $M_\odot$ mass range (Nomoto 1984, 1987; Wheeler 1990), and the fact that the LPVs in the Magellanic clouds appear to range in brightness up to $M_{bol} < -7$ (Wood, Bessell, and Fox 1983) may be an observational demonstration that this occurs. Theoretically, ONe core masses range from 1.1 to 1.4 $M_\odot$, and thus the calculations for CO cores in the 1.1–1.4 $M_\odot$ range may still be of observational relevance.

Using a linear reaction network which assumes that β decays occur instantaneously and using the detailed results of the AGB models with large cores, Truran and Iben (1977) demonstrated explicitly how neutron-rich isotopes are built up over successive thermal pulses into an asymptotic distribution (Ulrich 1973) which, for atomic number A in the range $70 < A < 204$, closely resembles the solar system distribution of *s*-process isotopes. Two things are responsible for this result: (1) the primary neutron absorbers are light elements with a mean neutron-capture cross section of ~3–5 mbarns, and (2) successive convective shells overlap so that a substantial amount of material appearing in a given convective shell has also been in the immediately preceding shell.

Studies with more sophisticated reaction chains which take β-decay lifetimes properly into account (Despain 1977, 1980; Howard *et al.* 1986; Busso *et al.* 1988; Malaney 1986; Malaney and Boothroyd 1987) show that the neutron densities achieved are so large ($\gg 10^8$ cm^{-3}) that very significant departures from the solar system distribution are produced near sensitive branch points. One must conclude that AGB stars of large core mass are not the major contributors to the Galactic production of *s*-process isotopes, and this is consistent with the observed short lifetimes of such stars. It will be interesting to see whether or not detailed abundance analyses of the LPVs in the Magellanic clouds will corroborate the predicted departures from the solar-system distribution that appear to be a characteristic of the ^{22}Ne neutron source. If they do not, one inference one might draw is that the cross section for the ^{22}Ne(α, n)^{25}Mg reaction is indeed as small as that suggested by Wolke *et al.* (1989); but then we would be faced with an observed excess of neutron-rich isotopes and the necessity of identifying another way of releasing neutrons to produce this excess.

The temperature at the outer edge of the helium- and carbon-rich zones in AGB stars of large core mass does not become small enough for carbon atoms to form and so the ^{13}C activation scheme which appears to work in low-mass AGB stars (see below) cannot operate. Several other possibilities should be kept in mind. With one exception, in all AGB models that have been constructed to date, the outer edge of the convective shell does not reach hydrogen-containing layers. This can be understood in terms of an entropy barrier (Iben 1976) the major contribution to which is the entropy of the radiation field through the hydrogen profile below the convective envelope. Schwarzschild and Härm (1967) found that, during one pulse out of 13 computed, the outer edge of the shell in a low-mass model actually extended into the tail of the hydrogen profile that had been produced during the preceding hydrogen-burning phase, but this can be understood as a consequence of the fact that radiation pressure was not included in their input physics. Nevertheless, even when radiation pres-

sure is included, the outer edge of the convective shell comes tantalizingly close to the tail of the hydrogen profile (within a fraction of a pressure scale height), and it is easy to imagine that some form of overshoot might mix hydrogen into the helium-burning convective shell.

Thus, the work of Sanders (1967), who capitalized on the mixing explicitly found by Schwarzschild and Härm to explore the consequences of injecting hydrogen into the helium-burning convective shell, is quite relevant. As hydrogen diffuses downward through the convective shell, it soon encounters temperatures large enough to initiate the reactions $^{12}C(p, \gamma)^{13}N(e+, \nu)^{13}C$, and as the product ^{13}C diffuses downward it soon reaches temperatures ($\sim 150 \times 10^6$ K) large enough to initiate the reaction $^{13}C(\alpha, n)^{16}O$. Because the temperature at the base of the convective shell is near its peak value ($\sim 300 \times 10^6$ K), the neutron-capture nucleosynthesis that subsequently takes place will differ significantly from that which occurs when ^{13}C is injected when the base temperature is only 150×10^6 K, and one may anticipate a final distribution of neutron-rich isotopes that differs from the solar system distribution in a way somewhat similar to the way in which the distribution formed when ^{22}Ne is the source (assuming that it operates at temperatures above 300×10^6 K). Hence, spectroscopic observations may not be able to distinguish easily between whether the ^{22}Ne source or the ^{13}C source is operating.

An imaginative proposal by Ulrich (1973) and Scalo and Ulrich (1973) deserves very serious consideration. These authors suppose that "plumes" of carbon- and helium-rich matter rise beyond the outer edge of the convective shell and, as the plumes plow through matter rich in hydrogen, hydrogen is entrained into their interiors where the sequence of reactions just discussed produces one neutron for every proton entrained. Still another scheme has been suggested by Sackman, Smith, and Despain (1974) who imagine that the outer edge of the helium convective shell actually reaches the base of the convective envelope and that continuous mixing throughout the combined convective regions take place.

The situation with regard to the production of *s*-process isotopes in AGB stars of small core mass appears to be somewhat clearer than in the case of AGB stars of large core mass. Some of the physics of what occurs in such models is shown in Figure 39, and additional physics is illustrated in Figure 42 (Hollowell and Iben 1988, 1989). In Figure 42, matter in both hatched regions is fully convective. As the convective shell grows in mass, the temperature at its base increases to a maximum of $\sim 300 \times 10^6$ K, at which point $\sim 1\%$ of the ^{22}Ne formed earlier from ^{14}N is converted into ^{25}Mg and neutrons over a period of less than 5 yr; this point is flagged by the vertical line labeled ^{22}Ne. The abundance of ^{12}C in the convective shell at its maximum extension is $\sim 20\%$ by mass. Following the disappearance of the convective shell, a semiconvective zone appears below the base of the convective envelope (where the temperature is $\sim 10^6$ K and a substantial number of carbon atoms with one K shell electron exist), forcing carbon to mix outward and a trace of hydrogen to mix inward. Simultaneously, the base of the convective envelope moves inward in mass to dredge up fresh carbon and neutron-rich isotopes.

Once the thermal pulse has subsided and once the helium-burning phase has run its course (after $\sim 10\%$ of the time between pulses has elapsed), the temperatures in the region which was earlier semiconvective (and over much of which the number abundances of ^{12}C and ^{1}H are comparable) become large enough that hydrogen burning takes place. Over the inner 80% of this region the dominant product is ^{13}C and over the outer 20% the dominant product is ^{14}N. The hydrogen-burning shell then gains strength and eats its way outward in mass, converting hydrogen into helium, until another thermal pulse is excited. When the outer edge of the convective shell reaches the region which earlier experienced semiconvection and in which fresh ^{13}C is found, ^{13}C begins to enter into the convective shell. At this point, flagged by the vertical line labeled ^{13}C, the temperature at the base of the convective shell is $\sim 150 \times 10^6$ K, and the density there is $\sim 40{,}000$ gm cm^{-3}.

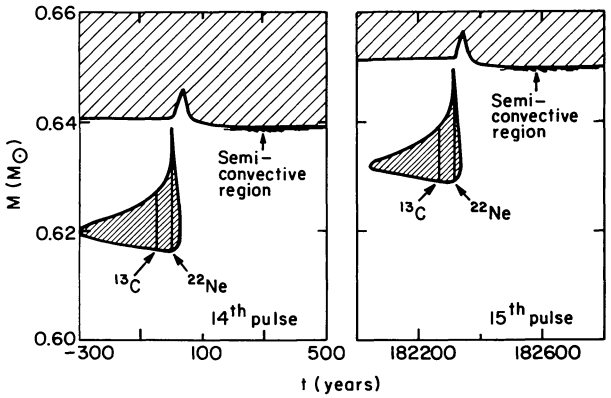

FIG. 42.—Mixing regions as a function of time and activation of neutron sources during two thermal pulses in an AGB model of small core mass. Fully convective zones are denoted by single hatching and the semiconvective region which extends downward from the base of the convective envelope is indicated schematically. The times at which the ^{13}C and ^{22}Ne neutron sources are activated are indicated by the vertical lines within the convective shells. From Hollowell and Iben (1989).

The duration of the ^{13}C ingestion episode is ~ 10 yr, and over this short period of time, the characteristics of the convective shell do not alter appreciably. The turnover time in the convective shell is $\sim \frac{1}{2}$ day and the lifetime of ^{13}C against destruction by the $^{13}C(\alpha, n)^{16}$ reaction ranges from ~ 10 days at the base of the shell to ~ 10 yr at the outer edge of the shell. The lifetime of most isobars involved in *s*-process nucleosynthesis ranges from years at the base of the convective shell to centuries at the outer edge of the shell. Thus, the abundance of ^{13}C and the abundances of these isobars are constant with regard to location within the convective shell, and nucleosynthesis is highly concentrated toward the base of the shell. The lifetime of a neutron against capture is of the order of 10^{-6} s everywhere within the shell, so the neutron density is determined locally by balancing the production rate with the destruction rate.

The mathematics of *s*-process nucleosynthesis is such that one can obtain the essential features in the framework of a one-zone model at slightly lower temperature and density than at the base of the convective shell (Hollowell and Iben 1990). With this model, one finds an effective mean neutron density of $n_n \sim 8.6 \times 10^6 Z_0^{-1}$ cm^{-3}, where Z_0 is the abundance by mass of heavy elements. Thus, expected neutron densities are very close to those required for producing *s*-process isotopes in the solar-system distribution and very far from those required for producing *r*-process isotopes in the solar system distribution (Clayton 1968).

Very complete calculations with full nuclear reaction networks have been carried out in the context of convective shell models by Gallino *et al.* (1988) and by Käppeler *et al.* (1990) and these show that the vast majority of *s*-process isotopes, including those near most sensitive branch points, are produced in nearly the solar system distribution during the ^{13}C ingestion phase. Three isotopes whose abundances are particularly sensitive to the temperature are not made in the solar-system distribution during this phase. Remarkably, however, they do emerge in the solar system distribution during the weak neutron irradiation which occurs when (and if) the ^{22}Ne source is activated (Gallino *et al.* 1988; Gallino 1989; Käppeler *et al.* 1990).

Käppeler *et al.* (1990) show that the ^{13}C-ingesting convective-shell model which is provided by stellar evolution calculations gives a distribution of *s*-process isotopes which is nearly identical with the distribution obtained by nuclear astrophysicists who have for so many years used a single-zone, exponential-neutron-exposure model without reference to the constraints imposed by considerations of stellar evolution. Of course, there are free parameters in the nuclear astrophysics model (mean neutron density, total neutron exposure, and slope of the exponential neutron exposure distribution) which are set by fitting to the solar-system distribution of *s*-process isotopes. The stellar evolution models permit one to estimate these same parameters and to estimate the distribution of *s*-process isotopes without reference to the solar system distribution. It is remarkable that the two independent approaches appear to have converged on a common solution. It is even more remarkable that real low mass AGB stars appear to agree with this solution (Lambert 1989).

d) Super–Lithium-rich Stars

Smith and Lambert (1989, 1990) have discovered that the brightest members of the sample of LPVs studied by Wood, Bessell, and Fox (1983) are super lithium rich, with surface lithium abundances typically three orders of magnitude larger than normal, and that the property of super richness does not extend to stars dimmer than about −6 mag. The fact that all of the brightest AGB stars are super lithium rich suggests that the phenomenon may not be a consequence of thermal pulses, but that it may be due to a process which requires some characteristic which varies monotonically with core mass to exceed a threshold value. A promising scenario for creating ^7Li in red giant envelopes was introduced by Cameron (1955) and by Cameron and Fowler (1971), who argued that, if the ^7Be produced in portions of the giant hot enough for the reaction $^3He(^4He, \gamma)^7Be$ to occur could be carried out to cool enough portions of the giant before the reaction $^7Be(e^-, \nu)^7Li$ occurred, the lithium eventually made by this last reaction could escape immediate destruction by proton capture. Building on this scheme, Ulrich and Scalo (1972), Sackman, Smith, and Despain (1973), Smith, Sackman, and Despain (1973), and Scalo, Despain, and Ulrich (1976) have studied lithium production in convective envelopes and find that, the hotter the base of the envelope, the larger is the surface lithium abundance which can initially be achieved. Since the temperature at the base of the convective envelope of an AGB model is hotter, the more massive the core of the model, it would appear that the basic theory for understanding the new observational results is already in hand.

In models of core mass $\sim 0.95\ M_\odot$, the temperature at the base of the convective envelope is large enough to sustain the reaction $^3He(\alpha, \gamma)^7Be$ (Iben 1975), but eventually all of the ^7Li made by the $^7Be(e^-, \nu)^7Li$ reaction in the cooler portions of the envelope is destroyed as it cycles inward to encounter the high temperatures at the base of the envelope (Iben 1975, 1983). Possibly, in real AGB stars with cores larger than $\sim 1.1\ M_\odot$, the base temperature becomes large enough that ^3He is replenished rapidly enough by the $p(p, e^+\nu)d(p, \gamma)^3He$ reactions that a large steady state surface abundance of ^7Li can be maintained.

IX. POST–AGB EVOLUTION AND WHITE DWARF SURFACE COMPOSITION

As discussed in the preceding section, comparison between quasi-static models of AGB stars and the observations tells us that most of the hydrogen-rich envelope of a real moderately low or intermediate mass star is ejected shortly after it has developed an electron-degenerate CO core and begun to experience thermal pulses. In a very low mass star ($0.8–1^-\ M_\odot$), ejection may be completed before hydrogen is reignited and thermal pulsing begins. AGB stars of moderately small core mass (those with initial total mass in the range $1^+–2^+\ M_\odot$) live long enough to become carbon stars before the ejection of a nebular shell and AGB stars of large core mass eject their hydrogen-rich envelopes very shortly after they reach the thermally pulsing stage. The remnant of AGB stars of initial mass in the 8–12 $M_\odot$ range will be an ONe white dwarf, if envelope ejection occurs before the mass of the CO core reaches $\sim 1.37\ M_\odot$, or a neutron star, if the core mass reaches $\sim 1.37\ M_\odot$ and electron captures on ^{24}Mg and on ^{20}Ne force the core to collapse. The OH/IR sources (exhibiting mass-loss rates of the order of $10^{-4}\ M_\odot\ yr^{-1}$) are probably high-mass ($>2–3\ M_\odot$) AGB stars in the process of nebular ejection (Habing, te Lintel Hekkert, and Van der Veen 1989).

Neither theory nor observation has succeeded thus far in demonstrating precisely where in a thermal pulse cycle the final ejection occurs or precisely how much hydrogen-rich material remains on the surface of the remnant at the termination of the ejection phase. Furthermore, winds continue to abstract matter from the surface of the remnant, but the strength of these winds is not unambiguously predicted by theory and the extent to which the remaining hydrogen-rich surface layer is depleted by these winds is therefore also not predictable. Given these lacunae in our knowledge, it is necessary to explore possible avenues for the evolution of the remnant and to hope that at some point the characteristics of real remnants will allow us to deduce the history of the last phases of ejection and the consequences of wind mass loss following ejection (Schönberner 1979, 1981, 1986; Renzini 1979, 1982; Iben 1989).

Figure 43 describes the evolutionary path of a model remnant of mass $0.6\ M_\odot$ which has retained $\sim 0.001\ M_\odot$ of hydrogen-rich material following an assumed shell-ejection (or "superwind") event. It has been supposed that ejection occurs during the quiescent hydrogen-burning interpulse phase, and the mass dM_{He} of the helium layer between the outer edge of the CO core and the base of the hydrogen-rich envelope re-

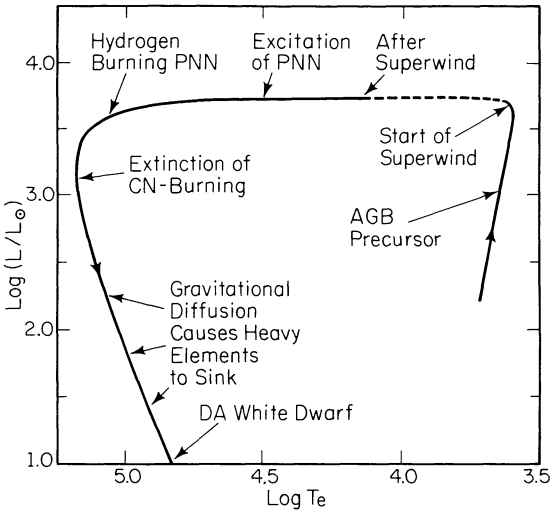

FIG. 43.—Evolutionary track of the hypothetical remnant of a nebular ejection event. The precursor AGB model of initial mass less than $\sim 2\ M_\odot$ has experienced 10 thermal pulses and ejection is assumed to occur when the precursor model is approximately halfway between the 10th pulse and (what would have been) the 11th pulse. The mass of the helium layer between the outer edge of the CO core and the base of the hydrogen-burning shell is $\sim 0.5 \times dM_H$, where dM_H is the mass processed by the hydrogen-burning shell between pulses. As mass is abstracted at a high rate from the model, it departs from the AGB branch and evolves rapidly to the blue when the mass in the remnant hydrogen-rich layer decreases below $\sim 0.01\ M_\odot$. Adapted from Iben (1984) and Iben and MacDonald (1985).

tained by the remnant can be anywhere between $0.2 \times dM_H$ and $0.8 \times dM_H$, where dM_H is the mass which the hydrogen-burning shell processes between helium shell flashes on the AGB. For a $0.6\ M_\odot$ core, $dM_H \sim 0.01\ M_\odot$. As the model evolves to the blue (initially at nearly constant luminosity), hydrogen burning at the base of the hydrogen-rich envelope is responsible for the luminosity and the surface temperature of the model is inversely correlated with the mass remaining in the hydrogen-rich surface layer. When its surface temperature exceeds 30,000 K, the remnant emits ionizing photons at a sufficient rate to cause the ejected nebula to fluoresce and the system of remnant and nebula adopts the characteristics of a planetary nebula. The nuclear-burning lifetime of the $0.6\ M_\odot$ remnant is $\sim 10^4$ yr, and this lifetime decreases as about the tenth power of remnant mass (eq. [14]).

The observations demonstrate that a real remnant also emits material particles in a hot, fast wind (Heap 1983; Perinotto 1983; Cerruti-Sola and Perinotto 1985) and this wind is probably of major importance in shaping the structure of the nebula (Kwok, Purton, and Fitzgerald 1978, Kahn and West 1985; Kwok 1987). Mass-loss rates of the order of 10^{-9}–$10^{-7}\ M_\odot\ \mathrm{yr}^{-1}$ are estimated, and these are of the order of or larger than the rate at which hydrogen-burning processes mass. Since the location in T_e along the plateau portion of the evolutionary track is correlated inversely with the amount of hydrogen remaining in surface layers, mass loss accelerates evolution to the blue.

Once the mass of the hydrogen-rich surface layer is reduced to $\sim 10^{-2}\ dM_H$ ($\sim 10^{-4}\ M_\odot$ when $M_{CO} \sim 0.6\ M_\odot$) hydrogen burning via CN-cycle reactions is extinguished (approximately at the bluest point along the track in Fig. 43). The hydrogen-rich surface layer contracts rapidly and the luminosity, now supplied primarily by the release of gravitational potential energy from the contracting envelope layer, drops by a factor of ~ 10 in 1000 yr, during which time the mass of the hydrogen-rich layer is probably not completely ejected due to wind mass loss (the wind, if radiatively driven, decreases in strength at least as rapidly as the luminosity). Thereafter, the surface luminosity is a complicated consequence of the release of gravitational potential energy, neutrino losses, and cooling of nondegenerate ions, and crystallization (Iben and Tutukov 1984*b*; D'Antona and Mazzitelli 1990; Koester and Chanmugam 1990).

The gravitational force in surface layers of the remnant is large enough that gravitationally induced diffusion becomes important (Schatzman 1949). Hydrogen, if it still remains, becomes the dominant element at the surface and the model approximates the characteristics of observed DA white dwarfs in which the number abundance of helium relative to hydrogen is typically less than 10^{-4}.

If, before envelope ejection is invoked, the model AGB precursor is allowed to burn hydrogen until the mass of the deposited helium layer dM_{He} is in excess of $\sim 0.8 \times dM_H$, a final helium shell flash is ignited after the model has departed from the AGB. In the example shown in Figure 44, $dM_{He} \sim 0.85 \times dM_H$ and the final flash is ignited after hydrogen burning by

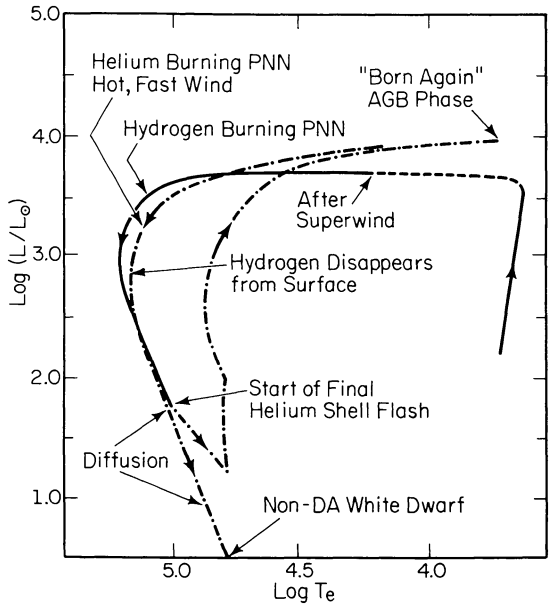

FIG. 44.—Evolutionary track of the hypothetical remnant of a nebular ejection event which occurs when the mass of the helium layer between the CO core and the base of the hydrogen-burning shell is $\sim 0.85 \times dM_H$. Other model characteristics are the same as those of the model described in Fig. 43. After hydrogen burning effectively ceases, the model envelope contracts rapidly and the conversion of gravitational potential energy into heat leads to the ignition of helium in the helium layer even though the mass of this layer is smaller than the critical mass dM_H for ignition on the AGB. In consequence of the hot, fast wind from the remnant, the remainder of the hydrogen-rich envelope is expelled, leaving only a trace of hydrogen which has escaped inward in consequence of chemical diffusion. The model adopts the characteristics of a non-Da white dwarf. Adapted from Iben *et al.* (1983) and Iben (1984).

the CN cycle as terminated and the remnant has adopted a white dwarf configuration. This type of behavior was predicted by Fujimoto (1977), and it is due to the conversion of gravitational potential energy into thermal energy during the rapid envelope-contraction episode following the extinction of hydrogen burning (Iben *et al.* 1983; Iben 1984).

The model returns to the region of the AGB where an envelope ejection mechanism was previously invoked, and it is reasonable to assume that this same ejection mechanism may again operate to abstract mass from the "born-again" AGB star. This time, however, the source of surface luminosity is helium burning, and departure from the AGB (and cessation of the ejection mechanism) requires that mass loss must continue until less than $\sim 10^{-5}\ M_\odot$ of hydrogen-rich material remains at the surface of the star. As it returns to the blue, the remnant again achieves high enough surface temperatures to excite the surrounding nebular material into fluorescence. The duration of this second planetary nebula phase powered by helium burning in the central star is ~ 3 times longer than that of the initial hydrogen-burning phase, and, over this time, the wind from the central star may be able to abstract what remains of the hydrogen-rich envelope. Eventually helium burning ceases to be effective and gravitational diffusion forces helium to become the dominant element at the surface; the model adopts characteristics of observed non-DA white dwarfs in which the abundance of hydrogen relative to helium is typically less than $\sim 10^{-4}$.

If ejection of the hydrogen-rich envelope occurs during a helium shell flash or shortly thereafter, the energy which powers the ensuing planetary nebula phase is contributed solely by helium-burning reactions. In this case, the helium "buffer" layer $dM_{\rm He}$ is quite small and the diffusion of carbon outward and of hydrogen inward due to the fact that "nature abhors a vacuum" may play a very significant role. Figure 45 shows the effect of diffusion in a model in which the buffer layer is $dM_{\rm He} \sim dM_{\rm H}/2$ (Iben and MacDonald 1986). Gravitational forces act to force the heavier elements to sink inward and the lighter elements to float outward. However, particles move in both directions and, despite gravitational forces, every element distribution develops a "tail" (via what may be called chemical diffusion) which extends into the region from which gravitational forces attempt to evacuate it. In the particular case illustrated, there are no observationally significant consequences, and evolution in the H-R diagram is as described in Figure 43.

However, if the hydrogen-rich envelope is ejected during a helium shell flash, the mass of the buffer layer is at a minimum, and the diffusion of carbon outward and of hydrogen inward can have dramatic consequences, as described in Figure 46 (Iben and MacDonald 1986). The luminosity of the model is sustained by helium burning during the planetary nebula stage, but $\sim 10^7$ yr after helium burning ceases to provide energy, the product of the carbon and hydrogen abundances have become so large in a region of high temperature below the surface that a hydrogen-burning thermonuclear runaway is ignited, leading to an outburst which exhibits the characteristics of a slow nova. This situation can be avoided only if essentially *all* of the hydrogen-rich envelope is removed before diffusion becomes important.

If there were some reason to believe that nebular ejections

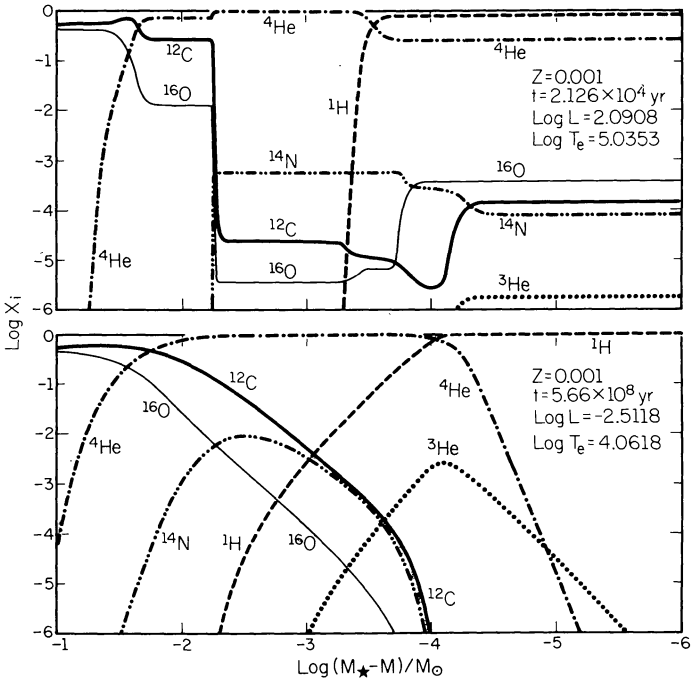

FIG. 45.—The distribution of several isotopes in the interior of a white dwarf compared with the distribution in its precursor, which is assumed to be the hydrogen-burning central star of a planetary nebula. Model mass is $0.6 M_\odot$ and the metallicity is that of a mild Population II star. The top panel gives the distribution which prevails at the end of the active hydrogen-burning phase of the precursor, and the lower panel gives the distribution after $\sim 6 \times 10^8$ yr of cooling. From Iben and MacDonald (1985).

occur preferentially during helium shell flashes (after all, the luminosity does rise briefly above the luminosity during the preceding quiescent hydrogen-burning phase [see Fig. 38]), and if every remnant followed an evolutionary course similar to the one depicted in Figure 46, then one might expect to see approximately one nova per year (roughly the white dwarf birth rate) which is not in a binary and therefore does not exhibit the characteristics of a cataclysmic variable after outburst. This prediction is presumably testable. Some support for the contention that all central stars of planetary nebulae are burning helium comes from the study by Kawaler (1988) of the pulsational instability of hydrogen-burning central star models. The models are unstable to g-mode pulsations which are driven in the nuclear-burning region. Several observational searches for central star pulsations have been negative (Grauer *et al.* 1987; Hine and Nather 1987), and Kawaler infers that central stars cannot be burning hydrogen. This interpretation requires, of course, that rotation and mass loss do not act to damp out oscillations in real central stars; further, the theoretical calculations do not predict the amplitude of the oscillations, which in the real case could be smaller than the observational detectability limit.

One consequence of this sort of evolution is that it provides a way for an erstwhile DA white dwarf to lose mass via a modified superwind (as a born-again AGB star which burns hydrogen) and still retain some hydrogen at the surface. This may help explain why DA white dwarfs at luminosities of $\sim 3 \times 10^{-3}\ L_\odot$ and surface temperatures $\sim$11,000–12,000 K (ZZ

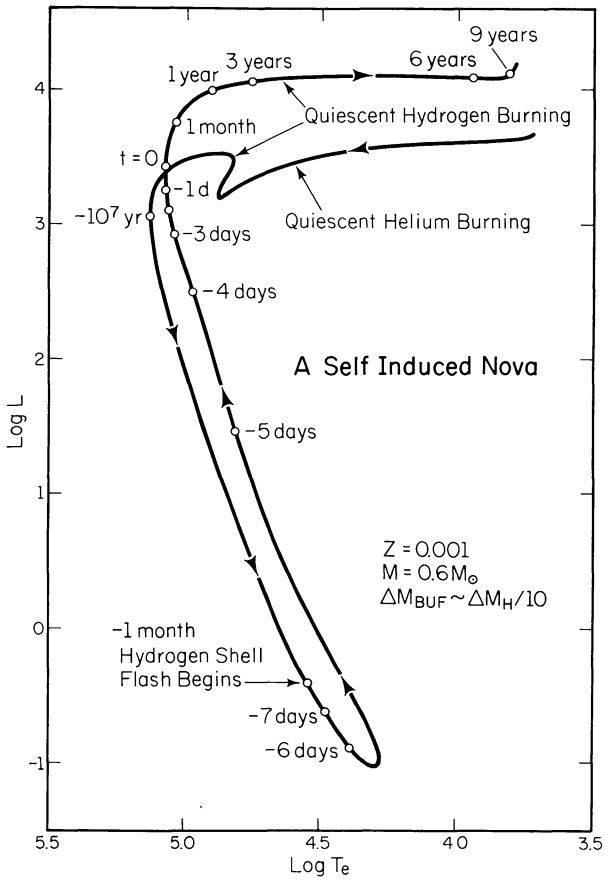

FIG. 46.—Evolutionary track of a model remnant of mass 0.6 $M_\odot$ and $Z = 0.001$ which results when it is assumed that the ejection of the hydrogen-rich envelope occurs shortly after a helium shell flash has occurred. From Iben and McDonald (1985).

Ceti stars) pulsate acoustically in nonradial modes (McGraw and Robinson 1976; McGraw 1979, 1980); an analysis of the excitation of such modes (Winget *et al.* 1982) suggests that the total mass of hydrogen in surface layers must be less than $\sim 10^{-7}\ M_\odot$ (but this has been questioned by Cox *et al.* 1987).

X. WHITE DWARF EVOLUTION

There are potentially other ways of determining which of the many possibilities for precursor evolution are actually realized, and in what proportion. In Figure 47 (Iben and Tutukov 1984*b*) is shown the time history of the luminosity of two models, one which burns hydrogen as a central star of a planetary nebula (case A) and the other which has no surface hydrogen and burns helium as a central star (case B). The abrupt drop in luminosity exhibited by the case A model is due to the extinction of hydrogen-burning by CN-cycle reactions, and Schönberner (1986) has made use of the distinction between the two cases at this point to argue that most central stars of planetary nebulae follow the case A route. If this is true, then either the reasoning which suggests that ZZ Ceti stars have hydrogen-rich envelopes of mass less than $10^{-7}\ M_\odot$ is faulty or, following the cessation of hydrogen burning at high luminosity, mass loss via a wind decreases the mass of the remaining hydrogen layer below this limit.

For times in the range 10^5–10^7 yr, the loss of energy by plasma neutrino emission is made good from the store of thermal energy in nondegenerate nuclei. Over the interval 10^7–10^8 yr, surface luminosity is supplied primarily by cooling of nondegenerate ions as neutrino losses become insignificant. During this time nuclear energy continues to be liberated at a modest rate by the reactions $p(p, e^+\nu)d(p, \gamma)^3$He and, over an interval of $\sim 2 \times 10^9$ yr beginning at $t \sim 10^8$ yr, nuclear energy is the major contributor to surface luminosity. Diffusion has not been included in the calculation of the case A model, and it turns out that, when diffusion is included, enough hydrogen is depleted by CN-cycle reactions during the earlier phases, that the energy subsequently liberated by ^{3}He-producing reactions accounts for at most 50% of the surface luminosity (Iben and McDonald 1985, 1986). In any case, when viewed in perspective, the quantitative influence on the cooling curve is small. In fact, the overall slope of the cooling curve is remarkably similar to the one which follows from the earliest theories of white dwarf cooling (Kaplan 1950; Mestel 1952; Schatzman 1953), even though neutrino losses, nuclear burning, and crystallization were not incorporated in the early models. An excellent summary of recent work on the construction of cooling curves is given by D'Antona and Mazzitelli (1990).

Cooling curves may be used to estimate both the birthrate of white dwarfs in the Galactic disk in a ring at the distance of the Sun from the Galactic center (e.g., Weidemann 1979; Iben and Tutukov 1984*b*) and the time at which active star formation began in this ring (D'Antona and Mazzitelli 1978; Winget *et al.* 1987). Assuming that (1) star formation began at a unique time in the past, (2) the total stellar birthrate has been a constant since this unique time, (3) the stellar mass function is as estimated by Salpeter (1955), and (4) cooling curves depend upon white dwarf mass as described by Winget *et al.* (1987), the distributions shown in Figure 48 result (Iben and Laughlin 1989). The observational distribution given by the open circles in this figure is from the work of Liebert, Dahn, and Monet (1988) as described by Winget *et al.* (1987).

Normalization of the theoretical distribution to the observed distribution in the range $0.5 < \log L < 4.0$ sets the birthrate of white dwarfs in the Galactic disk at $\sim 0.5\ \mathrm{yr}^{-1}$. An estimate of the age of the disk is based almost entirely on the observationally determined point at lowest luminosity (only two stars contribute to this point), and Figure 48 suggests an age of $\sim 9 \times 10^9$ yr for white dwarfs in the solar vicinity. This age, first deduced by Winget *et al.* (1987), is similar to the estimated age of NGC 188, one of the oldest Galactic clusters known (see § IV), but it is considerably smaller than the typical age of a globular cluster in the Galactic halo (see § V).

XI. WHITE DWARF MASSES IN CLOSE BINARIES

As discussed in § III*b*, the mass of the remnant of the mass donor in a Roche-lobe overflow event depends both on the initial mass of the donor and on its evolutionary state. An example of the consequence of abstracting mass at a rapid rate from an intermediate-mass model after it has become a red giant but before it ignites helium at the center (a late case B event) is shown in Figure 49 (Iben and Tutukov 1985). Mass has been abstracted in such a way as to maintain a constant model radius; transfer at a slightly more rapid rate would cause

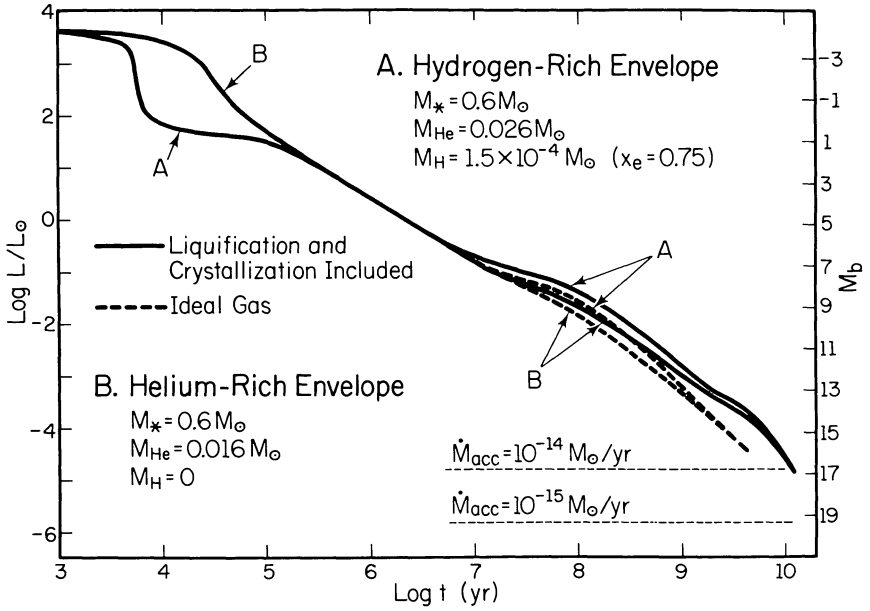

FIG. 47.—Time history of the luminosity of two models of mass 0.6 $M_\odot$ and $Z = 0.001$ which depart the AGB midway during a quiescent hydrogen-burning phase (case A) and during the quiescent helium-burning phase (B). From Iben and Tutukov (1984*b*).

the model to shrink to a smaller equilibrium radius. Eventually, layers are exposed which have been within a large convective core during the main-sequence phase (see Figs. 3*b* and 19) and which have therefore experienced a considerable degree of hydrogen burning; thereafter a constant radius can no longer be maintained even by reducing the assumed mass-loss rate to zero. At this point, mass loss is terminated, and the model evolves to the blue, while nuclear burning at the base of the hydrogen-rich layer continues to reduce the mass of this layer. The mass of the remnant is to a good approximation independent of the precise rate of mass loss (i.e., of the precise equilibrium radius assumed during the rapid mass-loss event) prior to the onset of this self-imposed shrinkage, and so one may accept this mass as a fairly reliable upper limit on the mass of the remnant of a common-envelope event in which orbital shrinkage requires the effective radius of the mass donor to shrink with time.

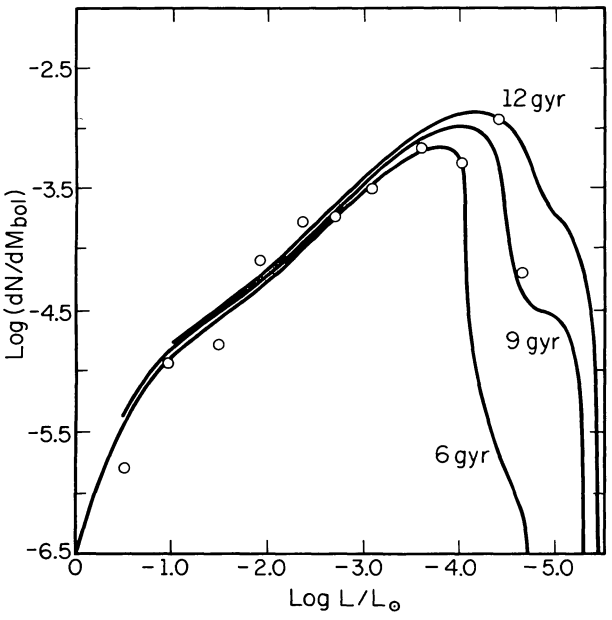

FIG. 48.—Theoretical number-luminosity distributions of white dwarfs in the Galactic disk as a function of the assumed age of the disk. Circles are interpretations of observational data (Winget *et al.* 1987). From Iben and Laughlin (1989).

In Figure 49, between the positions labeled F, where mass loss is terminated, and G, where core helium burning begins, hydrogen burning reduces the mass of the hydrogen-rich layer from $\sim 0.14\ M_\odot$ to $\sim 0.04\ M_\odot$. The separation in time between two solid points along the evolutionary track in Figure 49 is 3×10^5 yr, and, from the fact that $6 \times 10^{18} \times 0.36$ ergs is released for every gram of hydrogen-rich material burned (the abundance by mass of hydrogen near the surface is $X = 0.36$), one infers that the mass of the hydrogen-rich envelope is reduced by $\sim 0.007\ M_\odot$ between each pair of points along the plateau portion of the track as model radius decreases from $\sim 80\ R_\odot$ to $\sim 4\ R_\odot$. The position along the plateau portion of the track is determined primarily by the amount of mass in the hydrogen-rich envelope, and motion to the blue can be achieved just as well by abstracting mass from the surface as by allowing hydrogen burning to abstract mass from the envelope base. If, for example, it is supposed that the companion of the 5 $M_\odot$ model is a 2 $M_\odot$ star and that orbital shrinkage due to dissipation in a common envelope is as given by equation (7) with $\alpha \sim 1$, then the radius of the Roche lobe about the remant is $\sim 4\ R_\odot$, and consistency would demand that the mass-loss episode should have been continued until an additional ~ 0.03 $M_\odot$ had been abstracted from the model. Thus, the derived mass of the final remnant depends somewhat on the details of the common-envelope episode.

After emerging from the common envelope, the remnant

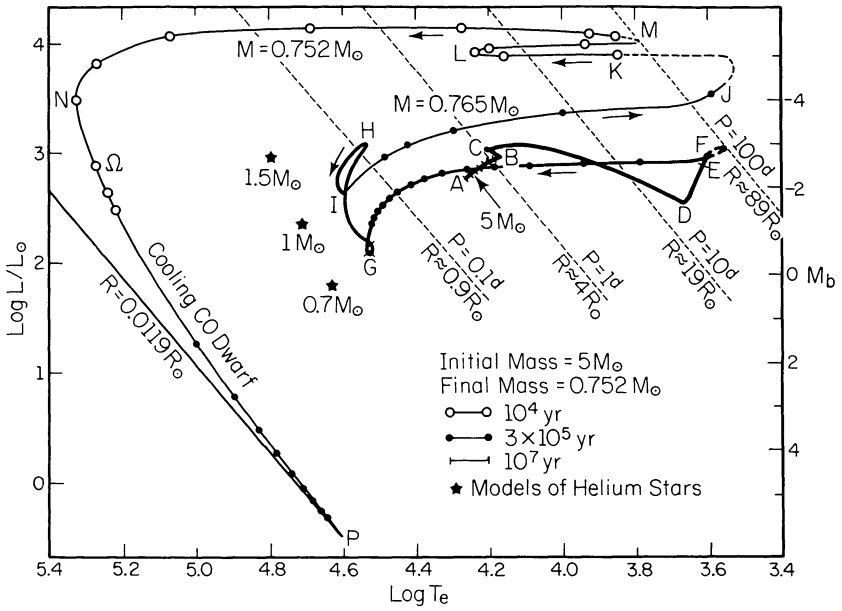

FIG. 49.—Evolutionary track in the H-R diagram of a model star of initial mass 5 $M_\odot$ from which mass is abstracted at a high rate just before helium is ignited in the core. The model exhausts hydrogen at its center at point B, evolves on a thermal time scale to point D, where it develops a deep convective envelope, and loses mass between points E and F in such a way as to maintain a nearly constant radius until exposure of highly processed interior matter causes radial shrinkage without further mass loss. The mass of the contracting remnant, which continues to burn hydrogen in its envelope as it evolves to the blue of the location of its main-sequence progenitor, is 0.765 $M_\odot$. Core helium burning occurs in the region near point G (the five-pointed stars mark the positions of core helium-burning models composed entirely of helium [Paczyński 1971*a*]), and a second phase of radial expansion takes place after helium is exhausted in a large region about the center (near point H). The model returns to the red and an additional, very slight, loss of mass in a second Roche-lobe filling episode forces evolution back to the blue (interrupted briefly by a mild hydrogen shell flash). During the final blueward evolution from point M to point N, which lasts for $\sim 6 \times 10^4$ yr, helium burning in a shell is the source of surface luminosity. Thereafter, the model evolves into a CO white dwarf. From Iben and Tutukov (1985).

continues to evolve to the blue and helium burning in a convective core eventually takes over as the major source of luminosity. The remnant spends $\sim 3 \times 10^7$ yr near point G in Figure 49 burning helium in the core; this is approximately half of the main-sequence lifetime of its precursor. The number ratio of helium to hydrogen at the surface of the remnant is $\sim \frac{1}{2}$, and the position of the remnant in the H-R diagram is quite close to the location of homogeneous models composed of pure helium, three representatives of which are shown by the five-pointed stars in Figure 49 (Paczyński 1971*a*). It is known that subdwarf B stars lie in this vicinity, and so one prediction of the model calculations is that, for some time after a Roche-lobe episode of the sort envisioned here, the system will consist of a main-sequence star with a close sdB or sdO companion. In the particular example chosen, the subdwarf will be bolometrically 10 times brighter than its main-sequence companion, and it will dominate this companion in the far ultraviolet.

Similar behavior is expected for other systems in which the primary, of initial mass in the 2–10 $M_\odot$ range, experiences a late case B mass-loss event. The less massive the primary, the larger is the lifetime of the core helium-burning remnant relative to the main-sequence lifetime of its precursor, so one might expect the frequency of systems consisting of a subdwarf and a main-sequence star to be larger, the smaller the mass of the system. The larger the initial mass of the primary, the smaller is the ratio of hydrogen to helium at the surface after mass-loss terminates and so, the more massive the core helium-burning remnant, the more it will resemble a subdwarf O star.

An example of this type of evolution may be UU Sge, the central star of the planetary nebula Abell 63 (Bond 1976). This system is an eclipsing binary with an orbital period of 11.2 hr (Miller, Krzminski, and Priedhorsky 1976; Bond, Liller, and Mannery 1978), the primary is an sdO star of mass ~ 0.9 $M_\odot$ and the secondary may be a dK main-sequence star of mass ~ 0.7 $M_\odot$. The surrounding planetary nebula is presumably the matter ejected in the common-envelope event which caused the orbital separation of the components to shrink to the present value of ~ 3 $R_\odot$. A further development of this theme may be found in Iben and Tutukov (1989*a*) and in Bond and Livio (1990).

Helium star models initially have convective cores, so when helium vanishes at the center, it also vanishes quickly over a large region about the center, leaving a compact core composed of carbon and oxygen. The subsequent evolution of the model remnant depends on the mass M_R of this remnant, as follows from the study by Paczyński (1971*a*) of helium model stars. If $M_R(M_\odot) < 0.75$, the model remains small as it burns helium in a shell; ultimately the model evolves into a white dwarf consisting of an electron-degenerate CO core capped by a helium layer. The mass of the helium layer relative to the mass of the CO core decreases with increasing M_R. For example, it is $\sim$25% of the total mass of the remnant when $M_r \sim 0.38$ $M_\odot$ and is $\sim$10% of the remnant mass when $M_R \sim 0.52$ $M_\odot$ (Iben and Tutukov 1985).

If $M_R > 2.5$, the model remains compact as it burns helium in a shell, and the helium-exhausted core continues to burn successive nuclear fuels until it has developed a Chandrasekhar-mass core of iron-peak elements; this core will collapse to become a neutron star. The accompanying explosion will be of supernova proportions and, except in very rare instances, it is expected that the binary system will become unbound in the process. If $0.75 < M_R < 2.5$, the CO core becomes electron degenerate and the model expands to giant proportions as helium burns in a shell. In this last case, the model star again encounters its Roche lobe and experiences a second phase of mass loss. This time, the mass of the remnant will be close to the mass of the CO core when Roche-lobe filling occurs.

The model of initial mass 5 $M_\odot$ whose evolutionary track is described in Figure 49 marginally fulfills the mass requirement for expansion after the exhaustion of helium at the center (between points I and J), and the ejection of an additional 0.023 $M_\odot$ is sufficient to expose very highly processed material and force the model to evolve again to the blue. The number ratio of helium to hydrogen at the surface becomes ~3. After experiencing a final, very mild hydrogen shell flash, the model then continues to evolve monotonically to the blue along a nearly horizontal track over a period of $\sim 5 \times 10^4$ yr. The source of surface luminosity is helium burning at the base of a small helium-rich envelope above a large CO electron-degenerate core. Ultimately, helium burning is extinguished, and the model evolves onto a cooling white dwarf sequence.

Qualitatively similar behavior is found for models of larger initial mass, but, as initial mass is increased above 5 $M_\odot$, more and more mass is lost in the second Roche-lobe overflow event and the surface abundance of hydrogen drops rapidly to zero. The hydrogen-deficient components in the rather wide binaries KS Per (Drilling and Schönberner 1982) and Upsilon Sagittarii (Schönberner and Drilling 1983) may be examples of this kind of evolution in which a second phase of mass loss abstracts all hydrogen-containing matter from the surface (see also Iben and Tutukov 1985), except that, in order to account for the large current orbital separation, it is necessary to give up the assumption of common-envelope formation. That is, one must suppose that the two components in the initial binary are of comparable mass and/or that the primary first fills its Roche lobe before developing a deep convective envelope. The final remnant mass will be approximately the same in such an early case B scenario as in the late case B scenario. Another possibility for explaining Upsilon Sgr and KS Per is that the primary fills its Roche lobe after it has developed an electron-degenerate CO core in a case C event (Lauterborn 1970); for primary masses larger than 5 $M_\odot$, there is no hydrogen remaining at the surface of the remnant after the mass-loss episode, and the time scale for evolving to the blue at high luminosity is $\sim 10^4$ yr (Iben 1986).

The remnant masses obtained in case B and case C events which produce CO white dwarfs are compared in Figure 50. The remnant mass in a late case C event is approximately the same as the mass of the white dwarf that a single star of the same initial mass is expected to form if it does not spend much time in the TPAGB phase, as suggested by the observations (§ VIII*a*). It is interesting that the upper limit on the mass of a CO white dwarf precursor in case B is larger than the upper limit for a single star, whereas in early case C it is smaller. The reason for the first result is that, when helium is first exhausted

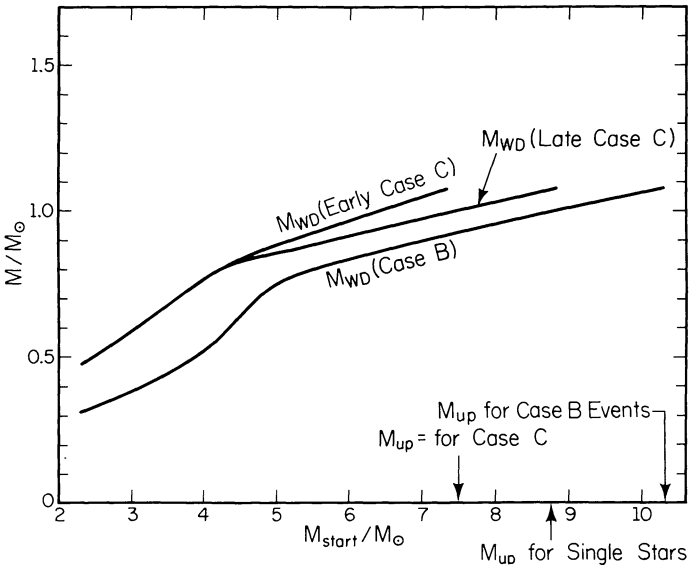

FIG. 50.—Mass of the remnant of a Roche-lobe overflow event experienced by an intermediate-mass model star of Population I composition in a late case B event, an early case C event, and a late case C event. Adapted from Iben (1986).

at the center, the mass of the hydrogen-exhausted core is smaller in a star which has undergone a case B event than it is in a single star of the same initial mass. The reason for the second result is that, at the same time that the mass of the convective envelope is being reduced by mass loss from the surface during an early case C event, the base of this envelope is extending inward into layers containing only helium (the second dredge-up process, see Fig. 4); the reduction in the total mass of the star has the effect of reducing the rate at which the base of the convective envelope can move inward in mass, and so the mass of the growing CO core exceeds 1.1 $M_\odot$, and carbon burning is triggered for smaller initial masses than in the case of a constant mass single star.

The evolution of a model star of modest initial mass (3 $M_\odot$) which experiences a late case B event is shown in Figure 51 (Iben and Tutukov 1985; Iben *et al.* 1986). Note that the core helium-burning phase of the remnant lasts over twice as long as the main-sequence phase of its precursor and that evolution to the red does not occur after the exhaustion of central helium. After undergoing two hydrogen shell flashes, the model experiences helium shell flashes which cause large variations throughout the entire model and large excursions in the H-R diagram. During an entire shell flash cycle, the model spends most of the time along the heavy solid portion of the evolutionary track, releasing gravitational potential energy as it contracts and heats. As it evolves downward along the lower dashed portion of the track, temperatures in the helium-containing layers nearest the center (approximately in the middle of the model in the mass coordinate) become large enough to ignite a thermonuclear runaway. A large amount of nuclear energy is converted locally into heat and the consequent overpressure causes the outer part of the model to expand. The reduction of the pressure on the CO core below the helium-containing layers causes this core to expand and cool adiabatically. In short, the entire model expands and its net store of

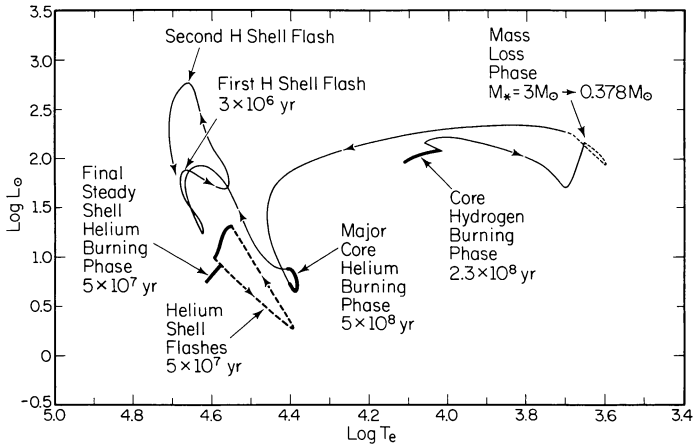

FIG. 51.—Evolutionary track of a 3 $M_\odot$ primary of Population I composition which fills its Roche lobe after having developed a deep convective envelope, but before having ignited helium at its center. Note that the duration of the core helium-burning phase of the remnant is over twice as large as the duration of the main-sequence phase of its precursor. After helium is exhausted at the center, the model experiences two hydrogen shell flashes of short duration followed by 30 helium shell flashes of much longer duration. Three of the four heavy segments along the tracks indicate where evolution occurs on a nuclear-burning time scale. During the helium shell-flashing stage the model evolves quickly in a counterclockwise fashion along the dashed curve and much more slowly along the fourth heavy segment. Two additional hydrogen shell flashes occur after the termination of the shell helium-burning episodes, and the model then evolves as a cooling white dwarf. From Iben and Tutukov (1985) and Iben *et al.* (1986).

thermal energy decreases. Ultimately, essentially all of the nuclear energy that is released in the flash is used up in decreasing the binding energy of the model as it expands and cools along the upper branch of the dashed track in Figure 51.

The nature of the shell flashes encountered by this model are quite different from the ones encountered by single stars in the AGB phase. In the AGB case, the thermonuclear runaway is a consequence of the buildup of a critical mass of helium between the CO core and the hydrogen-burning shell (this could be called an accumulation instability followed by a relaxation) and the more massive CO core is very little affected by the ensuing flash. In the case at hand, there is no buildup of a critical mass, and it is solely the heating of the contracting model that triggers the thermonuclear instability (this could be called a "pure" relaxation oscillation). Each successive shell flash is less powerful than the preceding flash and, after ~30 flashes, the model continues to burn helium quiescently for a time before helium burning is extinguished.

The distribution of composition parameters in the model remnant as it evolves into a white dwarf are shown in Figure 52. It is clear that the remnant cannot be called either a CO white dwarf or a helium white dwarf. For lack of a better name, such a remnant has come to be called a hybrid white dwarf. As discussed in § XIII, there are reasons to believe that mergers of pairs of low-mass white dwarfs may be responsible for the formation of some fraction of all sdO and sdB stars that are not in binaries, and the particular composition characteristics of hybrid white dwarfs play an important role in influencing the motion in the H-R diagram of a merger product and in accounting for the location of real subdwarfs in the H-R diagram.

XII. CATACLYSMIC VARIABLES, SYMBIOTIC STARS, HELIUM CVs, AND NOVAE

a) Hydrogen-accreting White Dwarfs

A basic understanding of the connection between cataclysmic variables (CVs) and classical novae has been known for some time (Walker 1954; Kraft 1959, 1964; Gallagher and Starrfield 1978; Patterson 1984; Shara 1989). The typical CV consists of a fairly massive ($\sim M_\odot$) white dwarf and a low-mass relatively unevolved companion which fills its Roche lobe and is transferring matter through a disk to its companion at a rate in the range 10^{-10}–$10^{-8}\ M_\odot\ \mathrm{yr}^{-1}$ (Patterson 1984).

The preponderance of known systems with massive white dwarf components is probably due to observational selection (Ritter and Burkert 1986; Truran and Livio 1986), and there may be many undetected systems containing less massive white dwarfs. On the other hand, CVs are very close systems ($P_{\rm orb} \sim$ 1–10 hr) which were presumably formed in a common envelope event, and this suggests that the mass of the progenitor of the white dwarf in typical systems may have been considerably larger than the mass of its low-mass companion, a requirement that itself leads to a relatively massive white dwarf. It is therefore not ruled out that the physics of CV formation is partially responsible for the preponderance of massive white dwarf components.

The accepted interpretation of the classical nova phenomenon is that, once enough hydrogen-rich material has been accumulated on the white dwarf, the temperature at the base of the accreted layer becomes large enough to ignite hydrogen, initiating a thermonuclear runaway; the rapid injection of nuclear energy forces the accreted layer to expand to red giant dimensions. The standard theoretical modeling of the outburst assumes the white dwarf to be an isothermal sphere of low temperature, and matter at the base of the accumulated layer is typically electron degenerate when ignition temperatures are reached; consequently, the outburst becomes a dynamical event, and the models indicate that much of the accreted layer

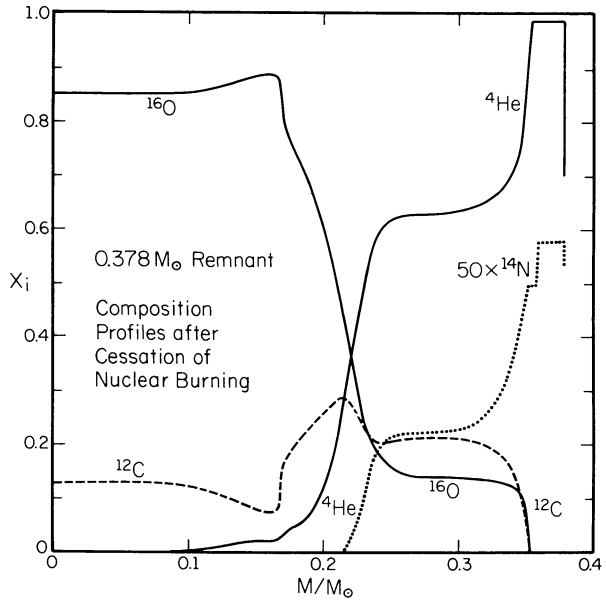

FIG. 52.—The abundances by mass of the major isotopes in the model white dwarf produced by the model whose evolutionary track is described in Fig. 51.

is completely expelled from the system, a result that seems to agree with the observational evidence for fast novae. Agreement between theoretical and observed light curves for fast novae can be achieved only by assuming an initial abundance of CNO elements in the burning layer which is an order of magnitude larger than implied by the spectrum of the mass donor (Starrfield, Truran, and Sparks 1978; Truran 1982; Fujimoto 1982; MacDonald 1983*a*). This requirement is corroborated by direct examination of the nova spectrum (Williams 1985), and the implication is that either some carbon and oxygen has been dredged up from the underlying CO white dwarf into the base of the accreted layer (MacDonald 1983*b*; Sparks and Kutter 1987; Livio and Truran 1987) or that, during a hybernation phase (Shara *et al.* 1986), hydrogen has diffused into the underlying white dwarf, forcing the thermonuclear runaway to begin in a layer rich in carbon and oxygen (Prialnik and Kovetz 1984; Kovetz and Prialnik 1985; Prialnik 1986; Prialnik and Shara, 1986). In either case, during an outburst, matter which was originally a part of the white dwarf is mixed by convection throughout the hydrogen-rich envelope and ejected from the system. Thus, the white dwarf may lose mass.

However, it is not obvious that this behavior will continue for many, many cycles or that it is a proper description for all classical novae. For typical model parameters, the critical mass of accumulated material is $\sim 10^{-5}\ M_\odot$, and this means that a typical CV should experience of the order of 10^5 nova outbursts in its lifetime as a CV. Furthermore, the temperature structure of a white dwarf is a function of its prior history, and the younger the white dwarf when accretion first begins, the weaker will be the degree of electron degeneracy at the base of the accreted layer when hydrogen is ignited and the less violent will be the subsequent outburst, even to the extent that it does not become dynamical (Paczyński and Zytkov 1978).

Figure 53 (Iben 1982*b*) demonstrates this for the case of a CO white dwarf of mass 1.01 $M_\odot$ accreting at a rate (1.5×10^{-9} $M_\odot$ yr^{-1}) which in the normal scenario would be expected to exhibit a dynamical outburst. The white dwarf has a thermal structure which would obtain if it had been accreting for a long time, burning hydrogen as rapidly as hydrogen is accreted and burning helium as rapidly as it is deposited below the hydrogen-burning shell; when the equilibrium assumption is dropped, the model at once begins to experience hydrogen shell flashes, the third of which exhibits the behavior shown in Figure 53.

Accretion requires the presence of a nearby donor. If this donor is a low-mass unevolved star, the system must be a CV, and as the accretor expands beyond the outer Lagrangian point in the equipotential system about the two components, matter will be lost from the system. However, just as in the case of the central star of a planetary nebula, the position along the plateau portion of the track (as the model evolves back to the blue) is directly related to the amount of hydrogen-rich material remaining above the underlying compact CO core, and thus blueward motion can be accelerated by mass loss from the surface. In the present situation, the mass M_e of the hydrogen-rich layer is $M_e \sim 2.7 \times 10^{-5}\ M_\odot$ when the model ignites a hydrogen shell flash, a return to the blue on a rapid time scale is initiated when this mass is reduced to $M_e = M_{e,\mathrm{crit}} \sim 1.3 \times 10^{-5}\ M_\odot$, and burning continues at a high surface temperature until $M_e \sim 4 \times 10^{-5}\ M_\odot$. Thus, only about half of the mass

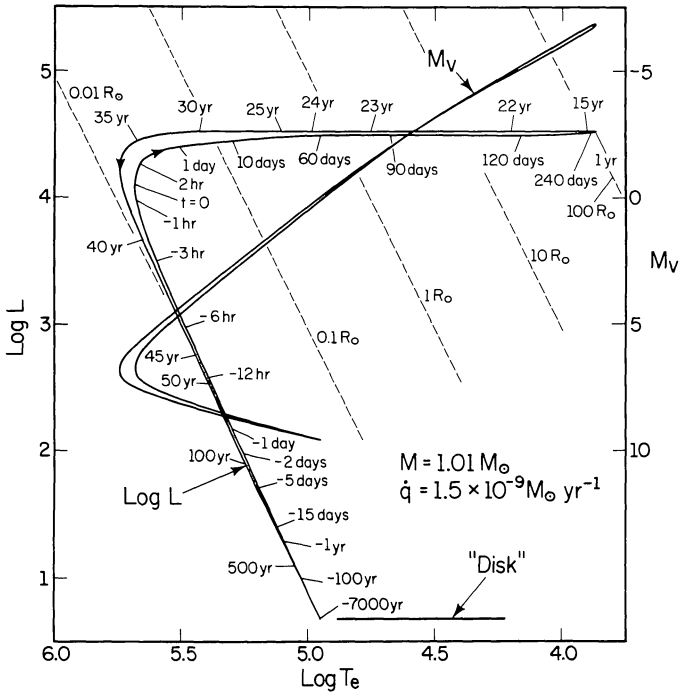

FIG. 53.—The evolutionary track of a "hot" white dwarf of near solar mass accreting at a rate $1.5 \times 10^{-9}\ M_\odot$ yr^{-1}. Evolution in both bolometric luminosity and in visual magnitude is shown.

accreted between outbursts is lost from the system, and, should this behavior persist, the white dwarf would reach the Chandrasekhar mass after 300,000 outbursts, or after the transfer of 0.8 $M_\odot$ of hydrogen-rich matter in more than 5×10^9 yr. Kato and Hachisu (1989) explore evolution similar to that envisioned here, taking wind mass loss into account, and conclude that evolution to supernova conditions is unlikely.

When the assumed accretion rate is increased, the mass of the accreted layer required for triggering the nova outburst is reduced. For example, if an accretion rate of $1.5 \times 10^{-8}\ M_\odot$ yr^{-1} is chosen, M_e at the start of the outburst is only half the value required when the accretion rate is 10 times smaller. The track in the H-R diagram is identical with that of the model with $dM/dt = 1.5 \times 10^{-9}\ M_\odot$ yr^{-1}, but the time scale for evolution prior to outburst is 20 times shorter, and the time spent formally as a red supergiant is only a few weeks rather than several decades. The reason for this last difference is that $M_e \sim M_{e,\mathrm{crit}}$ even before the large dM/dt model achieves red giant dimensions; the radius of the model remains larger than 1 $R_\odot$ for only 4 months, in contrast to the 23 yr for the smaller dM/dt model. Both models spend approximately the same time, $\sim$15 yr, along the bluest portion of the plateau track. One might expect the large dM/dt model to retain most of the mass accreted between outbursts and anticipate that the white dwarf would reach the Chandrasekhar mass after $\sim$300,000 outbursts, just as in the acse of the small dM/dt model.

However, after only $\sim$100 outbursts, the mass of the helium layer which builds up above the CO core becomes large enough that a helium shell flash will be ignited (Iben 1982*b*). The consequences of this flash have not been quantitatively explored, but one can anticipate that of the order of half of the accumulated helium layer is expelled from the system and

that, even if configurations consisting of a massive hot white dwarf accreting from a low-mass unevolved companion arise in nature, these systems will not in general reach conditions leading to a supernova explosion, but see Fugimoto and Sugimoto (1982).

Many slow novae exhibit characteristics similar to those exhibited by the models of hot accreting white dwarfs. These are in wide systems consisting of a white dwarf and an AGB or RGB star and they belong to the class of stars known as symbiotic stars. The white dwarf accretes matter from the wind emitted by its companion and thermonuclear outbursts must therefore occur just as in the case of CVs. Because the systems are very wide, the expansion phase will not be terminated by mass loss due to expansion beyond the outer Lagrangian point and, provided that the mass accretion rate is small enough, cases in which the nova remains for extended periods at both the red and blue portions of the plateau phase are to be expected. Examples of such "symbiotic novae" are RR Tel, PU Vul, and HM Sge. After its outburst in 1944, RR Tel spent $\sim$5 yr in the red phase and probably $\sim$25 yr in the blue (Thackeray 1977). In 1985, 6 yr after its outburst in 1979 (Ashbrook 1979), the characteristics of PU Vul placed it in the H-R diagram very near the brightest and coolest position along the evolutionary track in Figure 53 (Belyakina *et al.* 1984, 1985, 1989). After its outburst in 1975, HM Sge evolved rapidly to the red and then back to the blue in less than a year; between 1976 and 1985 the surface temperature of the hot component increased from 40,000 to 150,000 K at a constant bolometric luminosity estimated to be $\sim 10^4\ L_\odot$ (Nussbaumer and Vogel 1990). Other examples are discussed by Kenyon and Truran (1983).

In summarizing this discussion on white dwarfs which accrete hydrogen-rich matter, we may speculate that (1) in symbiotic systems, the white dwarf retains much of the matter accreted between nova outbursts and so the release of gravitational potential energy in outer layers of the white dwarf keeps these layers hot enough to prevent the outburst from becoming dynamical; and (2) in CVs, the white dwarf retains only a fraction of the matter accreted between outbursts, and outer layers in the white dwarf do not remain hot enough to prevent thermonuclear outbursts from eventually becoming dynamical, leading to a situation where the matter lost per outburst is even larger than the matter accreted between outbursts. It is possible that the accretion rate in symbiotic systems is in general much larger than in CVs and this circumstance would help understand the apparent difference in behavior of the two types of system.

The white dwarf component in many symbiotics appears to be brighter than at the bluest point along the model trajectories and shows no sign of varying in the manner of slow novae (Boyarchuk 1990). One interpretation of such systems is that the white dwarf is burning hydrogen at the same rate at which it is accreting new hydrogen, and this implies a mass-transfer rate that is quite large indeed, namely, $dM/dt > 1.3 \times 10^{-7}\ M_\odot\ \mathrm{yr}^{-1}\ (M_{\mathrm{WD}}/M_\odot)^{3.57}$ (Iben 1982*b*).

b) Helium Star Cataclysmic Variables

Although there are no examples in the observational literature of a nova whose spectrum indicates a complete absence of hydrogen, the theory of binary star evolution suggests that systems can arise in which a white dwarf accretes pure helium from a core helium-burning companion (Tornambè and Matteucci 1986; Iben and Tutukov 1987; Tutukov and Fedorova 1990) and that, after enough mass has been transferred, a thermonuclear runaway should occur in the accreted helium layer (Tutukov and Ergma 1979; Ergma and Tutukov 1980; Taam 1980*a, b;* Fujimoto 1980, 1982; Nomoto 1980, 1982*a, b;* Fujimoto and Sugimoto 1982).

These systems may be called helium star CVs (HeCVs), and they arise from systems consisting of a CO or ONe white dwarf and an intermediate-mass main-sequence star which eventually fills its Roche lobe and experiences a case B mass-loss event; orbital shrinkage in a common envelope phase leaves the helium star remnant nearly in Roche-lobe contact and angular momentum loss by GWR leads to establishment of contact. Transfer of helium to the white dwarf thereafter proceeds at the rate $dM/dt \sim 3 \times 10^{-8}\ M_\odot\ \mathrm{yr}^{-1}$ (Iben *et al.* 1987). One may estimate that HeCvs are formed at the rate of $\sim$0.01 yr^{-1} in the entire disk of our Galaxy (Tutukov and Fedorova 1989; Iben and Tutukov 1990*b*). In typical systems, with orbital periods between 20 minutes and an hour, the mass donor has a luminosity between 4 $L_\odot$ and 250 $L_\odot$ and a surface temperature between 30,000 K and 60,000 K. There may be one such system within 100 pc of the Sun, 300 within 1000 kpc, and 10^5 in the entire Galaxy.

Conditions within two model CO white dwarfs which have accreted at the rate $dM/dt \sim 3 \times 10^{-8}\ M_\odot\ \mathrm{yr}^{-1}$ for a time sufficiently long to achieve helium ignition are shown in Figure 54 (Iben 1990*b*; Iben and Tutukov 1991*b*). The mass of the accreted helium layer is nearly the same in both instances, but the density at the ignition point is much larger in the case of the more massive white dwarf, leading to a dramatic difference between the two cases in the outcome of the flash. The conditions at the outset of the flash in the less massive white dwarf are almost identical with those in the electron-degenerate helium core of a low-mass model star when it reaches the tip of the red giant branch and achieves helium ignition (Despain 1981), and it has been established that the ensuing thermonuclear runaway does not develop into a hydrodynamic event (Mengel and Sweigart 1981; Fujimoto, Iben, and Hollowell 1990). Thus, the low-mass case does not explode with the power of a supernova. However, the optical display is expected to be much more varied and long lasting than that of a classical nova. At least half of the $\sim$0.14 $M_\odot$ of accreted matter will, in consequence of expansion beyond the outer Lagrangian point, be expelled from the system. Furthermore, when the mass of the helium layer decreases to a few times 0.01 $M_\odot$, the remnant will contract and continue to burn at sufficiently high T_e to cause the ejected helium to fluoresce as a planetary nebula. The duration of the planetary-nebula–like phase would be $\sim 10^4$ yr if the nebular expansion velocities were of the order of 10 km s^{-1}. However, the violence of the explosion is such that one may anticipate expansion velocities on the order of the orbital velocities in the system ($\sim$1000 km s^{-1}), and this reduces the expected lifetime to only $\sim$100 yr. Assuming that $\sim 5 \times 10^4$ systems in the Galaxy can become "super novae" after transferring helium for $\sim 5 \times 10^6$ yr, one may anticipate about one super nova per century.

The impact of the outburst on the orbital separation is not obvious, as there are competing effects—frictional interaction between the helium-star companion and the escaping matter will act to decrease the separation, but mass loss in an approxi-

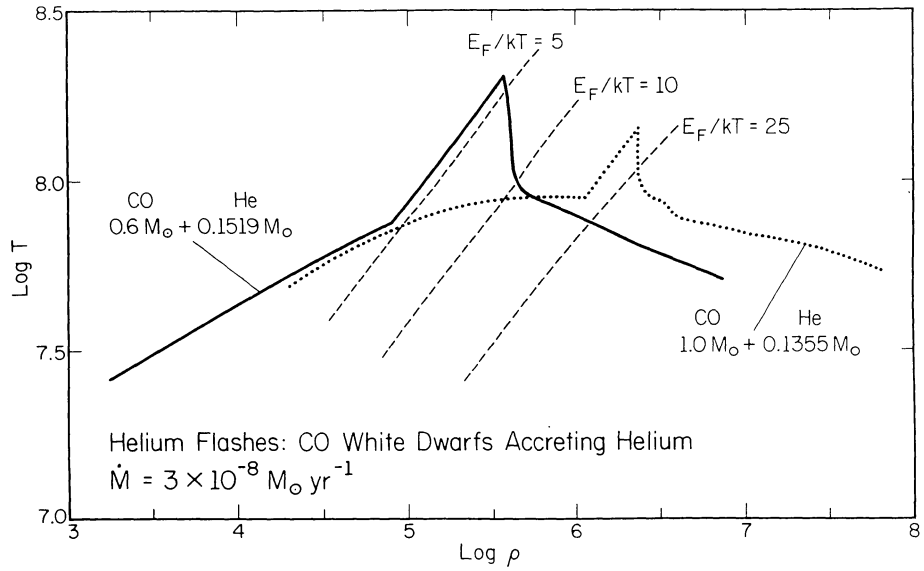

FIG. 54.—Thermal and density structure of cold CO white dwarfs accreting pure helium at a rate $dM/dt = 3 \times 10^{-8}\ M_\odot\ \mathrm{yr}^{-1}$. Lines of constant electron Fermi energy ϵ_F over kT indicate the degree of electron degeneracy. After accretion of the indicated amount of helium, each model is experiencing a helium shell flash. In the higher mass model, the flash is expected to develop into a dynamical event, with burning fronts propagating both inward and outward; complete disruption and an optical display of modest supernova proportions are expected. In the lower mass model, characteristics of the thermonuclear runaway are very similar to those in the core of a low-mass single star during the first core helium-burning flash, and the flash is expected to remain quasi-static, but the optical display is expected to be more dramatic than that of a typical classical nova; the amount of accreted material which the white dwarf retains has yet to be estimated.

mately spherically symmetric way will act to increase it. If an increase in separation is the net result, then angular momentum loss by GWR will bring the helium star back into Roche-lobe contact and mass transfer will recommence. In any case, it is likely that, over the lifetime of a typical low-mass system, several helium shell flashes will occur.

In the case of the more massive white dwarf accretor, an explosion of supernova proportions is expected. Helium ignition occurs at a point where the electron degeneracy is so great that the release mechanism which can operate when kT approaches the Fermi energy ϵ_F cannot be activated until the matter has been incinerated (burned all the way to iron peak nuclei). Calculations by Nomoto (1982*a, b*) and by Khokhlov (1990) show that a burning front travels outward from the ignition point (about midway in the accreted layer), incinerating and imparting greater than escape velocity to matter through which it passes. It is not clear whether a similar front also travels inward (Nomoto finds that it may, and Khokhlov finds that it does not). If a front does move inward, the model explodes as a full fledged supernova (e.g., Taam 1980*a, b;* Nomoto 1982*b*). If only an outwardly moving front is formed, then only the outer half of the accreted layer will be incinerated and blown off; the model will then appear as a "dwarf" supernova, developing a maximum luminosity some 10 times fainter than if the entire model were to explode. The supernova 1885A in Andromeda may be a real analog. Since there is no hydrogen in the system, the dwarf supernovae envisioned here cannot be mistaken for Type II supernovae, but could account for some fraction of Type Ib supernovae. Assuming $\sim 5 \times 10^4$ HeCV's in the galaxy which accrete for $\sim 5 \times 10^6$ yr before experiencing a star-disrupting explosion, one may anticipate one dwarf supernova per century. Given enough centuries of observation, the ratio of super novae to dwarf supernovae will provide a useful constraint on the model scenarios.

XIII. WHITE DWARF MERGERS AND THEIR CONSEQUENCES

Although there are as yet only two well-established close binary white dwarf pair known (the $P_{orb} = 1.6$ day pair L870-2 and the $P_{orb} = 1.15$ day pair WD 0957-666 [Bragaglia et al. 1990]), theoretical estimates suggest that the rate of formation of close white dwarf pairs is a substantial fraction of the total stellar birthrate. The most frequently forming pairs are helium white dwarfs and their formation rate in the Galaxy is estimated to be $\sim 0.1\ \mathrm{yr}^{-1}$ (Iben and Tutukov 1984*a*; 1986) or $\sim 20\%$ of the total stellar birthrate. Component masses range from a minimum of $\sim 0.13\ M_\odot$ to a maximum of $\sim 0.5\ M_\odot$, a typical component mass ratio being $q \sim 0.7$–0.8.

Because the mass of each white dwarf is directly related (see eqs. [1] and [2]) to the orbital separation when its progenitor fills its Roche lobe, lighter white dwarf pairs are in tighter orbits than heavier ones and orbital shrinkage due to the emission of GWR occurs at a more rapid rate for lighter pairs than it does for heavier ones. Roughly speaking, pairs of total mass less than $0.6\ M_\odot$ will merge within a Hubble time, whereas those of mass greater than $0.6\ M_\odot$ require longer than this.

Since the time scale for evolution to merger conditions decreases very rapidly with decreasing orbital period ($\tau_{GW}[\mathrm{yr}] \sim 10^{8.4}(P_{orb}[\mathrm{hr}])^{8/3}$ for two white dwarfs each of mass $0.25\ M_\odot$), the probability of discovering short period systems decreases very quickly with decreasing period and this (Iben and Tutukov 1991*a;* Iben 1990*a*) may account for the failure of several explicit searches for short-period pairs (Robinson and Shafter

1987; Foss, Green, and Wade 1990). It also explains why the observed number-mass distribution contains very few white dwarfs less massive than $\sim 0.3\ M_\odot$ (Koester, Shulz, and Weidemann 1979; Bergeron, Saffer, and Liebert 1990); the very lightest pairs merge shortly after formation and ultimately evolve into single white dwarfs (Iben and Tutukov 1986). The overall rate of mergers is estimated to be $\sim 0.05\ \mathrm{yr}^{-1}$.

The mass ratio is typically large enough that, when the lighter white dwarf fills its Roche lobe, mass transfer occurs at a rate which exceeds by orders of magnitude the Eddington accretion limit for the more massive white dwarf (Webbink 1984), and the net result is that the lighter white dwarf is transformed into a "thick disk" about the heavier white dwarf, as predicted by Tutukov and Yungelson (1979) and found by Mochkovich and Livio (1989) and by Benz *et al.* (1990). The thick disk is initially nearly spherically symmetric, and it is supported by thermal pressure forces rather than by "centrifugal" forces. However, it is expected that, in the real situation, magnetic fields will be present and that angular momentum will be transported outward very efficiently by Alfvén waves (Mestel and Weiss 1987) and expelled from the system by a wind which does not reduce the mass appreciably. Thus, the further evolution of the system may be explored by accreting helium onto a model helium white dwarf in a spherically symmetric way and at a rate greater than Eddington (Iben 1990*a*).

The accreted helium forms a large sphere of radius larger than the orbital separation of the progenitor white-dwarf pair. The maximum temperature, which occurs near the mass center of the accreted layer, does not become large enough to ignite helium during the accretion process. However, once accretion ceases, the model contracts nearly adiabatically until a first helium shell flash is ignited at the position of maximum temperature. Helium burning then proceeds inward in a series of flashes until a last flash is ignited at the center. Thereafter, the model embarks upon an extended period of burning helium in a convective core. Evolutionary tracks followed by several models from the onset of core helium burning are shown in Figure 55 (masses 0.38, 0.46, and 0.60 $M_\odot$). After exhausting central helium, the lowest mass models experience a series of helium shell flashes similar to those described in § XI, and then go on to become hybrid white dwarfs. The excursions in the H-R diagram during helium shell flashes are large and are therefore not shown. More massive models burn helium in a shell quiescently and evolve into CO white dwarfs.

The solid circles in Figure 55 are the positions of a collection of subdwarf O stars (Drilling 1986), and they are accurate to perhaps 1 mag in M_V and to perhaps 0.2 in log T_e. The locations of horizontal branch stars in the globular cluster M3 is shown for comparison. The models can account for the bluest and dimmest sdO stars, but not for the brightest. However, another configuration can be achieved by the merger of a helium white dwarf with a hybrid white dwarf. The evolutionary path of a model of mass 0.5 $M_\odot$ constructed by accreting pure helium onto a hybrid white dwarf model of mass 0.38 $M_\odot$ passes comfortably through the region defined by the brightest sdO stars.

Still different configurations can be achieved by merging CO and helium white dwarfs. The upshot is that, after a few helium shell flashes, the merger product burns helium quiescently in a

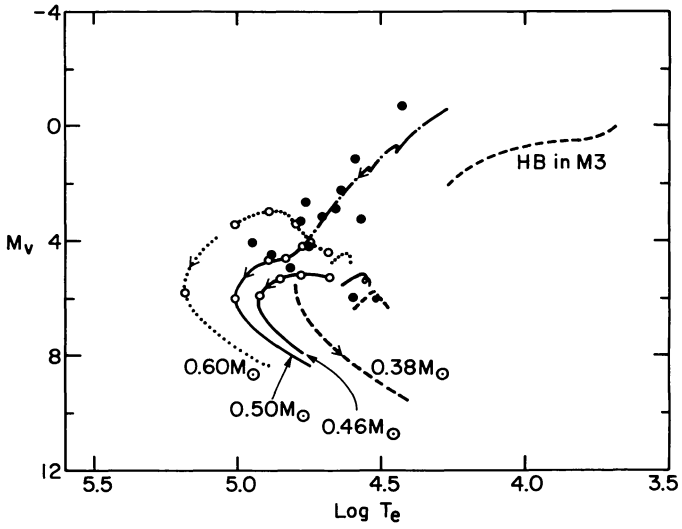

FIG. 55.—Theoretical tracks of models which arise from the merger of two helium white dwarfs (models of mass 0.38, 0.46, and 0.6 $M_\odot$) or of a helium white dwarf with a hybrid white dwarf (model of mass 0.5 $M_\odot$) compared with the positions of sdO stars (Drilling 1986). From Iben (1990).

shell and evolves in the H-R diagram through a region determined by the masses of the precursor white dwarfs. Approximating the radius of the CO core by the radius of a cold white dwarf of the same mass, Iben and Tutukov (1989*b*) predict that merger products define the band in Figure 56 labeled "superhorizontal branch." Fujimoto and Iben (1991) construct complete models, assuming a steady state thermal structure for the CO core and neglecting the liberation of gravitational potential energy. They find that the Iben-Tutukov assumption is a poor approximation for small CO cores, but that the prediction of a superhorizontal branch persists, albeit with considerable differences in detail. Experiments in which helium is accreted at high rates on models of cold white dwarfs show that the Fujimoto-Iben approximation can also be a poor one, in that the evolutionary track in the H-R diagram is a function of the prior thermal history of the CO white dwarf (Iben 1990*a*). A superhorizontal branch is still indicated, but its structure is more complex and its vertical extension in the H-R diagram is much larger than the more simple models suggest.

In any case, merger products of various sorts can be constructed to pass through the location of R CrB stars and near the location of the extreme hydrogen-deficient stars represented by the solid circles in Figure 56 above the superhorizontal branch (Drilling 1986). Although the surface temperatures of the observed stars are reliable, the luminosities have been arbitrarily chosen at $M_V \sim -5.5$ mag, and, so, a more meaningful comparison with theory must await the discovery of hydrogen-deficient stars for which reliable distance estimates can be made (as is already the case for several R CrB stars in the Magellanic clouds).

Mergers of pairs of CO white dwarfs are, of course, also expected. In experiments in which CO material is accreted onto a cold CO white dwarf model at less than the Eddington limit (requiring that the initial mass ratio satisfy $q < 0.6$), carbon is ignited in the accreted layer long before the mass of

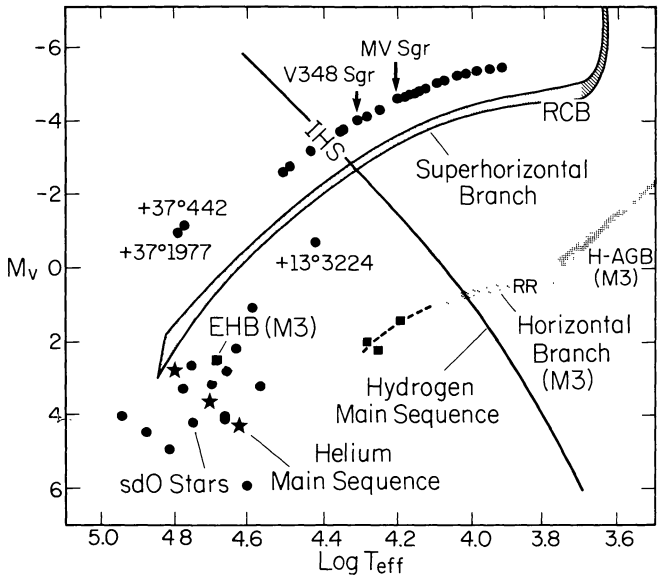

FIG. 56.—The locations of hydrogen-deficient stars in the H-R diagram relative to the position of the hydrogen-burning main sequence and the position of bright stars in the globular cluster M3. The luminous stipled band labeled "superhorizontal branch" is the predicted location of hydrogen-deficient stars which are the consequence of mergers between CO and helium white dwarfs (Iben and Tutukov 1989). The solid circles above the superhorizontal branch are defined by observed hydrogen-deficient stars whose surface temperatures have been assigned by comparing model atmosphere flux distributions with the observed flux distributions but whose bolometric magnitudes have been arbitrarily assigned as about −5.5 mag (Drilling 1986). The location of the R CrB stars is from Feast (1972). The solid five-pointed stars are defined by theoretical models composed of pure helium which are burning helium quiescently at the base of a convective core; they are the predicted consequence of mergers of two helium white dwarfs. The solid circles below the superhorizontal branch are defined by observed sdO stars (Drilling 1986). Data for stars in M3 is from Johnson and Sandage (1956).

the accreting white dwarf reaches the Chandrasekhar limit (Nomoto and Iben 1985) and carbon-burning proceeds inward in a series of flashes, converting the model into an ONe white dwarf (Saio and Nomoto 1985). If the total mass of the precursor white dwarf pair exceeds the Chandrasekhar limit, the system might experience core collapse triggered by electron capture and evolve into a neutron star (Nomoto 1984, 1987).

On the other hand, if $q > 0.6$, the rate of mass transfer will accelerate quickly to far beyond the Eddington limit (Webbink 1984; Webbink and Iben 1988), and, if the combined mass of the precursor white dwarfs is larger than the Chandrasekhar limit, the system may evolve into something akin to what Benz *et al.* (1990) find. In their model, carbon is burning at the base of the thick disk into which the lighter CO white dwarf has been formed. Assuming that the real analog is able to divest itself of enough angular momentum that the spherically symmetric approximation is legitimate, it might be supposed that the merger product would evolve first into an ONe white dwarf and then into a neutron star, as suggested by the study of Saio and Nomoto (1985). However, the Saio and Nomoto study explores the evolution of models less massive than the Chandrasekhar limit. In the more realistic situation where the combined mass of the CO core and the thick disk is larger than 1.4 $M_\odot$, it is quite possible that, when carbon burning dies down following the first carbon flash, the system collapses dynamically until carbon detonation or deflagration fronts arise, leading to a total disruption of the model. In short, the end result may indeed by a Type Ia supernova.

In that case, the scenario described in Figure 57 (Iben and Tutukov 1984*a*) is relevant. This scenario begins with a wide pair of relatively massive intermediate-mass stars which evolve through several common envelope phases (case C Roche-lobe filling episodes) into a pair of comparable-mass CO white dwarfs of total mass greater than 1.4 $M_\odot$ and orbital separation (1–3 $R_\odot$), such that merger will occur within 10^8–10^{10} yr. Presumably the distribution of a birthrate function of initial white-dwarf pairs with regard to initial separation is a continuous one. Therefore, even though the main phase of star formation may have been completed, as is thought to be the case in elliptical galaxies, many white dwarf pairs with the indicated initial properties which have been formed during the active star formation phase still exist and angular momentum loss by GWR is steadily forcing systems of larger and larger initial orbital separation into contact. Thus, this scenario is able to account for the occurrence of Type Ia supernovae in elliptical galaxies in which active star formation is not taking place and, since the rate at which white dwarf pairs move into contact decreases with increasing initial separation, and since one may expect a large spread in ages among galaxies, it is also able to account for the fact that the Type Ia SN rate per unit luminosity in the blue appears to vary by as much as a factor of 5 from one elliptical to another.

XIV. BLUE STRAGGLERS, STELLAR MERGERS, AND STAR BURSTS

Since they were first recognized in the globular cluster M3 as a distinct class (Sandage 1953), blue stragglers have remained a mystery whose solution has not followed in a straightforward fashion from either theoretical or observational considerations. The blue stragglers in M3 and those since identified in other old clusters both in the halo and in the disk appear to be main-sequence stars, but they are brighter and bluer than stars at the usually well-defined cluster turnoff point. With the traditional assumption that all stars in a cluster are coeval, apart from a small spread due to the finite duration of the formation process, the only way to account for the location of these stars in terms of single star evolution is to appeal to some sort of exotic mixing which extends their lifetime to become comparable with the lifetime of less massive stars which are clearly in the process of evolving away from the main sequence (Wheeler 1979). However, there are no indications from the surface characteristics of these stars, whether related to rotation rate, magnetic field strengths, or distribution of element abundances, to suggest that they are anything other than ordinary main-sequence stars.

Another explanation supposes that blue stragglers are the consequence of the merger of the components of a primordial binary (McCrea 1964). However, until the relatively recent appreciation of the role of tidal torques and of a MSW in causing orbital shrinkage and Roche-lobe filling, it has traditionally been assumed that mass transfer cannot begin until the primary has developed a compact hydrogen-exhausted core and has begun to evolve toward the giant branch. Following mass

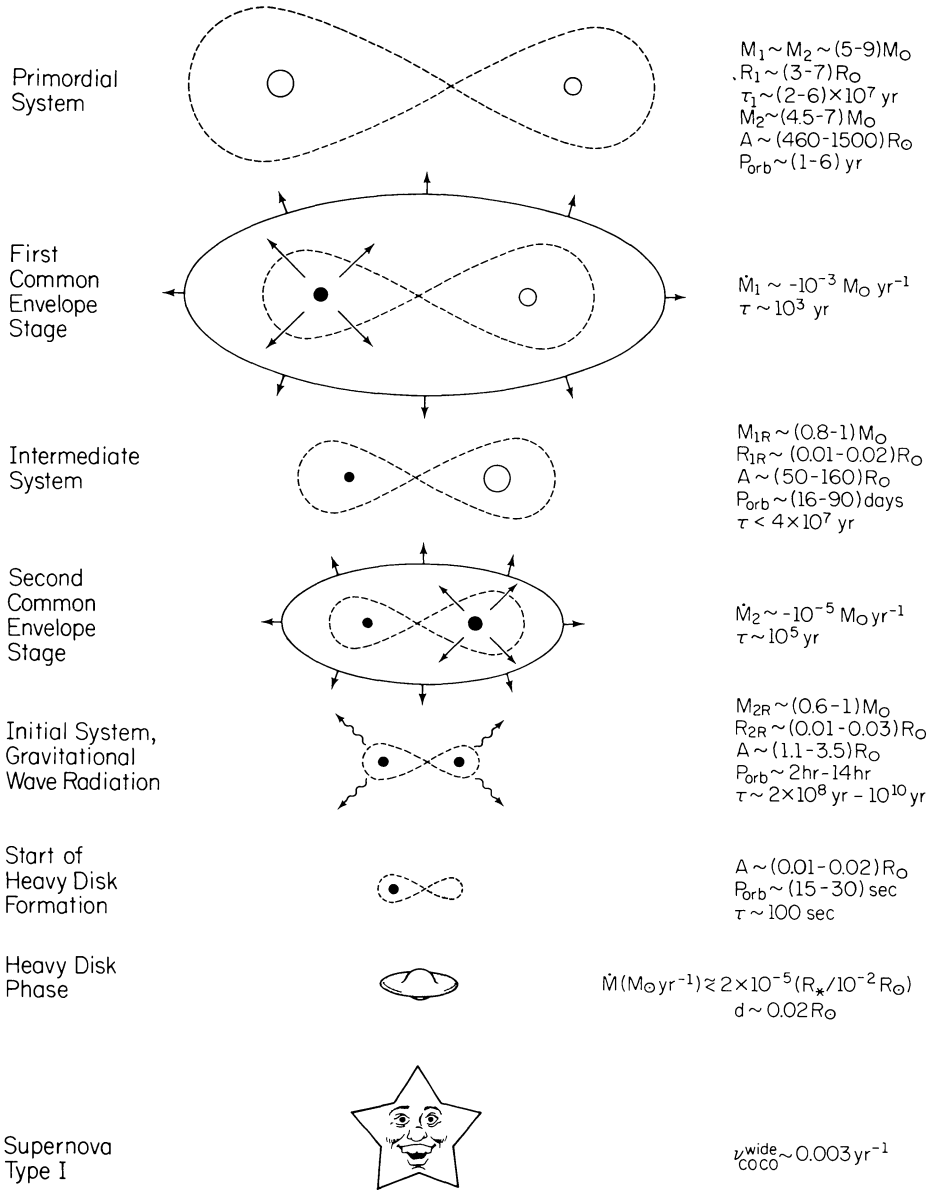

FIG. 57.—Scenario for the formation of a Type Ia supernova from a wide binary consisting of two relatively massive intermediate-mass stars which evolve through two common envelope phases into a close pair of CO white dwarfs whose combined mass exceeds the Chandrasekhar limit. The depiction of the final outcome is due to the draftsman Robert McFarlane, and its aspect has been inspired by the thought that this scenario may account for the formation of Type Ia supernovae in elliptical galaxies. From Iben and Tutukov (1984*a*).

transfer, the compact core of the mass donor would survive for a time as a subgiant (as in an Algol system) or as a helium star, and then evolve into a white dwarf. Efforts to detect the presence of a highly evolved companion have, except in rare instances, been unsuccessful.

Clues to possible solutions of the mystery are contained in the observational data, a part of which is summarized in Figures 58 (Eggen and Iben 1988) and 59 (Eggen and Iben 1989). The location in the H-R diagram of the brightest stars in the very young disk cluster α Persei are shown in Figure 58. There are several prominent distinctions in the properties of the stars represented by open circles (mode A stars) and those represented by solid circles (mode B stars). Those represented by open circles are brighter, rotate more rapidly, and are spatially much more concentrated to the center of the cluster than are those represented by the solid circles. Further, comparison with theoretical isochrones (Bertelli *et al.* 1987) suggests that the two groups of stars are of quite different age. Member stars in other very young disk clusters such as the Pleiades and IC 2602 may similarly be classified into two groups of different age, spatial concentration, and rotational properties. A possible inference is that there have been two major bursts of star formation in these very young clusters, and that the "blue stragglers" in them are simply stars which have been formed in the second burst. The properties of stars in young disk aggregates such as the Hyades cluster, the Hyades supercluster, and the Sirius supercluster provide additional evidence that burst activity in large enough systems may extend over $\sim 10^9$ yr.

In old disk clusters such as NGC 188 and M67 and in the very old halo clusters, differences in formation times of this order are not readily discernable. However, in some of these old systems, blue stragglers abound. There are two very tantalizing clues as to their origin. The first is that the one blue straggler in the old group HR 1614 (AW UMa in Fig. 59) is also a W UMa, or contact binary star with an exceedingly small mass ratio $q \sim 0.08$. The second clue is that the old disk aggregates M67 and NGC 188 contain W UMa stars side by side with blue stragglers (Eggen and Sandage 1969; Baliunas and Guinan 1985), whereas several still older halo clusters do not appear to contain any contact binaries, even though they may contain blue stragglers.

The logically most economic way of accounting for these facts is that, in large stellar aggregates, there is a primordial component of close low-mass main-sequence stars. As the aggregate ages, those systems which are close enough to be influenced by tidal torques and which contain at least one component which supports a MSW will lose orbital angular momentum until the initially more massive component fills its Roche lobe after having developed a partially evolved core, but before leaving the main sequence. The system rapidly evolves into a contact binary W UMa star. Forced by angular momentum loss due to a MSW emitted by the common envelope of the system, mass transfer from the slightly more evolved star continues until only one star remains, a bona fide single blue straggler. This last step is a total flight of the imagination (engaged in by others as well, e.g., van't Veer 1975, 1979; Vilhu 1982; Nemec 1989), but the star AW UMa in the HR 1614 group provides powerful circumstantial evidence for its validity. The apparent absence of contact binaries in some of the oldest halo aggregates may be explained by noting that, for large enough orbital separations, tidal torques cannot assist a MSW in bringing about orbital shrinkage; in the oldest aggregates which do not contain contact systems, then, we may speculate that all of those systems which are initially close enough to have evolved into contact have done so and have gone on to become single star blue stragglers. The recent discovery by Mateo *et al.* (1990) of both contact systems and blue stragglers in the halo globular cluster NGC 5466 shows that the process of blue straggler formation from mergers has not ceased in all halo clusters.

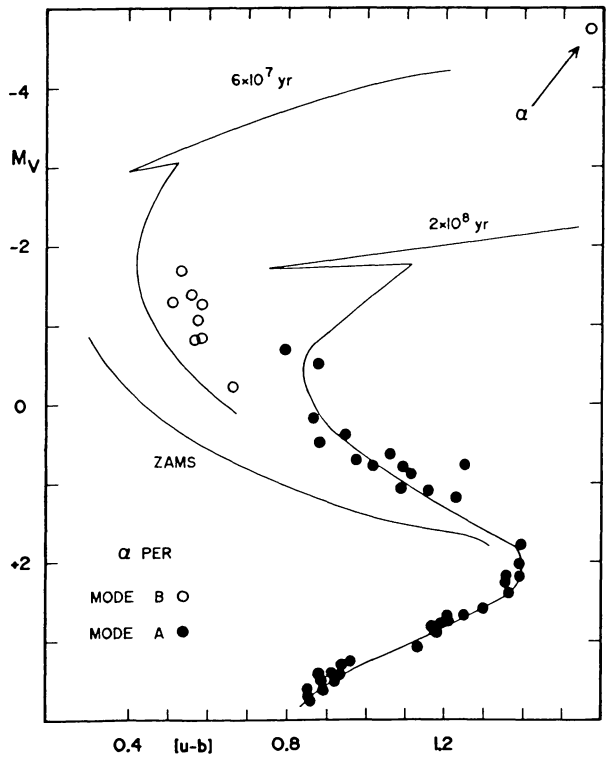

FIG. 58.—Location in the M_V-$(u-b)$ diagram of the brightest stars in the very young disk cluster α Per. The theoretical isochrones are from Bertelli *et al.* (1987). From Eggen and Iben (1988).

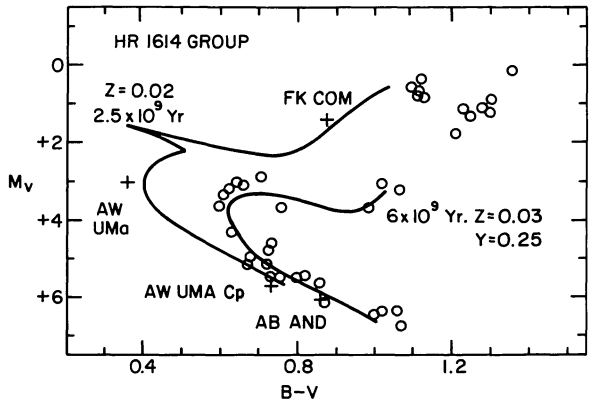

FIG. 59—Location in the M_V-$(B-V)$ diagram of stars in the very old disk aggregate HR 1614. Theoretical isochrones are from Bertelli, Bressan, and Chiosi (1985, 1986). From Eggen and Iben (1989).

It is a very great pleasure to acknowledge the instruction I have received from scientists with whom I have collaborated over the years. Most of those with whom I collaborated prior to 1984 and to whom I remain indebted are cited in the formal report of the 1984 George Darwin lecture (Iben 1985); to that list should be added Erica Böhm-Vitense, Paula Szkody, George Wallerstein, and Judah Schwartz. Since that time, I have enjoyed and benefitted from collaborations with Charles Bailyn, A. G. W. Cameron, Olin Eggen, Charles Evans, Tomoyuki Hanawa, Carl Hansen, Lew Hobbs, David Hollowell, Steve Kawaler, Greg Laughlin, Francesca Matteucci, Shigeki Miyaji, Jim MacDonald, Ken-ichi Nomoto, Catherine Pilachowski, Marty Richardson, Larry Smarr, Dai-ichiro Sugimoto, Ronald Webbink, Don Winget, and Stan Woosley. The continuing stimulation of work with A. V. Tutukov and M. Y. Fujimoto is gratefully acknowledged.

Thanks to editor Helmut Abt for agreeing to find several referees and thanks to the three patient referees who responded and whose most welcome suggestions for improvement have been incorporated in the text.

I thank the American Astronomical Society and many friends for giving me the privilege of representing the field of stellar structure and evolution in the 1989 Henry Norris Russell lecture.

REFERENCES

Abbott, D. C., and Conti, P. S. 1987, *Ann. Rev. Astr. Ap.*, **25,** 113.
Abraham, Z., and Iben, I., Jr. 1971, *Ap. J.*, **170,** 157.
Allen, C. W. 1973, *Astrophysical Quantities* (London: Athlone).
Arnett, W. D. 1969, *Ap. Space Sci.*, **5,** 150.
Arnett, W. D., Bahcall, J. N., Kirschner, R., and Woosley, S. E. 1989, *Ann. Rev. Astr. Ap.*, **27,** 629.
Ashbrook, J. 1979, *Sky and Tel.*, **58,** 11.
Baade, W., and Swope, H. H. 1963, *A.J.*, **68,** 435.
Backer, D. C., and Kulkarni, S. R. 1990, *Phys. Today*, **43,** No. 3, 26.
Bailyn, C. D., and Iben, I., Jr. 1989, *Ap. J.(Letters)*, **347,** L21.
Baker, N., and Kippenhahn, R. 1962, *Zs.Ap.*, **54,** 114.
———. 1965, *Ap. J.*, **142,** 868.
Baliunas, S., and Guinan, E. 1985, *Ap. J.*, **294,** 207.
Barkat, Z., and Wheeler, J. C. 1990, *Ap. J.*, **355,** 602.
Barlow, M. J., and Cohen, M. 1977, *Ap. J.*, **213,** 737.
Becker, S. A. 1981, in *Physical Processes in Red Giants*, ed. I. Iben, Jr., and A. Renzini (Dordrecht: Reidel), p. 141.
Becker, S. A., and Iben, I., Jr. 1980, *Ap. J.*, **237,** 111.
Becker, S. A., Iben, I., Jr., and Tuggle, R. S. 1977, *Ap. J.*, **218,** 633.
Belyakina, T. S., *et al.* 1984, *Astr. Ap.*, **132,** L12.
———. 1985, *Izv. Krymsk. Astrofiz. Obs.*, **72,** 3.
———. 1989, *Astr. Ap.*, **223,** 119.
Benz, W., Bowers, R. L., Cameron, A. G. W., and Press, W. 1990, *Ap. J.*, **348,** 647.
Bergeron, P., Greenstein, J. S., and Liebert, J. 1990, preprint.
Bergeron, P., Saffer, R. A., and Liebert, J. 1990, in *Confrontation between Stellar Pulsation and Evolution, P. A. S. P. Conf. Ser.*, ed. C. Cacciari (San Francisco: A. S. P.), p. 513.
Bergeron, P., Wesemael, F., Liebert, J., and Fontaine, G. 1989, *Ap. J. (Letters)*, **345,** L91.
Bertelli, G., Bressan, A., and Chiosi, C. 1985, *Astr. Ap. Suppl.*, **59,** 33.
———. 1986, *Astr. Ap. Suppl.*, **66,** 191.
Bertelli, G., Bressan, A., Chiosi, C., Nasi, E., and Pigatto, L. 1987, preprint.
Bethe, H. 1986, *Phys. Rev. Letters*, **56,** 1305.
Blanco, V. M., McCarthy, M. F., and Blanco, B. M. 1980, *Ap. J.*, **242,** 938.
Blöcher, T., and Schönberner, D. 1990, private communication.
Boesgaard, A. M. 1988, *Vistas Astr.*, **31,** 167.
Böhm-Vitense, E., Szkody, P., Wallerstein, G., and Iben, I., Jr. 1974, *Ap. J.*, **194,** 125.
Bond, H. E. 1976, Pub. A. S. P., **88,** 192.
Bond, H., Liller, W., and Mannery, E. J. 1978, *Ap. J.*, **223,** 252.
Bond, H. E., and Livio, M. 1990, *Ap. J.*, **355,** 568.
Boothroyd, A. I., and Sackmann, I.-J. 1988*a*. *Ap. J.*, **328,** 653.
———. 1988*b*. *Ap. J.*, **328,** 671.
Boyarchuk, A. 1990, in *Frontier Objects in Astrophysics and Particle Physics*, ed. F. Giovanelli, in press.
Bragaglia, A., Greggio, L., Renzini, A., and D'Odorico, S. 1988, *Messenger*, **52,** 35.
———. 1990, *Ap. J. (Letters)*, **365,** L13.
Burbidge, E. M., Burbidge, G. R., Fowler, W. A., and Hoyle, F. 1957, *Rev. Mod. Phys.*, **29,** 547.
Busso, M., Picchio, G., Gallino, R., and Chieffi, A. 1988, *Ap. J.*, **326,** 196.
Cameron, A. G. W. 1955, *Ap. J.*, **121,** 144.
———. 1960, *A.J.*, **65,** 485.
Cameron, A. G. W., and Fowler, W. A. 1971, *Ap. J.*, **164,** 111.
Cassinelli, J. P. 1979, *Ann. Rev. Astr. Ap.*, **17,** 275.
Castellani, V., Giannone, P., and Renzini, A. 1971*a*, *Ap. Space Sci.*, **10,** 340.
———. 1971*b*, *Ap. Space Sci.*, **10,** 355.
Cerrutti-Sola, M., and Perinotto, M. 1985, *Ap. J.*, **291,** 237.
Chandrasekhar, S. 1931, *Phil. Mag.*, **11,** 592.
———. 1939, *An Introduction to the Study of Stellar Structure* (Chicago: University of Chicago Press).
———. 1958, *Ap. J.*, **102,** 223.
Charbonneau, P., and Michaud, G. 1990, *Ap. J.*, **352,** 681.
Chiosi, C., and Maeder, A. 1986, *Ann. Rev. Astr. Ap.*, **24,** 205.
Christy, R. F. 1962, *Ap. J.*, **136,** 887.
———. 1966, *Ap. J.*, **144,** 108.
Clayton, D. D. 1968, *Principles of Stellar Structure and Nucleosynthesis* (New York: McGraw Hill).
Clayton, D. D., Fowler, W. A., Hull, T. C., and Zimmerman, B. 1961. *Ann. Phys.* **12,** 121.
Cogan, B. C. 1970, *Ap. J.*, **162,** 139.
Colgate, S. A., and White, R. H. 1966, *Ap. J.*, **143,** 626.
Conti, P. S. 1978, *Ann. Rev. Astr. Ap.*, **16,** 371.
Couch, R. G., and Arnett, W. D. 1975, *Ap. J.*, **196,** 791.
Cox, A. N. 1980*a*, *Ann. Rev. Astr. Ap.*, **18,** 15.
———. 1980*b*, *Space Sci. Rev.*, **27,** 478.
Cox, A. N., Starrfield, S. G., Kidman, R. B., and Pesnell, W. D. 1987, *Ap. J.*, **317,** 303.
Cox, A. N., and Stewart, J. N. 1970, *Ap. J. Suppl.*, **174,** 24.
Cox, J. P. 1963, *Ap. J.*, **138,** 487.
Cox, J. P., and Whitney, C. A. 1958, *Ap. J.*, **127,** 561.
Davis, R., Jr., Harmer, D. S., and Hoffman, K. C. 1968, *Phys. Rev. Letters.*, **20,** 1205.
Davis, R., Jr., Lande, K., Lee, C. K., Cleveland, B. T., and Ullman, J. 1990, in *Inside the Sun*, ed. C. Berthomieu and M. Cribier (Dordrecht: Kluwer), in press.
D'Antona, F., and Mazzitelli, I. 1978, *Astr. Ap.*, **66,** 453.
———. 1990, *Ann. Rev. Astr. Ap.*, **28,** 205.
Demarque, P. 1980, in *Star Clusters*, ed. J. E. Hesser (Dordrecht: Reidel), p. 281.
Despain, K. H. 1977, *Ap. J.*, **212,** 774.
———. 1980, *Ap. J. (Letters)*, **236,** L165.
———. 1981, *Ap. J.*, **251,** 639.
Drilling, J. S. 1986, in *Hydrogen-Deficient Stars and Related Objects*, ed. K. Hunger, D. Schönberner, and K. Rao (Dordrecht: Reidel), p. 9.
Drilling, J. S., and Schönberner, D. 1984, *Astr. Ap.*, **113,** L22.
Eddington, A. S. 1926, *The Internal Constitution of the Stars* (Cambridge: Cambridge University Press).
———. 1941, *M.N.R.A.S.*, **101,** 182.
———. 1942, *M.N.R.A.S.*, **102,** 154.
Eggen, O. J. 1989, *Fund. Cosmic Phys.*, **13,** 1.
Eggen, O. J., and Iben, I., Jr. 1988, *A.J.*, **96,** 635.
———. 1989, *A.J.*, **97,** 431.
———. 1991, *A.J.*, in press.
Eggen, O. C., and Sandage, A. R. 1969, *Ap. J.*, **158,** 669.
Ergma, E. V., and Tutukov, A. V. 1980, *Astr. Ap.*, **84,** 123.
Fabian, A. C., Pringle, F. E., and Rees, M. J. 1975, *M.N.R.A.S.*, **172,** 15p.
Feast, M. W. 1972, *M.N.R.A.S.*, **158,** 11p.
Feast, M. W., and Walker, A. R. 1987, *Ann. Rev. Astr. Ap.*, **25,** 345.
Flannery, B. P. 1976, *Ap. J.*, **205,** 217.
Foss, D., Wade, R. A., and Green, R. F. 1991, *Ap. J.*, in press.
Fowler, W. A., Caughlan, G. R., and Zimmerman, B. A. 1975, *Ann. Rev. Astr. Ap.*, **13,** 69.
Fowler, W. A., and Hoyle, F. 1964, *Ap. J. Suppl.*, **9,** 201.
Frogel, J. A., Mould, J., and Blanco, V. M. 1990, *Ap. J.*, **352,** 96.
Fujimoto, M. Y. 1977, *Pub. Astr. Soc. Japan*, **29,** 331.
———. 1980, in *Type I Supernovae*, ed. J. C. Wheeler (Austin: University of Texas), p. 115.
———. 1982*a*, *Ap. J.*, **257,** 752.
———. 1982*b*, *Ap. J.*, **257,** 767.
Fujimoto, M. Y., and Iben, I., Jr. 1991, *Ap. J.*, in press.
Fujimoto, M. Y., Iben, I., Jr., and Hollowell, D. 1990, *Ap. J.*, **349,** 580.
Fujimoto, M. Y., Nomoto, K., and Sugimoto, D. 1976, *Pub. A.S.P.*, **28,** 89.
Fujimoto, M. Y., and Sugimoto, D. 1982, *Ap. J.*, **257,** 291.
Fullerton, L. W., and Hills, J. G. 1982, *A.J.*, **87,** 1.
Gallagher, J. S., and Starrfield, S. 1978, *Ann. Rev. Astr. Ap.*, **16,** 171.
Gallino, R. 1989, in *Evolution of Peculiar Red Giants*, ed. H. R. Johnson and B. Zuckerman (Cambridge: Cambridge University), p. 176.
Gallino, R., Busso, M., Picchio, G., Raiteri, C. M., and Renzini, A. 1988, *Ap. J. (Letters)*, **334,** L45.
Grauer, A. D., and Bond, H. E. 1983, *Ap. J.*, **271,** 259.
Grauer, A. D., Bond, H. E., Liebert, J., Fleming, T. A., and Green, R. F. 1987, *Ap. J.*, **323,** 271.
Grindlay, J. E., and Bailyn, C. D. 1988, *Nature*, **336,** 48.
Habing, H. J., te Lintel Hekkert, P., and Van der Veen, W. E. C. J. 1989, in *Planetary Nebulae*, ed. S. Torres-Peimbert (Dordrecht: Reidel), p. 359.
Hamada, T., and Salpeter, E. E. 1962, *Ap. J.*, **134,** 683.
Hayashi, C. 1961, *Pub. A.S. Japan*, **13,** 450.
Hayashi, C., and Cameron, R. C. 1962, *Ap. J.*, **136,** 166.
Hayashi, C., Hoshi, R., and Sugimoto, D. 1962, *Progr. Theor. Phys. Suppl.*, **22,** 1.

Heap, S. R. 1982, in *Planetary Nebulae,* ed. R. D. Flower (Dordrecht: Reidel), p. 375.
Heggie, D. C. 1975, M.N.R.A.S., **173,** 729.
Heney, L. G., LeLevier, R., and Levée, R. D. 1955, *Pub. A.S.P.,* **67,** 154.
Hertzsprung, E. 1911, *Publ. Astrophysikalische Obs. Potsdam,* No. 63.
Hills, J. G. 1975*a*, *A.J.,* **80,** 809.
———. 1975*b*, *A.J.,* **80,** 1075.
———. 1978, *A.J.,* **219,** 550.
Hine, B. P., and Nather, R. E. 1987, in *IAU Colloquium 95, 2d Conf. on Faint Blue Stars,* ed. A. G. D. Davis-Philip, D. Latham, and J. Liebert (Schenectady: L. Davis), p. 619.
Hirata, K. S., *et al.* 1989, *Phys. Rev. Letters,* **63,** 16.
Hobbs, L. M. Iben, I., Jr., and Pilachowski, C. 1989, *Ap. J.,* **347,** 817.
Hobbs, L. M., and Pilachowski, C. A. 1988, *Ap. J.,* **334,** 734.
Hogg, H. S. 1955, *Pub. David Dunlop Obs.,* **2,** 35.
Hollowell, D. 1988, Ph.D. thesis, University of Illinois.
Hollowell, D., and Iben, I., Jr. 1988, *Ap. J. (Letters),* **333,** L25.
———. 1989, *Ap. J.,* **340,** 966.
———. 1990, *Ap. J.,* **349,** 208.
Howard, W. M., Mathews, G. J., Takahashi, K., and Ward, R. A. 1986, *Ap. J.,* **309,** 633.
Hoyle, F., and Fowler, W. A. 1960, *Ap. J.,* **132,** 565.
Hoyle, F., and Schwarzschild, M. 1955*a*, *Ap. J. Suppl.,* **2,** 1.
———. 1955*b*, *Ap. J. Suppl.,* **13,** 1.
Huenemoerder, D. P., Buzasi, D. L., and Ramsey, L. W. 1989, *Pub. A.S.P.,* **98,** 1398.
Hundhausen, A. J. 1972, *Coronal Expansion and Solar Wind* (Berlin: Springer Verlag).
Hut, P., and Paczyński, B. 1984, *Ap. J.,* **284,** 675.
Hut, P., and Verbunt, F. 1985, in *Cataclysmic Variables and Low-Mass X-Ray Binaries,* ed. D. Q. Lamb and J. Patterson (Dordrecht: Reidel), p. 103.
Iben, I., Jr. 1964, *Ap. J.,* **140,** 1631.
———. 1965*a*, *Ap. J.,* **141,** 993.
———. 1965*b*, *Ap. J.,* **142,** 1447.
———. 1966*a*, *Ap. J.,* **143,** 483.
———. 1966*b*, *Ap. J.,* **143,** 516.
———. 1967*a*, *Ap. J.,* **147,** 624.
———. 1967*b*, *Ap. J.,* **147,** 650.
———. 1967*c*, *Ann. Rev. Astr. Ap.,* **5,** 571.
———. 1967*d*, *Science,* **155,** 785.
———. 1968, *Phys. Rev. Letters,* **21,** 1208.
———. 1969, *Ann. Phys.,* **54,** 164.
———. 1971*a*, *Ap. J.,* **166,** 131.
———. 1971*b*, *Pub. A.S.P.,* **83,** 697.
———. 1973a, in *Explosive Nucleosynthesis,* ed. D. W. Schramm and W. D. Arnett (Austin: University of Texas), p. 115.
———. 1973*b*, *Ap. J.,* **186,** 209.
———. 1974, *Ann. Rev. Astr. Ap.,* **12,** 215.
———. 1975*a*, *Ap. J.,* **196,** 525.
———. 1975*b*, *Ap. J.,* **196,** 549.
———. 1976, *Ap. J.,* **208,** 165.
———. 1977*a*, *Ap. J.,* **217,** 788.
———. 1977*b*, in *Advanced Stages of Stellar Evolution,* ed. P. Bouvier and A. Maeder (Geneva Observatory: Sauverny), p. 1.
———. 1978*a*, *Ap. J.,* **219,** 213.
———. 1978*b*, *Ap. J.,* **226,** 996.
———. 1981, *Ap. J.,* **246,** 278,
———. 1982*a*, *Ap. J.,* **253,** 248.
———. 1982*b*, *Ap. J.,* **259,** 244.
———. 1982*c*, *Ap. J.,* **260,** 821.
———. 1983, *Ap. J. (Letters),* **275,** L65.
———. 1984, *Ap. J.,* **277,** 333.
———. 1985, *Quart. J.R.A.S.,* **26,** 1.
———. 1986, *Ap. J.,* **304,** 201.
———. 1988, *Ap. J.,* **324,** 355.
———. 1989, in *Evolution of Peculiar Red Giants,* ed. H. R. Johnson and Ben Zuckerman (Cambridge: Cambridge University Press), p. 205
———. 1990*a*, *Ap. J.,* **353,** 215.
———. 1990*b*, in *Proc. 9th North American Conf. on CV's and LMXB's, Accretion Powered Compact Binaries,* ed. C. Mauche (Cambridge: Cambridge University Press), p. 409.
Iben, I., Jr., Fujimoto, M. Y., Sugimoto, D., and Miyaji S. 1986, *Ap. J.,* **304,** 217.
Iben, I., Jr., and Huchra, J. P. 1971, *Astr. Ap.,* **14,** 293.
Iben, I., Jr., Kaler, J. B., Truran, J. W., and Renzini, A. 1983, *Ap. J.,* **264,** 605.
Iben, I., Jr., and Laughlin, G. 1989, *Ap. J.,* **341,** 312.
Iben, I., Jr., and MacDonald, J. 1985, *Ap. J.,* **296,** 615.
———. 1986, *Ap. J.,* **301,** 164.
Iben, I., Jr., Nomoto, K., Tornambe, A., and Tutukov, A. V. 1987, *Ap. J.,* **317,** 717.
Iben, I., Jr., and Renzini, A. 1982*a*, *Ap. J. (Letters),* **259,** L79.
———. 1982b. *Ap. J. (Letters),* **263,** L23.
———. 1983. *Ann. Rev. Astr. Ap.,* **21,** 271.
———. 1984, *Phys. Repts.,* **105,** 329.
Iben, I., Jr., and Rood, R. T. 1970*a*, *Ap. J.,* **159,** 605.
———. 1970*b*, *Ap. J.,* **161,** 587.
Iben, I., Jr., and Tuggle, R. S. 1972, *Ap. J.,* **173,** 135.
———. 1975, *Ap. J.,* **197,** 39.
Iben, I., Jr., and Tutukov, A. V. 1984*a*, *Ap. J. Suppl.,* **54,** 335.
———. 1984*b*, *Ap. J.,* **282,** 615.
———. 1984*c*, *Ap. J.,* **284,** 719.
———. 1985, *Ap. J. Suppl.,* **58,** 661.
———. 1986, *Ap. J.,* **311,** 753.
———. 1987, *Ap. J.,* **313,** 727.
———. 1989*a*, *IAU Symposium 131, Planetary Nebulae,* ed. S. Torres-Peimbert (Dordrecht: Kluwer), p. 505.
———. 1989*b*, *Ap. J.,* **342,** 430.
———. 1991*a*, in *Frontiers of Stellar Astronomy, A Symposium in Celebration of the Fiftieth Anniversary of McDonald Observatory,* ed. D. Lambert, in press.
———. 1991*b*, *Ap. J.,* in press.
Iben, I., Jr., and Webbink, R. F. 1988, in *IAU Colloquium 114, White Dwarfs,* ed. G. Wegner (New York: Springer), p. 477.
Johnson, H. L., and Sandage, A. 1955, *Ap. J.,* **121,** 616.
———. 1956, *Ap. J.,* **124,** 379.
Kahn, F. D., and West, K. A. 1985, *M.N.R.A.S., 212,* 837.
Kaplan, S. A. 1950, *Astr. Zh.,* **27,** 31.
Käppeler, F., Gallino, R., Busso, M., Picchio, G., and Raiteri, C. M. 1990, *Ap. J.,* **354,** 630.
Kato, M., and Hachisu, I. 1989, *Ap. J.,* **346,** 424.
Kato, M., Hachisu, I., and Saio, H. 1989, *Ap. J.,* **340,** 509.
Kawaller, S. D. 1988, *Ap. J.,* **334,** 220.
Keller, G., and Meyerott, R. E. 1955, *Ap. J.,* **122,** 32.
Kenyon, S. J., and Truran, J. W. 1983, *Ap. J.,* **273,** 280.
Khokhlov, A. M. 1990, private communication.
Kippenhahn, R., and Weigert, A. 1967, *Zs. Ap.,* **65,** 251.
Koester, D., and Chanmugam, G. 1990, *Rept. Progr. Phys.,* **53,** 837.
Koester, D., Schulz, H., and Weidemann, V. 1979, *Astr. Ap.,* **76,** 26.
Kopal, Z. 1978, *Dynamics of Close Binary Systems* (Dordrecht: Reidel).
Kovetz, A., and Prialnik, D. 1985, *Ap. J.,* **291,** 812.
Kraft, R. P. 1959, *Ap. J.,* **130,** 110.
———. 1964. *Ap. J.,* **139,** 457.
———. 1967, *Ap. J.,* **150,** 551.
Kraicheva, Z. T., Popova, E. T., Tutukov, A. V., and Yungelson, L. R. 1978, *Astr. Zh.,* **56,** 1118.
Krolik, J., Meiksin, A., and Joss, P. C. 1984, *Ap. J.,* **282,** 466.
Kwok, S. 1987, *Phys. Rept.,* **157,** 3, 111.
Kwok, S., Purton, G. R., and Fitzgerald, M. P. 1978, *Ap. J. (Letters),* **219,** L125.
Lamb, S. A., Iben, I., Jr., and Howard, M. 1976, *Ap. J.,* **207,** 209.
Lambert, D. L. 1989, in *Evolution of Peculiar Red Giants,* ed. H. R. Johnson and B. Zuckerman (Cambridge: Cambridge University Press), p. 101.
Lambert, D. L., Dominy, J. F., and Sivertsen, S. 1980, *Ap. J.,* **235,** 114.
Lambert, D. L., and Ries, L. M. 1981, *Ap. J.,* **248,** 228.
Lambert, D. L., and Slovak, M. H. 1982, *Pub. A.S.P.,* **93,** 477.
Landau, L. D., and Lifshitz, E. 1962, *The Classical Theory of Fields* (London: Pergamon).
Lattanzio, J. 1986, *Ap. J.,* **311,** 708.
———. 1987, *Ap. J. (Letters),* **313,** L15.
———. 1988, in *The Origin and Distribution of the Elements,* ed. G. J. Mathews (Singapore: World Scientific), p. 398.
Lauterborn, D. 1970, *Astr. Ap.,* **7,** 150.
Lee, Y.-W., Demarque, P., and Zinn, R. 1990, *Ap. J.,* **350,** 155.
Liebert, J., Dahn, C. C., and Monet, D. G. 1988, *Ap. J.,* **332,** 891.
Lipunov, V. M., and Postnov, K. A. 1988, *Ap. Space Sci.,* **145,** 2.

Livio, M., and Soker, N. 1988, *Ap. J.*, **329,** 764.
Livio, M., and Truran, J. W. 1987, *Ap. J.*, **318,** 316.
Luck, R. E., and Lambert, D. L. 1982, *Ap. J.*, **256,** 189.
Lynden-Bell, D., and Pringle, T. E. 1974, *M.N.R.A.S.*, **168,** 603.
Lubow, S. H., and Shu, F. H. 1976, *Ap. J.*, **207,** 653.
Lucy, L. 1976, *Ap. J.*, **205,** 208.
MacDonald, J. 1983*a*, *Ap. J.*, **267,** 732.
———. 1983*b*, *Ap. J.*, **273,** 289.
Maeder, A. 1982, *Astr. Ap.*, **105,** 149.
Malaney, R. A. 1986, *M.N.R.A.S.*, **223,** 709.
Malaney, R. A., and Boothroyd, A. I. 1987, *Ap. J.*, **320,** 866.
Massevitch, A. G., Popova, E. I., Tutukov, A. V., and Yungelson, L. R. 1979, *Ap. Space Sci.*, **62,** 451.
Massevitch, A. G., and Tutukov, A. V. 1988, *Stellar Structure and Evolution: Theory and Observation* (Moscow: Nauk).
Mateo, M., Harris, H. C., Nemec, J., and Olszewski, E. W. 1990, *A. J.*, **100,** 469.
McCrea, W. H. 1964, *M.N.R.A.S.*, **128,** 147.
McGraw, J. T. 1979, *Ap. J.*, **229,** 732.
———. 1980, *Space Sci. Rev.*, **27,** 601.
McGraw, J. T., and Robinson, E. L. 1976, *Ap. J. (Letters)*, **205,** L155.
Mengel, J. G., and Sweigart, A. V. 1981, in *Astrophysical Parameters for Globular Cluster Stars,* ed. A. G. D. Davis Philip (Dordrecht: Reidel), p. 277.
Merrill, P. W. 1952, *Science,* **115,** 484.
Mestel, L. 1952, *M.N.R.A.S.*, **112,** 583.
Mestel, L., and Weiss, N. O. 1987, *M.N.R.A.S.*, **226,** 123.
Meyer, F., and Meyer-Hofmeister, E. 1979, *Astr. Ap.*, **78,** 176.
Mikheyev, S. P., and Smirnov, A. Yu. 1986, *Nuovo Cimento,* 9C, **17,** 1.
Miller, J. S., Krzeminski, W., and Priedhorsky, W. 1976, *IAU Circ.*, No. 2974.
Miyaji, S., Nomoto, K., Yokoi, K., and Sugimoto, D. 1980, *Pub. Astr. Soc. Japan,* **32,** 303.
Mochkovich, R., and Livio, M. 1989, *Astr. Ap.*, **202,** 211.
Mochnacki, S. W. 1981, *Ap. J.*, **245,** 650.
Morton, D. C., 1967*a*, *Ap. J.*, **147,** 1017.
———. 1967*b*, *Ap. J.*, **150,** 535.
Morton, D. C., Jenkins, E. B., and Brooks, N. 1969, *Ap. J.*, **155,** 875.
Nather, R. E., Robinson, E. L., and Stover, R. J. 1981, *Ap. J.*, **244,** 269.
Nemec, J. M. 1989, in *IAU Colloquium 111, The Use of Pulsating Stars in Fundamental Problems of Astronomy,* ed. E. Schmidt (Cambridge: Cambridge University Press), in press.
Nomoto, K. 1980, in *Type I Supernovae,* ed. J. C. Wheeler (Austin: University of Texas), p. 164.
———. 1982*a*, *Ap. J.*, **253,** 798.
———. 1982*b*, *Ap. J.*, **257,** 780.
———. 1984, *Ap. J.*, **277,** 791.
———. 1987, *Ap. J.*, **322,** 206.
Nomoto, K., and Iben, I., Jr. 1985, *Ap. J.*, **297,** 531.
Nomoto, K., Nariai, K., and Sugimoto, D. 1979, *Pub. Astr. Soc. Japan,* **31,** 287.
Nussbaumer, H., and Vogel, M. 1990, *Astr. Ap.*, in press.
Paczyński, B. 1970, *Acta Astr.*, **20,** 47; erratum **20,** 287.
———. 1971*a*, *Acta Astr.*, **21,** 1.
———. 1971*b*, *Ann. Rev. Astr. Ap.*, **9,** 183.
———. 1972, *Ap. Letters,* **11,** 53.
———. 1976, in *IAU Symposium 73, Structure and Evolution of Close Binary Systems,* ed. P. P. Eggleton, S. Mitton, and J. Whelan (Dordrecht: Reidel), p. 75.
———. 1983, *Nature,* **304,** 421.
Paczyński, B., and Zytkow, A. N. 1978, *Ap. J.*, **222,** 604.
Patterson, J. 1984, *Ap. J. Suppl.*, **54,** 443.
Payne-Gaposchkin, C. 1971*a*, in *Galactic Astronomy,* Vol. **2,** ed. H.-Y. Chiu and A. Muriel (New York: Gordon & Breach), p. 245.
———. 1971*b*, in *The Magellanic Clouds,* ed. A. B. Muller (New York: Springer Verlag), p. 34.
Perinotto, M. 1983, in *Planetary Nebulae,* ed. R. D. Fowler (Dordrecht: Reidel), p. 323.
Pilachowski, C. 1986, *Ap. J.*, **300,** 289.
Popova, E. I., Tutukov, A. V., and Yungelson, L. R. 1982, *Ap. Space Sci.*, **88,** 155.
Prialnik, D. 1986, *Ap. J.*, **310,** 222.
Prialnik, D., and Kovetz, A. 1984, *Ap. J.*, **281,** 367.
Prialnik, D., and Shara, M. M. 1986, **311,** 172.
Rappaport, S., Verbunt, F., and Joss, P. C., *Ap. J.*, **275,** 713.
Ray, A., Kembhavi, A. K., and Antia, H. M. 1989, *Astr. Ap.*, **184,** 164.
Reimers, D., and Koester, D. 1982, *Astr. Ap.*, **116,** 341.
Renzini, A. 1977, in *Advanced Stages of Stellar Evolution,* ed. P. Bouvier and A. Maeder (Geneva Observatory: Sauverny), p. 151.
———. 1979, in *Stars and Stellar Systems,* ed. B. E. Westerlund (Dordrecht: Reidel), p. 155.
———. 1982, in *Wolf-Rayet Stars,* ed. C. W. H. de Loore and A. J. Willis (Dordrecht: Reidel), p. 413.
Renzini, A., and Fusi-Pecci, F. 1988, *Ann. Rev. Astr. Ap.*, **26,** 199.
Richer, H. B., Olander, N., and Westerlund, B. E. 1979, *Ap. J.*, **230,** 724.
Ritter, H., and Burkert, A. 1986, *Astr. Ap.*, **158,** 161.
Robertson, J. A., and Eggleton, P. P. 1977, *M.N.R.A.S.*, **179,** 359.
Robinson, E. I., and Shafter, A. W. 1987, *Ap. J.*, **322,** 296.
Roche, E. A. 1849*a*, *Mem. Acad. Sci. Montpellier,* **1,** 243.
———. 1849*b*, *Mem. Acad. Sci. Montpellier,* **1,** 383.
———. 1851, *Mem. Acad. Sci. Montpellier* **2,** 21.
———. 1873, *Ann. de l'Acad. Sci. Montpellier,* **8,** 235.
Rood, R. T. 1972, *Ap. J.*, **177,** 681.
———. 1973, *Ap. J.*, **184,** 815.
———. 1990, in *Astrophysical Ages and Dating Methods,* ed. E. Vangioni-Flam, M. Casse, J. Audouze, and J. Vanthran (Gif-sur-Yvette: Editions Frontières), p. 313.
Rosen, S. P., and Gelb, J. M. 1986, *Phys. Rev. D.*, **34,** 969.
Rosenberg, H. 1911, *Astr. Nach.*, **186,** No. 4445, 71.
Russell, H. N. 1914*a*, *Popular Astronomy* **22,** 275.
———. 1914*b*, *Popular Astronomy,* **22,** 331.
Sackman, I.-J. 1980, *Ap. J. (Letters)*, **241,** L37.
Sackman, I.-J., Smith, R. L., and Despain, K. H. 1974, *Ap. J.*, **187,** 555.
Saffer, R. A., Liebert, J. W., and Olszewski, E. 1988, *Ap. J.*, **334,** 947.
Saio, H., and Nomoto, K. 1985, *Astr. Ap.*, **150,** L21.
Salpeter, E. E. 1955, *Ap. J.*, **121,** 161.
Sandage, A. R. 1953, *A. J.*, **58,** 61.
———. 1981, *Ap. J.*, **248,** 161.
———. 1982, *Ap. J.*, **252,** 553.
Sandage, A. R., and Tammann, G. A. 1969, *Ap. J.*, **157,** 683.
———. 1971, *Ap. J.*, **167,** 293.
Sanders, R. H. 1967, *Ap. J.*, **150,** 971.
Scalo, J. M., Despain, K. H., and Ulrich, R. K. 1975, *Ap. J.*, **196,** 805.
Scalo, J. M., and Ulrich, R. K. 1973, *Ap. J.*, **183,** 151.
Schatzman, E. 1949, *Pub. Kobenhavns Obs.*, No. 149.
———. 1953, *Ann. d'Ap.*, **16,** 162.
Schönberg, M., and Chandrasekhar, S. 1942, *Ap. J.*, **96,** 161.
Schönberner, D. 1979, *Astr. Ap.*, **79,** 108.
———. 1981, *Astr. Ap.*, **103,** 119.
———. 1986, in *Late Stages of Stellar Evolution,* ed. S. Kwok and S. R. Pottash (Dordrecht: Reidel), p. 337.
Schönberner, D., and Drilling, J. S. 1983, *Ap. J.*, **268,** 225.
Schwarzschild, K. 1906, *Gottinger Nachr.*, 41.
Schwarzschild, M., and Härm, R. 1962, *Ap. J.*, **136,** 158.
———. 1965, *Ap. J.*, **142,** 855.
———. 1967, *Ap. J.*, **150,** 961.
Seeger, P. A., Fowler, W. A., and Clayton, D. D. 1965, *Ap. J. Suppl.*, **11,** 121.
Shara, M. M. 1989, *Pub. A.S.P.*, **105,** 5.
Shara, M. M., Livio, M., Moffat, A. F. J., and Orio, M. 1986, *Ap. J.*, **311,** 163.
Simoda, M., and Iben, I., Jr., 1970, *Ap. J. Suppl.*, **22,** 81.
Simon, N. R. 1982, *Ap. J. (Letters)*, **260,** L87.
Skumanich, A. 1972, *Ap. J.*, **171,** 565.
Smarr, L. L., and Blandford, R. D. 1976, *Ap. J.*, **207,** 574.
Smith, R. L., Sackman, I.-J., and Despain, K. H. 1973, in *Explosive Nucleosynthesis,* ed. D. W. Schramm and W. D. Arnett (Austin: University of Texas), p. 169.
Smith, V. V., and Lambert, D. L. 1989, *Ap. J. (Letters)*, **345,** L75.
———. 1990, *Ap. J. (Letters)*, **361,** 69.
Sneden, C., Truran, J. W., and Wheeler, J. C. 1989, *Ann. Rev. Astr. Ap.*, **27,** 279.
Sparks, W. M., and Kutter, S. G. 1987, *Ap. J.*, **321,** 394.
Stahler, S. W. 1988, *Pub. A.S.P.*, **100,** 1474.
Starrfield, S., Sparks, W. M., and Truran, J. W. 1985, *Ap. J.*, **291,** 136.
Starrfield, S., Truran, J. W., and Sparks, W. M. 1978, *Ap. J.*, **226,** 186.

Stellingwerf, R. F. 1975, *Ap. J.*, **199,** 705.
Strom, S. E., Strom, K. M., Rood, R. T., and Iben, I., Jr. 1970, *Astr. Ap.*, **8,** 243.
Sugimoto, D., and Nomoto, K. 1975, *Pub. Astr. Soc. Japan,* **27,** 197.
Sweigart, A. V., 1990, in *Confrontation between Stellar Pulsation and Evolution,* ed. C. Cacciari (San Francisco: A.S.P.), in press.
Sweigart, A. V., and Demarque, P. 1972, *Astr. Ap.*, **20,** 445.
Sweigart, A. V., and Gross, P. G. 1976, *Ap. J. Suppl.*, **32,** 367.
———. 1978, *Ap. J. Suppl.*, **36,** 405.
Taam, R. E. 1980*a, Ap. J.*, **237,** 142.
———. 1980*b, Ap. J.*, **242,** 749.
Taam, R. E., and Bodenheimer, P. 1989, *Ap. J.*, **337,** 849.
Taylor, J. H., and Weisberg, J. M. 1982, *Ap. J.*, **253,** 908.
Taylor, R. J. 1989, *Q.J.R.A.S.*, **30,** 125.
Thackeray, A. D. 1977, *Mem. R.A.S.*, **83,** 1.
Thomas, H. C. 1967, *Zs. Ap.*, **67,** 420.
Tornambè, A., and Matteucci, F. 1986, *M.N.R.A.S.*, **223,** 69.
Truran, J. W. 1982, in *Essays in Nuclear Astrophysics,* ed. C. A. Barnes, D. D. Clayton, and D. N. Schramm (Cambridge: Cambridge University Press), p. 467.
Truran, J. W., and Iben, I., Jr., 1977, *Ap. J.*, **216,** 797.
Truran, J. W., and Livio, M. 1986, *Ap. J.*, **308,** 721.
Tuchman, V., Sack, N., and Barkat, Z. 1978, *Ap. J.*, **219,** 183.
———. 1979, *Ap. J.*, **234,** 217.
Tutukov, A. V., and Ergma, E. V. 1979, *Soviet Astr. Letters,* **5,** 284.
Tutukov, A. V., and Fedorova, A. V. 1989, *Astr. Zh.*, **66,** 1172.
Tutukov, A. V., and Yungelson, L. R. 1973, *Nauch. Inf.* **27,** 57.
———. 1979, *Acta Astr.*, **23,** 665.
———. 1979, *IAU Colloquium 83, Dynamics of Comets: Their Origin and Evolution,* ed. A. Carusi and G. B. Valsecchi (Dordrecht: Reidel), p. 401.
———. 1987*a, Comm. Ap.*, **XII,** 51.
———. 1987b, in *IAU Colloquium 95, 2d Conf. on Faint Blue Stars,* ed. A. G. Davis Philip, D. S. Hayes, and J. Liebert (Schenectady: L. Davis), p. 435.
———. 1988*a, Nauch. Inf.* **65,** 30.
———. 1988*b, Soviet Astr. Letters,* **14,** 265.
———. 1990, *Astr. Zh.*, **67,** 109.
Ulrich, R. K. 1973, in *Explosive Nucleosynthesis,* ed. D. N. Schramm and D. W. Arnett (Austin: University of Texas), p. 139.
Ulrich, R. K., and Scalo, J. M. 1972, *Ap. J.*, **176,** L37.
Uus, U. 1970, *Nauch. Inf.*, **17,** 3.
VandenBerg, D. A. 1983, *Ap. J. Suppl.*, **51,** 29.
———. 1985, *Ap. J. Suppl.*, **58,** 711.
VandenBerg, D. A., Bolte, M., and Stetson, P. B. 1990, *A.J.*, **100,** 445.
van't Veer, F. 1975, *Astr. Ap.*, **40,** 167.
———. 1979, *Astr. Ap.*, **80,** 287.
Verbunt, F., Lewin, W. H. G., and van Paradijs, J. 1989, *M.N.R.A.S.*, **241,** 51.
Verbunt, F., and Zwaan, L. 1981, *Astr. Ap.*, **100,** L7.
Vilhu, O. 1982, *Astr. Ap.*, **109,** 17.
Walker, M. F. 1954, *Pub. A.S.P.*, **66,** 230.
Wallerstein, G. 1988, *Science,* **240,** 1743.
Webbink, R. F. 1976, *Ap. J.*, **209,** 829.
———. 1984, *Ap. J.*, **277,** 355.
Webbink, R. F., and Iben, I., Jr. 1988, in *Faint Blue Stars,* ed. A. G. Davis Philip, D. S. Hayes, and J. W. Liebert (Davis: Schenectady), p. 401.
Webbink, R. F., Rappaport, S., and Savonije, G. J. 1983, *Ap. J.*, **270,** 678.
Weber, E. J., and Davis, L. 1976, *Ap. J.*, **148,** 217.
Weidemann, V. 1979, in *White Dwarfs and Variable Stars,* ed. H. Van Horn and V. Weidemann (Rochester: University of Rochester), p. 206.
———. 1987, *Astr. Ap.*, **188,** 74.
———. 1990, *Ann. Rev. Astr. Ap.*, **28,** 103.
Weidemann, V., Jordan, S., and Iben, I., Jr. 1991, in preparation.
Weidemann, V., and Koester, D. 1983, *Astr. Ap.*, **121,** 77.
———. 1984, *Astr. Ap.*, **132,** 195.
Weigert, A. 1966, *Zs. Ap.*, **64,** 395.
Wheeler, J. C. 1979, *Ap. J.*, **234,** 569.
———. 1990, in *Supernovae,* ed. J. C. Wheeler, T. Piran, and S. Weinberg (Singapore: World Scientific), p. 1.
Whelan, J., and Iben, I., Jr., 1973, *Ap. J. (Letters),* **253,** L61.
Wildt, R. 1939, *Ap. J.*, **89,** 295.
———. 1940, *Ap. J.*, **90,** 611.
Williams, R. E. 1985, in *Production and Distribution of CNO Elements,* ed. I. J. Danziger (Garching ESO), p. 225.
Wilson, J. 1980, *Proc. N.Y. Acad. Sci.*, **336,** 358.
———. 1983, in *Numerical Astrophysics,* ed. J. Centrella, R. Bowers, J. LeBlanc, and M. LeBlanc (Boston: Jones and Bartlett), p. 422.
Winget, D. E., Hansen, C. J., Liebert, J., Van Horn, H. M., Fontaine, G., Nather, R. E., Kepler, S. O., and Lamb, D. Q. 1987, *Ap. J. (Letters),* **315,** L77.
Winget, D. E., Van Horn, H. M., Tassoul, C. J., Fontaine, G., and Carrol, B. W. 1982, *Ap. J. (Letters),* **252,** L65.
Wolfenstein, L. 1978, *Phys. Rev. D,* **17,** 1.
Wolfenstein, L., and Beier, E. W. 1989, *Phys. Today,* **42,** 28.
Wolfe, K., *et al.* 1989, *Zs. Phys. A,* **334,** 491.
Wood, P. R. 1974, *Ap. J.*, **190,** 609.
———. 1979, *Ap. J.*, **227,** 220.
Wood, P. R., Bessell, M. S., and Fox, M. W. 1983, *Ap. J.*, **272,** 99.
Wood, P. A., and Zarro, D. M. 1981, *Ap. J.*, **247,** 247.
Woosley, S. E., and Weaver, T. A. 1986, *Ann. Rev. Astr. Ap.*, **24,** 205.
Zhevakin, S. A. 1953, *Soviet Astr.—A. J.*, **30,** 161.
———. 1954*a, Soviet Astr.—A. J.*, **31,** 141.
———. 1954*b, Soviet Astr.—A. J.*, **31,** 335.

ICKO IBEN: Department of Astronomy, University of Illinois, Astronomy Building, 1002 West Green Street, Urbana, IL 61801